Deltares

Enabling Delta Life

Mud dynamics in the Ems-Dollard, phase 2

Analysis soil samples

Deltares

Mud dynamics in the Ems-Dollard, phase 2

Analysis soil samples

Julia Vroom
Bas van Maren
Maria Ibanez
Miguel de Lucas Pardo
Han Winterwerp
Luca Sittoni

1205711-001

Deltares

Title
Mud dynamics in the Ems-Dollard, phase 2

Client	Project	Reference	Pages
Rijkswaterstaat	1205711-001	1205711-001-ZKS-0006	75

Keywords
Settling velocity, Atterberg limits, Cohesive sediment, Erosion, Ems Estuary.

Summary
The Water Framework Directive (WFD) obliges the EU member states to achieve good status of all designated water bodies (rivers, lakes, transitional and coastal waters) by 2015. In the management plan for the implementation of the WFD (and Natura 2000) in the Netherlands, the context, perspectives, targets and measures for each designated water body (also including the Ems-Dollard) have been laid out. To achieve a good status of the Ems-Dollard Estuary (as the WDF obliges), knowledge on the mud dynamics in this region has to be improved, and the reasons for the increase in turbidity have to be identified before 2015. Therefore Rijkswaterstaat has initiated the project "Onderzoek slibhuishouding Eems-Dollard" (Research mud dynamics Ems-Dollard). This project explores the reasons for the historic increase in turbidity, and which measures can be designed to improve the water quality in the area.

Part of this research is the collection and analysis of sediment samples. These samples have been analysed to (1) determine changes in the mud content with respect to 1989, (2) obtain parameters for input and calibration of numerical models, and (3) increase insight in the mud dynamics in the Ems Estuary by focussing on spatial variations and differences w.r.t. 1989.

The most important parameters for input of the numerical model, which can be derived from the bed samples, are the critical shear stress for erosion τ_{cr} and the sediment settling velocity w_s. The critical shear stress for erosion for a consolidated bed ranges typically between 1 and 1.5 Pa. The settling velocity, determined with the settling tests, varies between 1 and 1.2 mm/s. The mud content measured in 2013 is at some locations larger than the mud content measured in 1989 and at other locations smaller, even if part of this difference may be due to methodological differences in laboratory analysis and collection of the samples. The bed of the main tidal channel in the Dollard (the Groote Gat) has become muddier, as well as the bed of the lower Ems River and the direct vicinity of the port of Delfzijl.

References
Offertenummer 1205711-000-ZKS-0004, toekenningsbrief RWS/WD-2011/3497

Version	Date	Author	Initials	Review	Initials	Approval	Initials
1.0	Mar. 2014	Bas van Maren		Thijs van Kessel			
2.0	Jun. 2014	Julia Vroom		Thijs van Kessel			
2.1	Oct. 2014	Bas van Maren	BM	b/a GB		Frank Hoozemans	

State
final

Contents

1 Introduction

1.1 Research mud dynamics Ems-Dollard study overview

The Water Framework Directive (WFD) requires EU member states to achieve good ecological and chemical status of all designated water bodies (rivers, lakes, transitional and coastal waters) by 2015. In the management plan (Rijkswaterstaat, 2009) for the implementation of the WFD (and Natura 2000) in the Netherlands, the context, perspectives, targets and measures for each designated water body have been defined. The requirements for the Ems Estuary (see Figure 1.1 for location) are that the mud dynamics need to be better understood (before 2015), and driving forces for increase in turbidity need to be identified. Therefore Rijkswaterstaat has initiated the project 'Research mud dynamics Ems Estuary' (*Onderzoek slibhuishouding Eems-Dollard*). The aim of this project is to (I) determine if and why the turbidity in the Ems Estuary has changed, (II) to determine how the turbidity affects primary production, and (III) to investigate and quantify measures to reduce turbidity and improve the ecological status of the estuary – see also the flow chart of the project structure (Figure 1.2).

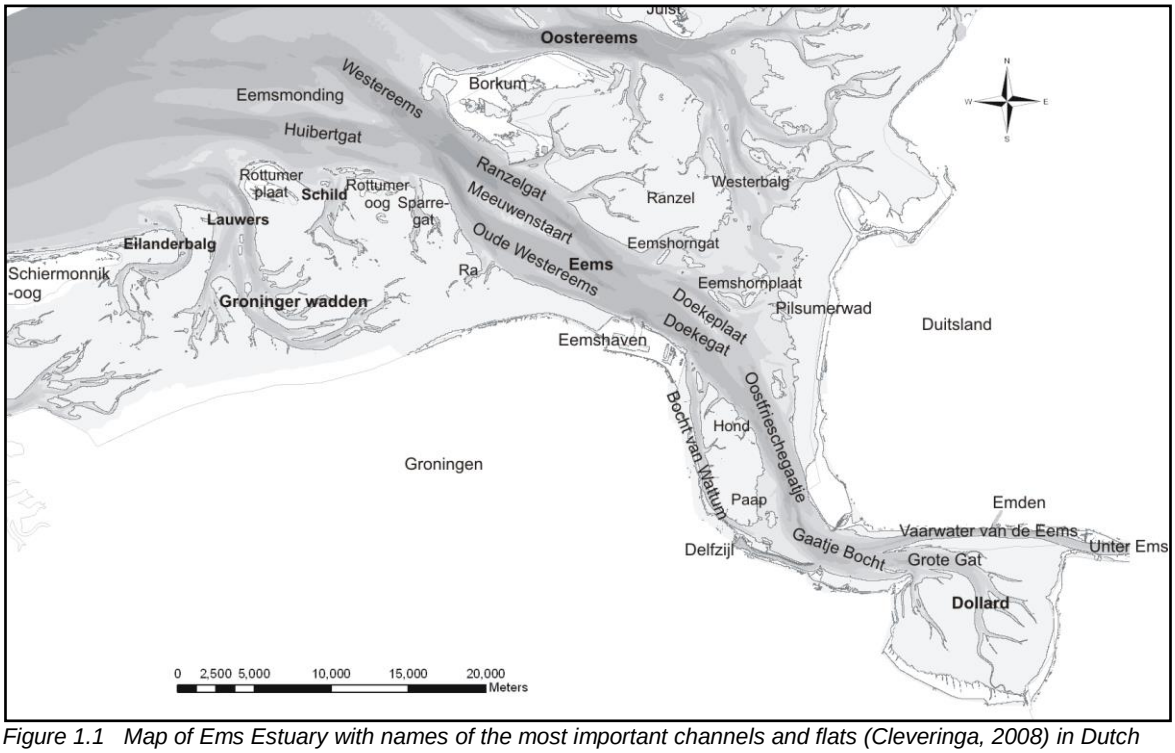

Figure 1.1 Map of Ems Estuary with names of the most important channels and flats (Cleveringa, 2008) in Dutch and German. The English name of the 'Vaarwater van de Eems' is the Emden navigation channel or Emden Fairway. The English name of 'Unter Ems' is the lower Ems River.

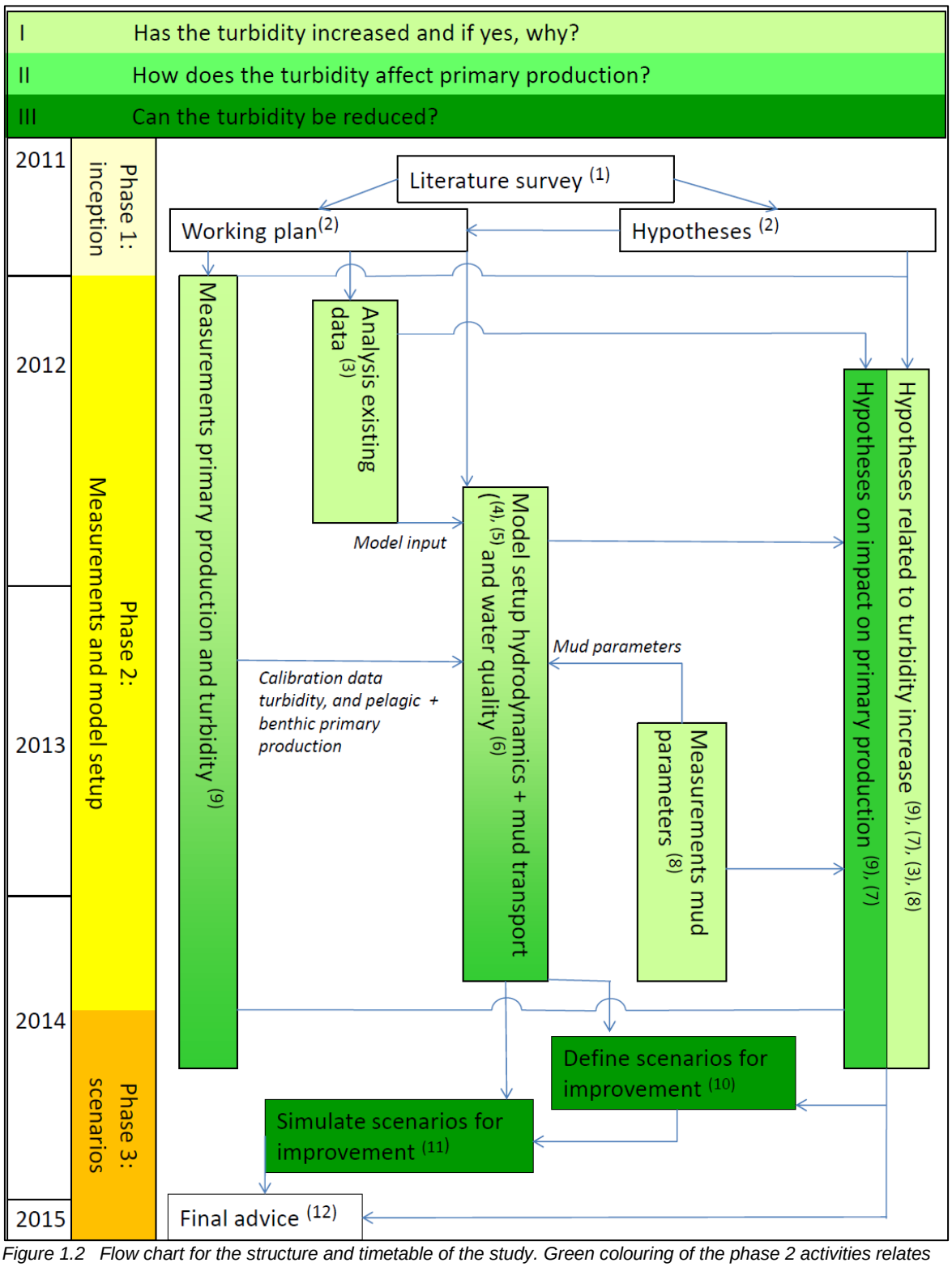

Figure 1.2 Flow chart for the structure and timetable of the study. Green colouring of the phase 2 activities relates to the colour of the main research questions I, II, and III. See Box 1 for a description and Table 1.1 for the references (1) – (12)

This research project explores mechanisms that may be responsible for the present-day turbidity of the estuary and measures to reduce the turbidity. To achieve this, an effect-chain model is setup in which relates human interventions to changes in hydrodynamics, sediment transport, and water quality. This model is supported as much as possible by existing data and new data collected within this project. However, the long-term effect of human interventions on suspended sediment dynamics in an estuary such as the Ems Estuary is complex, and data supporting such an analysis is limited. Although the absolute values of the model predictions should therefore be carefully interpreted, it is a powerful tool to investigate trends. This work provides indicative explanations for the current turbidity patterns and a first exploration of restoration options, but also reveals important gaps in knowledge and next steps to be taken. Additional research is required to further substantiate the results of this project.

The overall study is divided into three stages: an inception phase (phase 1) in which gaps in knowledge are identified and a research approach is defined; phase 2, in which measurements are done and models are set up and calibrated; and phase 3 in which the models are applied to investigate measures to improve the ecological and chemical status of the estuary. The overall structure and timeline of this study is summarized in Figure 1.2 and Box 1. An overview of the deliverables (reports and notes) produced during the project is given in Table 1.1. The numbers 1 to 12 of the deliverables are part of the project layout in Figure 1.2.

BOX 1: SET UP OF THE STUDY (with Figure 1.2; references in Table 1.1)

The primary objective of this study is to address the following:

q1: Has the turbidity increased and why?

q2: If yes, what is the impact on primary production?

q3: Can the turbidity be reduced?

These questions are presented in a flow chart (see Figure 1.2). During phase 1, existing gaps in knowledge were identified (see report 1 in Table 1.1), and a number of hypotheses were formulated related to q1 and q2 (report 2 in Table 1.1), to be addressed during phase 2 of the study.

Phase 2 consists of measurements, model set up and analysis. Measurements of primary production and turbidity are carried out from January 2012 to December 2013, and reported mid 2014 (report 9 in Table 1.1). These measurements are carried out to address hypotheses related to q1 and q2, and to calibrate the sediment transport and water quality models. Existing abiotic data (such as water levels, bed level, dredging, and sediment concentration) are analysed in this phase to address hypotheses related to q1 and to provide data for model calibration (report 3 in Table 1.1). Soil samples in the Ems estuary and Dollard basin have been collected to determine changes in mud content (hypotheses relates to q1) and determine parameter settings of the sediment transport model (report 8 in Table 1.1).

The effect-chain model set up for this study consist of three modules: a hydrodynamic module (report 4 in Table 1.1), a sediment transport module (report 5), and a water quality module (report 6). These models are applied to address the hypotheses related to q1, q2, and q3 (report 7 in Table 1.1).

In phase 3, a number of scenarios are defined to reduce turbidity / improve the water quality (q3) of the estuary (report 10 in Table 1.1). Their effectiveness is tested in reference (report 11). A final report, synthesizing the most important findings and recommendations (report 12) concludes the project.

Table 1.1 Reports / notes delivered during phase 1 to 3 of the Mud dynamics in the Ems estuary project (with numbers referencing to Figure 1.2). The current report is in bold.

Number	Year	Phase	Main research question	Report
1	2011	1	-	Literature study
2	2011	1	-	Working plan phase 2 and 3
3	2012	2	1	Analysis existing data
4	2014	2	-	Set up hydrodynamic models
5	2014	2	-	Set up sediment transport models
6	2014	2	-	Set up water quality model
7	2014	2	1, 2	Model analysis
8	**2014**	**2**	**1**	**Analysis soil samples**
9	2014	2	1, 2	Measurements primary production
10	2014	3	3	Scenario definition (note)
11	2014	3	3	Model scenarios
12	2015	3	1, 2, 3	Final report

The current reports described the results of soil sampling measurements carried out in 2013. In section 1.2, the purpose and general methodology of the study is described. The methodology is described in more details in Chapter 2, and results are presented in Chapter 3. The data is interpreted, and the main purposes of this study are addressed, in Chapter 4. Conclusions and recommendations for future work follow in Chapter 5.

1.2 Purpose and methodology of this study

This report presents the results of 'measurements mud parameters' as part of Phase 2 of the study, in which a large number of mud samples have been collected and analysed. The purpose of the field samples collection and laboratory analysis is to:

1. Determine changes in the mud content with respect to 1989.
2. Obtain parameters for input and calibration of the numerical models (typical values for settling velocity w_s and critical shear stress for erosion τ_{cr}).
3. Increase the insight in the mud dynamics in the Ems-Dollard (transport and segregation).

Data analysis is an important support to the modelling study. While data quantifies change in the system, models are specifically developed to understand the processes responsible for changes qualitatively. Models can also be used to predict the influence of measures on the system (Phase 3 of this project).

Phase 1 was focussing on the analysis of existing data (report 3) and revealed changes in the suspended sediment concentration in a number of regular sampled stations in the Ems Estuary. Changes in the mud dynamics and distribution in the estuary can also be derived from changes in the bed composition, which was measured for the last time in 1989 (van Heuvel, 1989). Resampling these observations applying the same method may therefore also provide valuable information on changes in mud distribution in the last decades.

Recently, a methodology was setup to relate the erosional behaviour of sediments using bulk sediment properties (Winterwerp et al., 2012). This methodology consists of measuring simple bulk properties (i.e. grain size distribution, pH, dry density ρ_{dry} and water and carbon content) on all collected samples, and focuses more complex laboratory techniques (Atterberg Limits, zeta potential, settling tests, Vane test, CST test and the Sedigraph) on a limited number of samples. As described in the measurement plan (report 2), this approach was applied to the Ems Estuary as part of Phase 2.

In this report, first the theory, explaining why and how the measurements are conducted, is described in section 2.1. The collection of samples in the field and the laboratory and data analyses are described in section 2.2 and 2.3, respectively. The results are given in Chapter 3. Consequently, the results, interpreted with respect to the three aims of the field campaign, are discussed in Chapter 4. Section 4.1 gives a general interpretation of the results of the laboratory analyses. In section 4.2 the changes in mud content w.r.t. 1989 are explained, i.e. purpose 1 of the field campaign. Consequently, the increase in insight in the mud dynamics based on temporal and spatial patterns (purpose 3), is described in section 4.3. Section 4.4 focusses on the implications of the data analyses for the numerical modelling study (purpose 2). A proposal for re-calibration of the model, by changing values of user-defined variables is given. Conclusions are drawn in Chapter 5.

2 Methods

2.1 Theoretical framework

One of the goals of the field campaign is to derive values for certain variables (being the settling velocity w_s, erosion parameter M and the critical shear stress for erosion τ_{cr}) in the numerical modelling study. The erosion rate of cohesive sediment E is governed by the bed shear stress, the critical shear stress for erosion τ_{cr} and the erosion parameter M. The critical shear stress for erosion τ_{cr} and the erosion parameter M vary in time, depth and space and are dependent on the degree of consolidation, sand content and organic content. These two parameters (erosion parameter M and the critical shear stress for erosion τ_{cr}) can be measured in the field. However, these measurements are labour-intensive, show a large variation and are not well applicable outside intertidal areas. An alternative is to determine erosion properties of the bed sediment in the laboratory, by collecting an undisturbed sample and bringing this to the laboratory for analysis. The drawback of these experiments is that they are still labour-intensive and costly, and the results are strongly dependent on the way of collection and the transportation to the laboratory. A third option is determination of bulk properties, which can be used to determine the erodibility of the bed sediment. This methodology is used and summarised here, and explained more extensively in van Maren (2013) and Winterwerp et al. (2012).

The methodology of Winterwerp et al. (2012) quantifies the erodibility of a sediment bed in relation to simple sediment properties. The erodibility is based on a relation between the erosion parameter M (proportional to the erosion rate or velocity), the critical shear stress for erosion τ_{cr} (which determines threshold for erosion) and bulk sediment properties (particle size distribution, dry density ρ_{dry}, void ratio e_i). These relationships will be provided in section 2.3.7 of this report. The bulk properties are easy to measure and can be obtained for a large number of samples. In addition, more detailed and time-consuming measurements are needed for linking the parameters derived from those detailed experiment to the bulk properties. Those more detailed and time-consuming experiments are executed on a subset of samples and extrapolated to the remaining samples, which are analysed with easy to measure bulk properties. In this way spatially varying information on the erosion parameter M and the critical shear stress for erosion τ_{cr} can be obtained.

In this study, particle size distribution (PSD) with the Malvern, pH, conductivity and water and organic content, which are relatively easy to measure, are determined for all samples. With the particle size distribution the (clay and) mud content of the sample can be computed, as well as the median grain size d_{50}, the dry density ρ_{dry} and the water content W. The water content W gives insight in the erodibility of the bed sediment. The mud distribution throughout the estuary will be analysed to increase our insight in the mud dynamics in the Ems-Dollard estuary. By comparing the mud content in 2013 to the mud content in 1989 changes over time can be observed. These temporal variations of changes in mud content will also increase the insight in mud dynamics, especially when linked to changes in hydrodynamics, suspended sediment concentrations and bed level changes. In this way, purpose 1 and 3 of this study can be met.

The particle size distribution with the Sedigraph, Atterberg Limits, Vane test, Zeta Potential, CST test and settling column test are more elaborated tests, and are carried out on a limited number of samples (Table 2.1, Figure 2.1 and appendix B). Samples and laboratory testing were selected to assure good spatial coverage (so samples originate from the entire sampled

area, see Figure 2.1) and varying mud content (using the measured grain size distribution, representing all ranges in mud content. Subsequently, the measured simple properties allow extrapolation of less standard soil properties to all samples.

The critical shear stress for erosion τ_{cr} can be determined from the Plasticity Index PI of the bed material. The Plasticity Index PI is the difference between the *Atterberg Limits*, i.e. the Liquid Limit LL minus the Plastic Limit PL. The Liquid Limit LL is the transition from fluid behaviour to plastic behaviour and the Plastic Limit PL marks the transition from plastic to solid behaviour. The Atterberg Limits define the water content (defined as the mass of water divided by the mass of dry solids) of the soil at these limits. The relation between the Liquid Limit LL and the Plasticity Index PI is dependent on the type of material and the organic content. The Plasticity Index PI for sand is zero, while for certain types of clay it can be very high. If the Plasticity Index PI is larger than 7%, the soil behaves cohesively. The Atterberg Limits can be derived from the samples directly, although this analysis is labour intensive. Therefore, a linear relation between the clay content and the Plasticity Index PI ('Activity plot') is determined with the Atterberg Limits. Using this relation, the results can be extrapolated to the remaining samples for which only the clay content is measured. The clay content is derived from the particle size distribution. Due to underestimation of the clay content in the Malvern analysis, a linear relation between the mud content and the Plasticity Index PI has been used to extrapolate the Plasticity Index PI to all samples. With this Plasticity Index PI, the critical shear stress for erosion is computed.

The erosion parameter (M_E) is related to several parameters: the consolidation coefficient c_v, the undrained shear strength c_u, the volumetric mass concentration ϕ, the dry density ρ_{dry} and the median grain size d_{50}. The consolidation coefficient c_v can be derived both from the *CST test* and *settling column tests.* Comparison of the consolidation coefficient c_v from those two independent tests, gives a good check of the results. The undrained shear strength c_u of the material can be obtained with a *vane test*. In this project an empirical relation between the strength and void ratio e_i from Winterwerp et al. (2012) is used, due to malfunctioning of the *vane test* the results could not be used. Since the void ratio e_i is determined for all samples, the undrained shear strength c_u can also be thereby computed for all samples. The volumetric mass concentration ϕ and the dry density ρ_{dry} are computed with the mass of water and solids in each sample. The median grain size d_{50} follows from the particle size distribution.

The settling column test is also used to determine the settling velocity w_s of flocculated material. An indication of the degree of flocculation in the estuary can be obtained with Zeta Potential measurements. In addition, these measurements give some insight in the type of mud present in the sample, and provide an independent result of the type of mud determined with the Atterberg Limits. Table 2.1 gives an overview of all tests and parameters discussed above.

Table 2.1 Laboratory tests carried out in the FL, including resulting properties. In the right column is indicated for which purpose the results of the experiments are used.

Laboratory Test	#	Property	Used to derive	Used for purpose
Malvern	307	PSD	mud and clay content, d_{50}	Determine changes in the mud content with respect to 1989. Increase the insight in the mud dynamics in the Ems-Dollard. Obtain erosion parameter and critical shear stress for erosion τ_{cr} for input and calibration of the numerical models.
pH, conductivity	247 222	pH, conductivity	pH, conductivity	
Oven drying at 105 ^{o}C and 400 ^{o}C	278	Water and organic content	dry density ρ_{dry}, void ratio e_i, water content W, volumetric mass concentration ϕ	Increase the insight in the mud dynamics in the Ems-Dollard. Obtain erosion parameter M for input and calibration of the numerical models.
Sedigraph	25	PSD	mud and clay content	Increase the insight in the mud dynamics in the Ems-Dollard.
Atterberg Limits	25	Liquid Limits LL and Plastic Limit PL	Liquid Limit LL, Plasticity Index PI	Obtain erosion parameter M and critical shear stress for erosion τ_{cr} for input and calibration of the numerical models.
Vane test**	22	Peak shear strength, undrained shear strength c_u	Not used, empirical relation with void ratio of Winterwerp et al. (2012) is used instead.	Obtain erosion parameter M for input and calibration of the numerical models.
Zeta potential	38	Zeta potential	Zeta potential	Increase the insight in the mud dynamics in the Ems-Dollard.
CST	4	Gibson coefficient C_{gib}	Gibson coefficient C_{gib}	Obtain erosion parameter M for input and calibration of the numerical models.
Settling columns tests	4	Permeability parameter K_k, fractal dimension D, effective stress coefficient K_p and settling velocity w_s	Consolidation coefficient c_v, settling velocity w_s	Obtain erosion parameter M and settling velocity w_s for input and calibration of the numerical models.

* The pH and conductivity could only be measured for samples with a thick enough water layer on top of the sample.

** not used in this report due to malfunctioning of the instrument

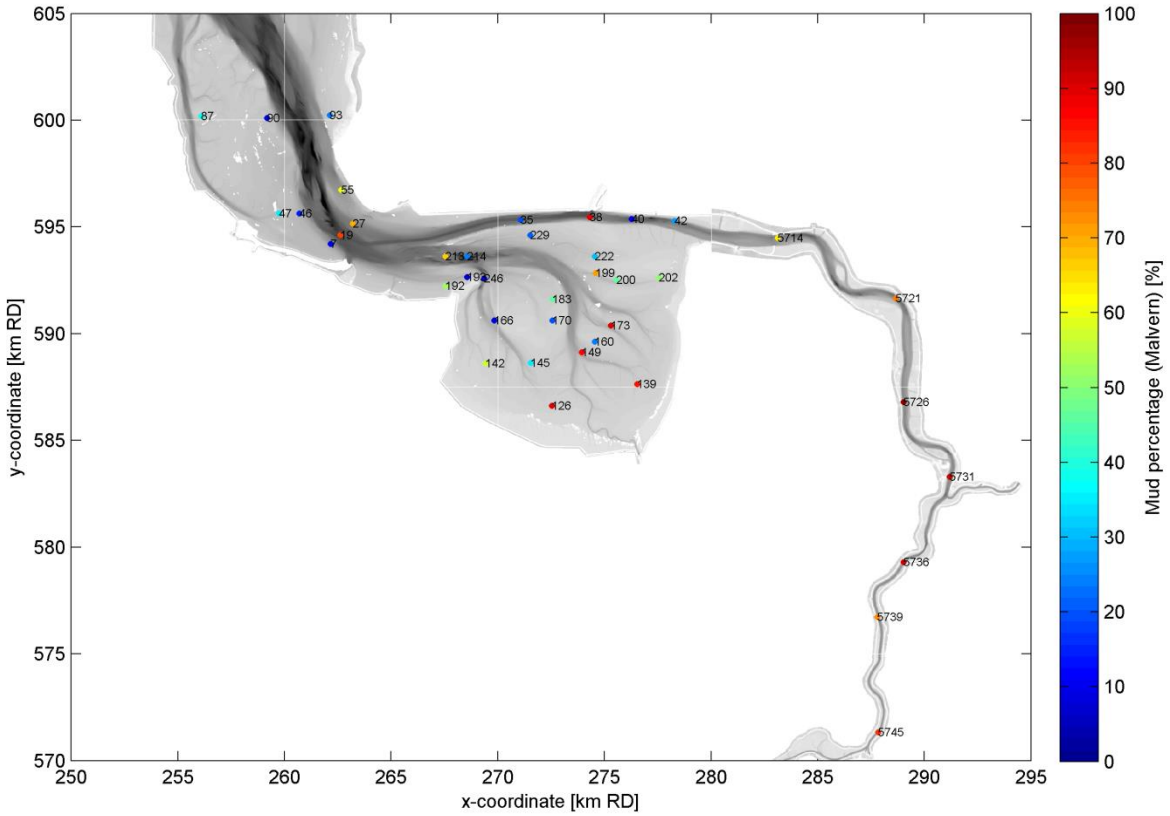

Figure 2.1 Location of samples used for additional experiments and their mud percentage based on the Malvern measurement 2013.

A second purpose of this study is to compare the mud distribution in the estuary in 1989 versus 2013. In 1989, the soil samples were subsampled with a spoon, representing the upper 8-10 cm of the larger sample (van Heuvel, 1991). The material with a diameter larger than 1 mm was sieved. The remaining material (sand and mud) was measured with a Malvern through laser beam diffraction with different lenses. The overlap areas of the separate measurements were compared and used to reprocess the Malvern results into a single distribution. Before introducing the sample into the Malvern, the sample was completely dispersed through mechanical and ultrasonic dispersion. No chemical treatment was applied (McLaren et al. 1998).

2.2 Field sampling

Between September 25th and December 13th, 1989 a total of 668 sediment samples has been collected in the Ems-Dollard and the Wadden Sea (van Heuvel, 1991). During the sampling period, no dredging activities were executed and the weather was relatively calm (no storms). The samples were taken with a large van Veen grab (10-20 L) at the locations in Figure 2.2.

Between August and October 2013, 272 bed samples were taken at the approximately same locations as the sampling in 1989 (Figure 2.2) in the area between Eemshaven and Papenburg, allowing for a comparison between both periods. The sampling area is restricted to mud-dominated areas, including Hond-Paap tidal flat (Figure 1.1 shows a map with names of important flats and channels) and adjacent tidal channels, the Dollard basin, and parts of the Ems River. In order to sample on the same location, the coordinates of the old measurements where retrieved from the Open Earth database. After sampling and initial

processing, it was revealed that the coordinates of the samples stored in the Open Earth database where incorrectly converted to latitude / longitude. As a result, the new samples were collected 130 m from the original location. This is not expected to strongly influence the historic comparison, for reasons discussed in section 3.2.2.

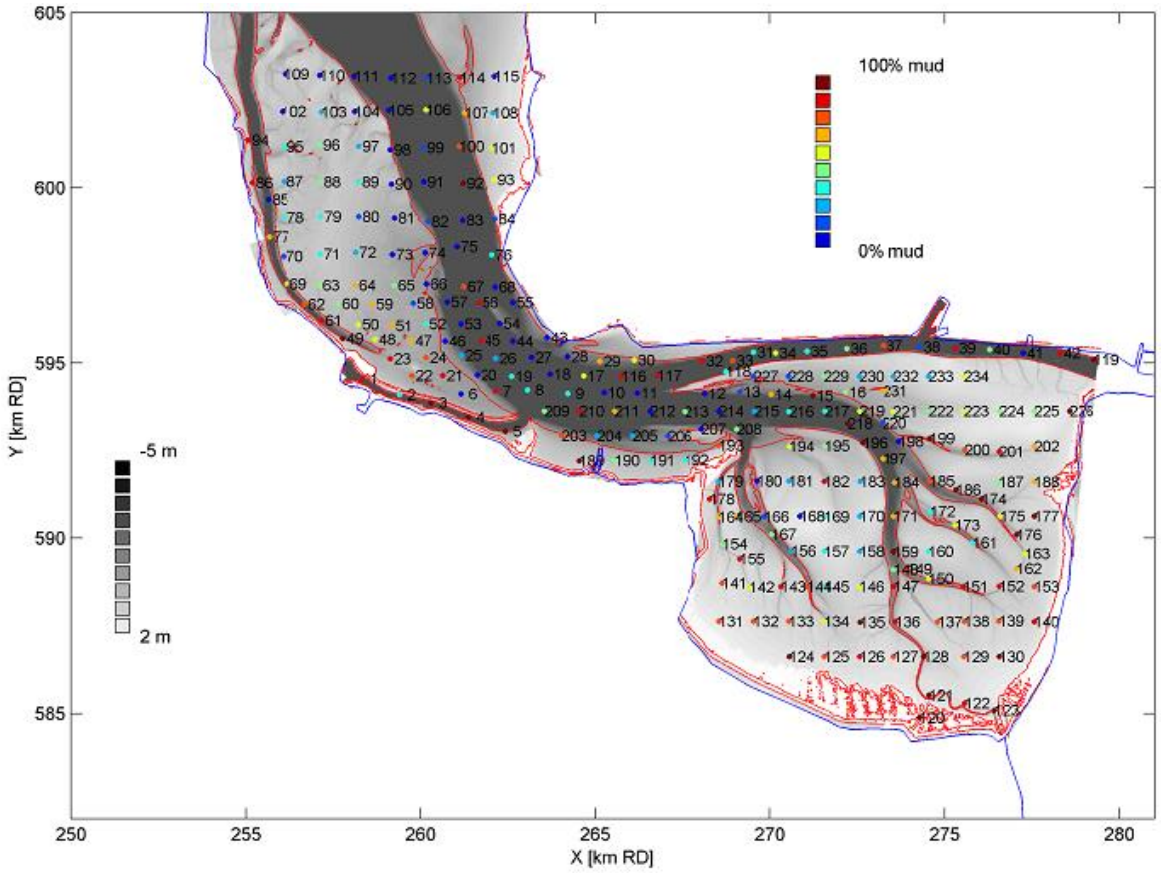

Figure 2.2 Samples and mud content in 1989 in the area of interest (excluding the lower Ems River), to be repeated during the field campaign 2013. Sample locations taken from taken from the Open Earth database. Note that on this scale of plotting the difference between the 1989 and 2013 measurements is very small.

Most samples have been collected using a Box corer frame with a cylindrical tube (Figure 2.3). In this way an 'undisturbed' sample could be collected. When the water depth was too shallow (< 1 m) to be reached by the vessel, a smaller boat was used (Figure 2.4). From the small boat a vacuum tube[1] was used to collect samples instead of a box corer for practical reasons. Most samples in shallow water could be collected at high water levels in this way. The remaining samples were taken by hand, by pushing the sample cylinder into the soil. After sampling, the sampling date and time and a visual estimate of the soil type were recorded.

In 1989, the samples were collected with a van Veen grab, which collects a disturbed sample. In order to identify the effect of sample collection methodology, 28 samples have been collected with a van Veen grab additionally to the Box corer/vacuum tube. The sampling with the Box corer/Vacuum tube and van Veen grab have not been executed at the same moment due to practical reasons. The van Veen grab samples were collected during a separate

[1] *The vacuum tube consists of a pole with the sample cylinder fixed to it. The pole is positioned at the sampling location and pushed into the soil. After the valve is closed, the cylinder including the sample can be taken out of the bed.*

cruise. This might be an (additional) source of differences between the samples. This will be addressed in more details in section 3.2.2.

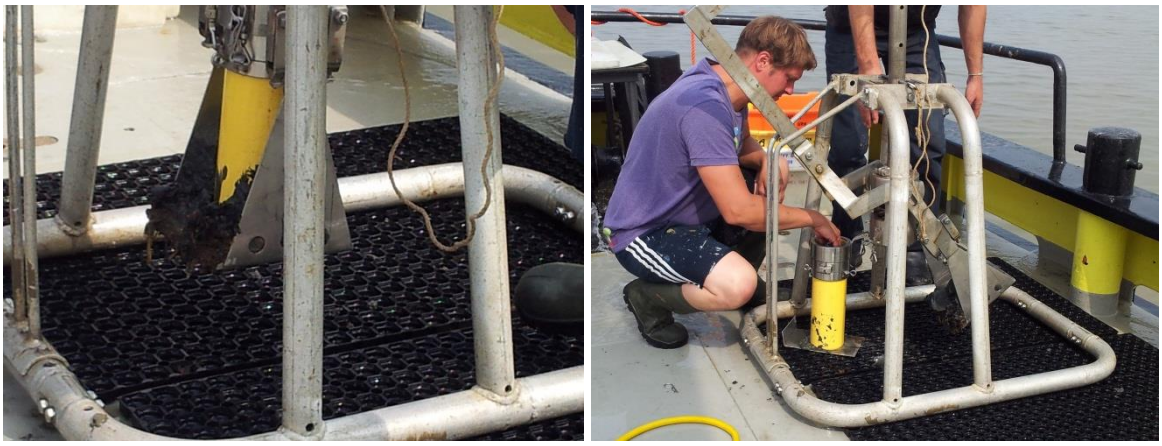

Figure 2.3 Sample collected with the Box corer frame (left) and the sample just released from the Box corer frame (right).

Figure 2.4 Fixing the lid with tape to avoid opening of the sample cylinder (left) and the smaller boat used to collect samples in shallow water using the vacuum tube (right).

The samples collected during the field campaign arrived to the laboratory of Deltares (Fysisch Lab, FL), where they were stored in the basement at 11^{o}C. The samples were collected between August and October, and analysed between October and March. The samples have a water layer on top of the sediment to prevent dehydration of the sample. Especially with clayey samples dehydration should be prevented, because the platelets can stick together (irreversibly). During transport and storage, a layer of relatively clear water formed above the sediment due to some settling and consolidation. The conductivity and pH of this water layer has been measured. For the determination of the water and organic content, the water layer has not been taken into account.

2.3 Laboratory and data analysis

2.3.1 Bulk properties

2.3.1.1 pH, conductivity and water and organic content

The pH and conductivity of the supernatant water of all the samples (except the van Veen grabbed samples) were measured first. Then, for each sample a subsample was taken with a cylinder with a diameter of 2 cm, to a depth of 10 cm. From each homogenised subsample 1 g of material was taken and diluted in 800 ml of tap water for determination of the particle size distribution (PSD). The remainder of the subsample extracted from the sample was weighed and heated for one day at 105^{o}C and weighed again to measure water mass (difference in mass before and after heating at 105^{o}C). The sample was then heated at 400^{o}C and weighing again to measure the organic mass (difference in mass before and after heating at 400^{o}C).

With the weight of the dry sample without organic content and the mass of water in the samples, the water content W, the dry density ρ_{dry} and the void ratio e_i are computed. The water content W is a parameter to quantify the amount of water in a soil sample, which is often used in soil mechanics. The water content W is defined as:

$$W = M_w / M_{s,dry}$$

With:

W	water content [-]
M_w	mass of water [kg]
$M_{s,dry}$	mass of dry solids [kg]

The dry density ρ_{dry} of the sediment is defined as the mass of dry material divided by the wet volume of the sample:

$$\rho_{dry} = \frac{M_{s,dry}}{V_{wet}} = \frac{M_{s,dry}}{\frac{M_{s,dry}}{\rho_s} + \frac{M_w}{\rho_w}}$$

With:

ρ_{dry}	dry density [kg/m^3]
$M_{s,dry}$	mass of dry solids [kg]
V_{wet}	volume of the wet solids [m^3]
M_w	mass of water [kg]
ρ_s	density of solids [kg/m^3], assumed to be 2650 kg/m^3 in this study
ρ_w	density of water [kg/m^3], dependent on salinity

The void ratio e_i of the samples is computed as follows:

$$e_i = \frac{M_w / \rho_w}{M_{mud} / \rho_{mud}}$$

With:

e_i	void ratio [-]
M_w	mass of water [kg]

ρ_w	density of water [kg/m^3], dependent on salinity
M_{mud}	mass of dry solids with d < 63 µm [kg]
ρ_{mud}	density of solids with d < 63 µm [kg/m^3], assumed to be 2650 kg/m^3

With the mass of the organic material, the organic content can be computed:

$$OC = \frac{M_{organic}}{M_{s,dry}}$$

With:

OC	organic content [-]
$M_{organic}$	mass of organic material [kg]
$M_{s,dry}$	mass of dry solids [kg]

2.3.1.2 *Malvern particle size distribution*

Before measuring the particle size distribution (PSD) with the Malvern, the diluted sample needs to be pre-treated. Within a consolidated bed, clay particles have aggregated into flocs which are not representative for their distribution in the water column. Several methods exist to disperse the flocs. Chemical pre-treatment with a deflocculant will destroy all flocs, and a subsequent grain size analysis will measure the PSD of the primary particles. However, some degree of flocculation does exist in the natural Ems-Dollard suspended sediments. Therefore, in order to approximate the PSD of the original suspension, a less rigorous pre-treatment is applied, being ultrasonic treatment. It is remarked that due to ultrasonic treatment, sand particles may break up, resulting in an overestimation of the finer fraction (Blok & Arentz, 2012). For consistency with the 1989 samples (which also did not use chemical pre-treatment) the ultrasonic treatment is applied, but the effect of the ultrasonic treatment on the PSD is verified first.

The diluted sample underwent ultrasonic treatment for 10 minutes. Based on tests with different duration of the ultrasonic treatment on various samples, a duration of 10 minutes was chosen because for longer treatment the particles size distribution of the primary particles does change hardly, see Figure 2.5. After the ultrasonic treatment, the particle size distribution was measured with the Malvern MasterSizer 2000 by Static Light Scattering. Ten measurements for each sample were done, and the particle size distribution is the average of these ten measurements.

The van Veen grab samples were only taken for comparison of the PSD with the boxcore samples, and therefore only the PSD of these samples is measured (and not the pH and conductivity), applying the same ultrasonic treatment.

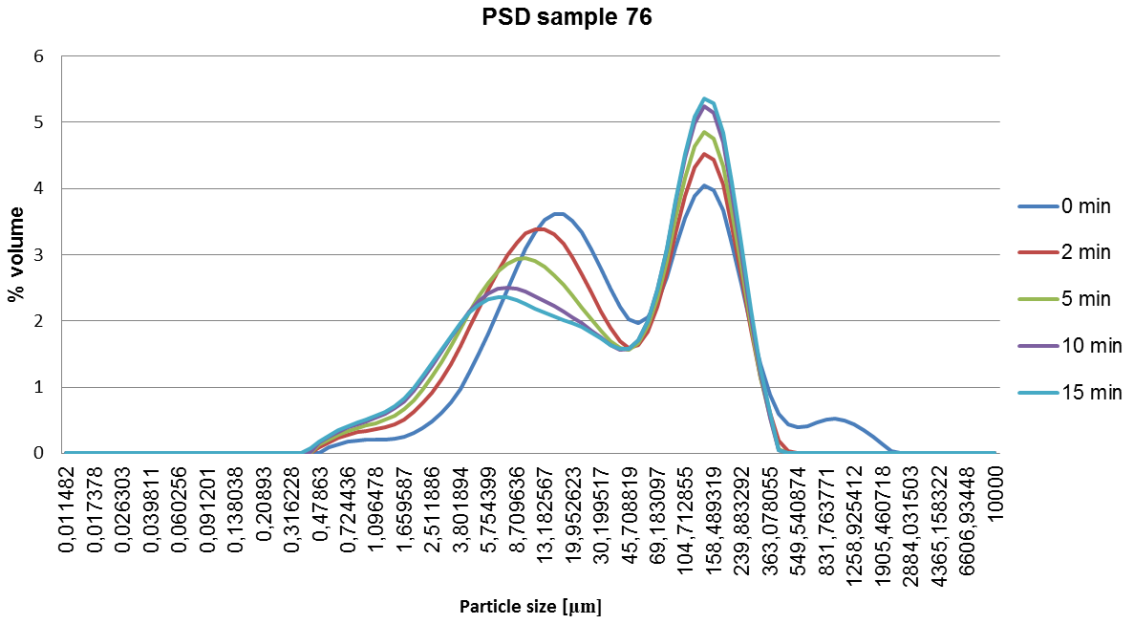

Figure 2.5 Particle size distribution resulting from varying ultrasonic treatment time in minutes.

With the Malvern, the total PSD is measured within one single measurement, ranging from clay to sand. However, using a Malvern, the detailed particle size distribution of especially the finer fraction (d < 63 µm; mud) may be influenced by particles with d > 63 µm (sand). Therefore a sensitivity test has been done to verify the effect of sand-sized grains on the distribution of mud. These tests (Figure 2.8) revealed that although there is an effect of sand on the particle size distribution, the effect on the measured clay, silt and sand fraction is low. Hiding of particles only influences the PSD when particles with d > 2 mm are present in the sample. However, this is not the case for the samples in this report as none of the presented distributions show a large amount of particles larger than 2 mm.

Table 2.2 Setting of the Malver MasterSizer 2000

Settings of the Malvern MasterSizer 2000	
Dispersant name	water
refractive index	1.33
Material name	Kaolinite high
refractive index	1.57
absorption	0.1
blue light	1.57

Figure 2.6 The Malvern MasterSizer 2000

The Malvern is an attractive instrument to determine the PSD because the measurement is fast and simple. However, the Malvern is also known to underestimate the clay fraction (d < 2 µm). Therefore, the particle size distribution was also analysed with the Sedigraph. Because the Sedigraph measurements are time-consuming, a selection of the samples was used for

this analysis. The difference between the PSD from the Malvern and Sedigraph and the application of the results is discussed in more detail in section 2.3.1.3.

2.3.1.3 Sedigraph particle size distribution

Similarly to the Malvern, the Sedigraph is used to determine the particle size distribution. The sample is dried, after which the PSD of the sediment with a diameter d > 38 µm is determined by sieving (38 µm is standard protocol; large silt or sand particles settle rapidly and may increase the settling velocity of finer material through the wake effect). The material with a grain size less than 38 µm is suspended and its settling velocity is directly measured by X-ray absorption technic. The settling velocity is converted to a PSD using Stokes' law. This conversion introduces an error, since Stokes' law is valid for spherical particles, whereas clays consist of plate-like particles which settle much slower. Hence, the Sedigraph will underestimate the particle size in the silt range and overestimate the clay fraction. The distribution of sediment with d > 38 µm is determined by sieving, and subsequently added to the sedigraph measurements to obtain the full PSD. To be coherent with the 1989 samples, the samples were pre-treated by ultrasonic stirring, but not dispersed chemically. A single-sample comparison (Figure 2.7) suggested that the effect of chemical pre-treatment is limited. Therefore, in order to be consistent with the Malvern analyses and the 1989 measurements, and to best approximate the suspended sediment PSD (see section 2.3.1.2), the samples are not chemically pre-treated.

The main differences between the Malvern and the Sedigraph are that:

- The Malvern measures particle volume and area (through light scattering) whereas the Sedigraph measures particle mass (through settling).
- The Sedigraph measures settling velocity, which is subsequently converted to a PSD.
- The Sedigraph samples are dried and sieved to remove particles larger than 38 µm before analysis, the Malvern samples are not.

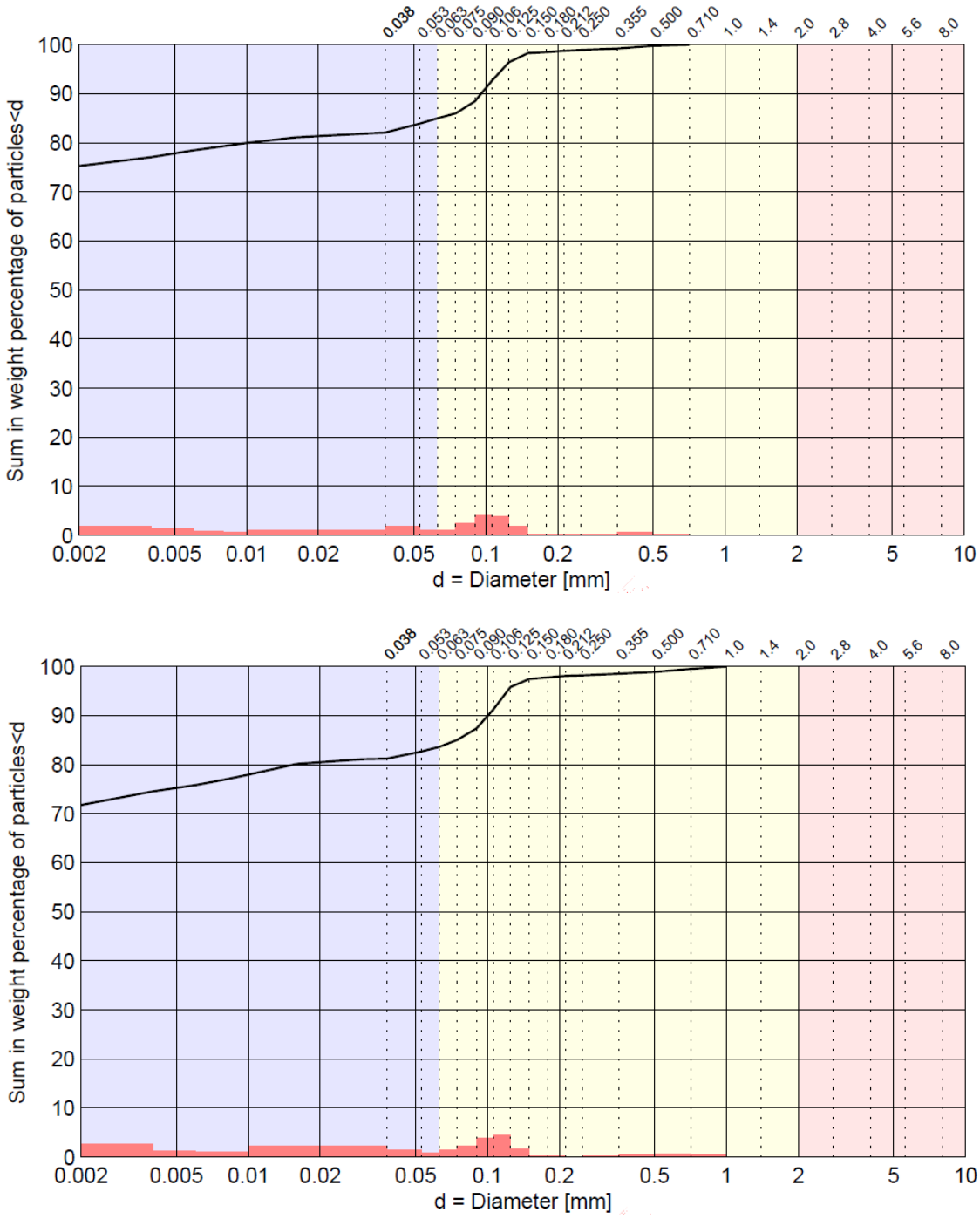

Figure 2.7 Grain size distribution measured with the Sedigraph with (left) and without chemical pre-treatment (right). On the y-axis the cumulative distribution [%] is given, the diameter [mm] is on the logarithmic x-axis.

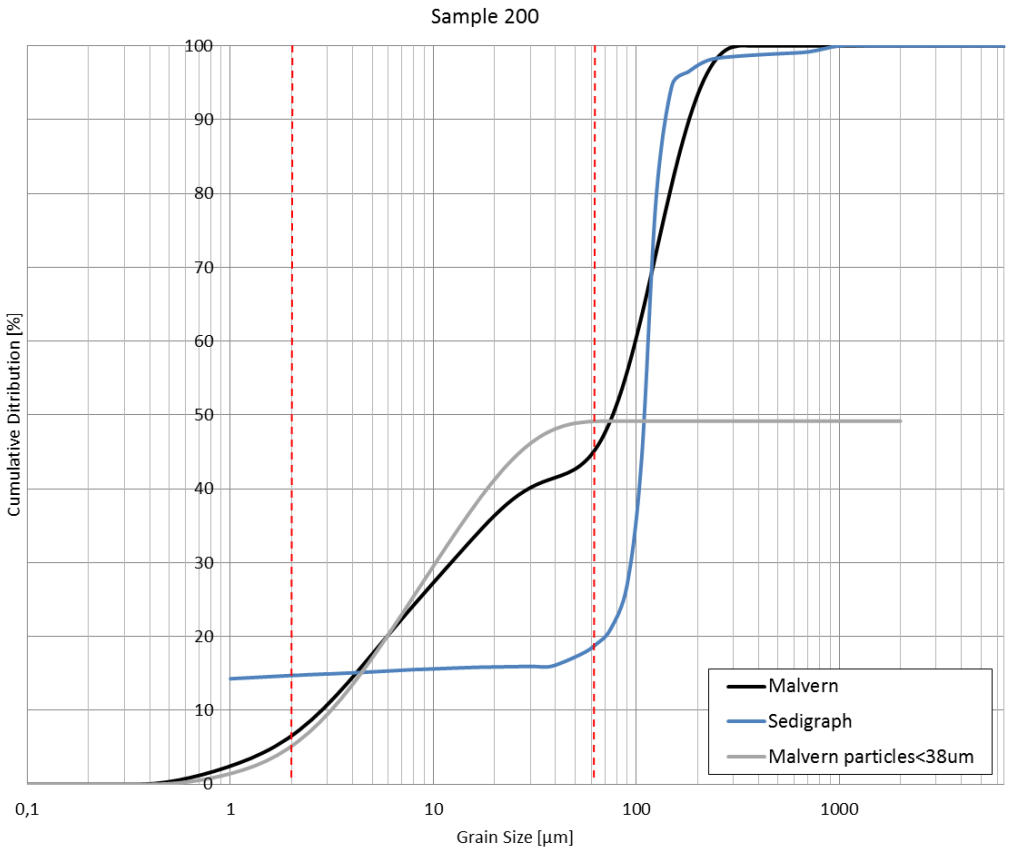

Figure 2.8 Particle size distribution for sample 200 as determined with Malvern (black) and Sedigraph (blue). Particle size distribution of part of sample 200 with d < 63 µm as determined with Malvern (grey).The sedigraph measures only particle sizes larger than 1 µm; the offset of 15% implies that 15% has a grain size below 1 µm

With the particle size distribution, the clay, mud and sand content of the sample is derived, as well as the median particle diameter d_{50}. The clay content is the percentage of material with a diameter equal to or smaller than 2 µm. The silt content is the percentage of material with a diameter larger than 2 µm and equal to or smaller than 63 µm. The remaining material is classified as sand. The median particle diameter d_{50} is determined by the Malvern and is defined as the grain size for which 50% of the material is smaller and 50% of the material is larger.

2.3.2 Atterberg Limits

The measured Atterberg Limits of the samples are the Liquid Limit LL and the Plastic Limit PL. The Liquid Limit LL is determined by making a groove in a sample at different water contents. When the groove becomes closed after a certain number of blows on the sample, the Liquid Limit LL is reached. The limit is expressed as the water content. The Plastic Limit PL is determined by making sausage shaped samples at different water content. When deformed, the samples begin to crumble at the Plastic Limit PL (Winterwerp & van Kesteren, 2004). The Atterberg Limits (the Liquid Limit LL and the Plastic Limit PL), and their relation to clay content, provide a good indication of the soil-mechanical properties.

A key parameter deductible form the Atterberg Limits is the Plasticity Index PI (defined as $PI = LL - PL$). The Plasticity Index PI is a measure for the amount of water bounded within the

sediment. A plasticity chart, the relation between the Liquid Limit LL and Plasticity Index PI, gives an indication of the type of clay mineral.

An activity chart relates the clay content to the Plasticity Index PI. When the mechanical behaviour of the soil is determined by the clays and not by sand, the relation between clay content ζ^{cl} (d < 2 µm) and the Plasticity Index PI is linear. The slope of this relation is a measure for the type of clay mineral, with typical values of 0.4 for illite, 0.9 for kaolinite, and as high as 7 for montmorillonite.

2.3.3 Vane test

The peak shear strength and undrained shear strength c_u can be determined with a vane test. A vane (Figure 2.9) is placed into the soil and rotated with a constant angular velocity. The resistance of the sample is measured by a torque transducer between the rotating vane and motor. The recorded signal (Figure 2.9) is multiplied by the A-factor, which is dependent on the properties of the vane. The peak strength is a function of the rotation speed, stress history and the sample preparation. The undrained or remoulded shear strength c_u is a material property at given water content of the sample (Winterwerp & van Kesteren, 2004) and is defined as the residual stress in the bed after failure of a sample. It gives an indication of the resistance of the sediment bed to erosion.

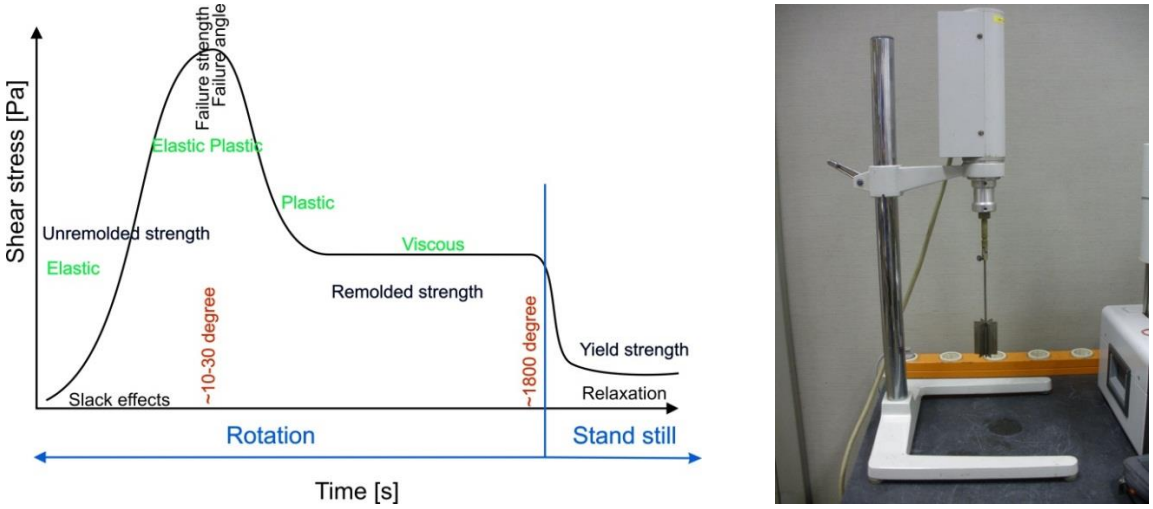

Figure 2.9 Left: example of vane measurement. Right: Vane instrument with vane element FL10. Taken from Cornelisse, 2011.

Unfortunately, due to malfunctioning of the equipment, no reliable results for the Vane test could be obtained for the present samples. The malfunctioning of the device was discovered shortly after the execution of the experiments, but the damage in the equipment was permanent, and therefore repeating the test did not become an option. As an alternative for the Vane test, we use the relationship by Winterwerp et al. (2012), to relate the peak and undrained shear strength c_u to the void ratio. In this way no specific undrained shear strength for the Ems-Dollard is obtained, but an approximation for the undrained shear strength c_u can also be used. This value for the undrained shear strength c_u is then used to compute the erosion parameter M. Based on previous experiments, a linear relationship should exist between the void ratio and the undrained shear strength c_u, see Figure 2.10. This relation yields:

$$c_u = 1000 \cdot \left(\frac{3.5}{e_i} \right)^5$$

With:

c_u undrained shear strength [Pa]

e_i void ratio [-]

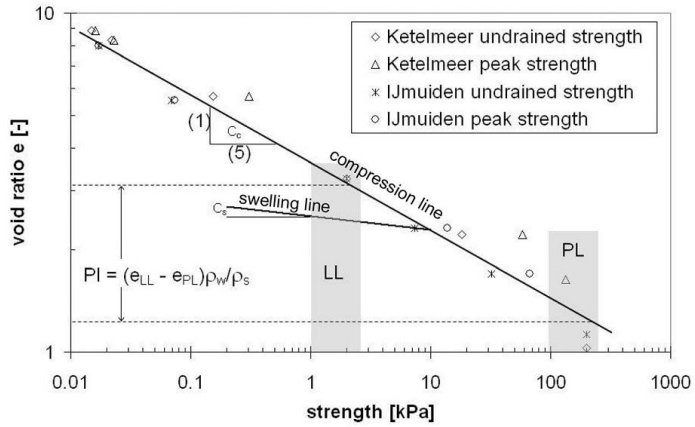

Figure 2.10 Relation between void ratio and undrained and peak strength. Taken from Winterwerp et al. (2012).

2.3.4 Zeta Potential

The ζ-potential reflects the charge of a particle at its shear plane, giving an estimate for flocculation activities of the suspended sediments. The ζ-potential influences the likelihood that a particle will aggregate with other particles or not. It is a function of pH, anion or cation concentration and absorbed surfactants. The sensitivity of the ζ-potential to these ambient conditions is influenced by clay mineral activity (Winterwerp & van Kesteren, 2004). The ζ-potential is measured with the Malvern Zeta Nano Sizer.

The ζ-potential of a mud or silt particle indicates its sensitivity to flocculation. It is a measure for the balance between repulsive and attractive forces acting on the clay particles. A high ζ-potential (larger than 30 mV in absolute value) means that repulsion is larger than attraction, therefore a stable suspension with little flocculation activity. When the ζ-potential is low (smaller than 30 mV in absolute value), the repulsive forces are weak and the suspension instable. As a result particles may easily flocculate and settle due to increased settling velocity resulting from the larger size of flocs. The ζ-potential depends on the pH and the salt concentration, and therefore these 2 parameters (in addition to the effect of the clay mineral itself) influence the capacity of the clay minerals to coagulate and form flocs (schematized in Figure 2.11).

The procedure for measuring the ζ-potential is as follows. A suspension of with a 1% volumetric sediment concentration was created by adding the sample to demi water. The natural pH of the sediments is lowered for some samples by adding a solution of HCl. This solution is inserted with a syringe into a cell which is placed in the Malvern Zeta Nano Sizer. The resulting measurements can be compared to standard measurements of ζ-potential of pure minerals as a function of pH to establish a classification.

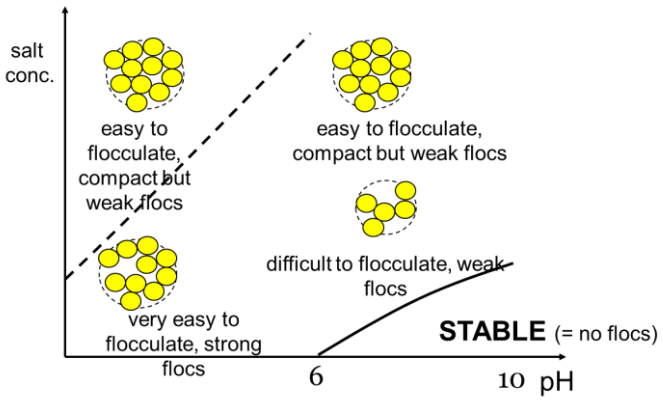

Figure 2.11 Conceptual floc-stability diagram (Chassagne, 2012, personal communication).

2.3.5 CST test

With a CST meter the Capillary Suction Time (CST) of a sample is measured. It is a measure for the permeability of the sample at certain void ratio (or water content). A sample is put into a cylindrical ring, which is located on top of a filter paper (Figure 2.12). Water is sucked into the paper and spreading out in a circle. At a distance from the sample, two electrodes are placed at a fixed distance. The time it takes for the waterfront to 'flow' from the first to the second electrode is dependent on the permeability of the sample and is the CST. The CST can be determined at different void ratios for the same sample. The void ratio needs to be decreased by pre-consolidation of the sample. The relation between the void ratio and the CST for each sample can be used to determine the Gibson coefficient (Huisman & van Kesteren, 1998). When the void ratio is plotted against 1/√CST, a linear relation is obtained. The slope of this line determines the Gibson coefficient. The equation relating the void ratio to the CST and Gibson coefficient is given by:

$$e = e_{CST}^{\infty} + \frac{L\sqrt{\pi}}{2\sqrt{C_{gib}}}\frac{1}{\sqrt{CST}}$$

With:

e	void ratio [-]
e_{CST}^{∞}	void ratio with infinite capillary suction time [-]
L	characteristic length [m], dependent on CST device and filter paper
C_{gib}	Gibson coefficient [m^2/s]
CST	capillary suction time [s]

The intercept with the vertical axis (e_{CST}^{∞}) is the void ratio for which the CST approaches infinity and is not used in the analysis because we are only interested in the Gibson coefficient. The Gibson coefficient is determined with:

$$C_{gib} = \left(\frac{L\sqrt{\pi}}{2 \cdot slope}\right)^2$$

With:

C_{gib}	Gibson coefficient [m^2/s]
L	characteristic length [m], dependent on CST device and filter paper
$slope$	slope of the 'void ratio against 1/√CST'-line [$s^{0.5}$]

The parameter L is dependent on the properties of the CST device and the properties of the filter paper. In Huisman & van Kesteren (1998), a value of $1.3*10^{-3}$ m is suggested for a CST with the dimensions used in our analysis. This value is used to compute the C_{gib} in §3.6.

The Gibson coefficient C_{gib}, or consolidation coefficient, is important to determine erosion rates E. The coefficient is similar to the consolidation coefficient c_v which follows from the settling column tests (see section 3.7), and provides evidence meant for comparison of the results. The consolidation parameter c_v is used to compute the erosion parameter M.

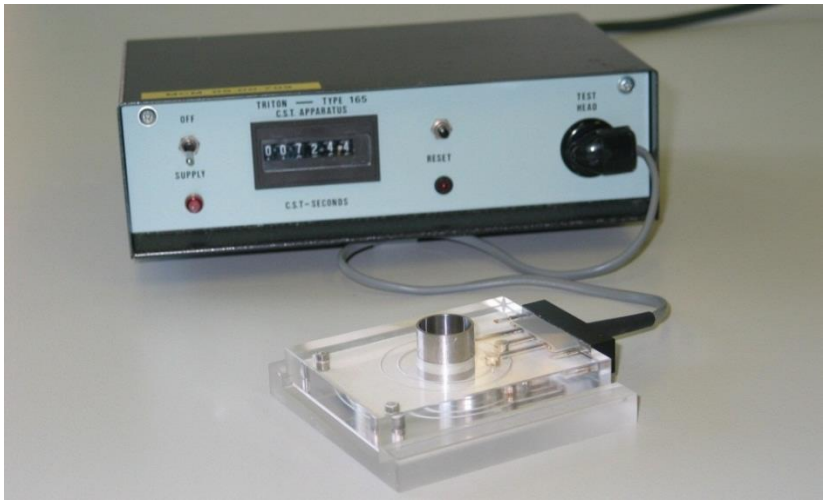

Figure 2.12 The CST device

2.3.6 Settling column / Consolidation test

Standard consolidation experiments were performed with the settling columns, aiming at determining settling and consolidation parameters. These experiments are based on the work of Dankers (2007), Merckelbach and Kranenburg (2004), and Merckelbach (2000). Essentially, the experiments consist in letting settle and consolidate a high-concentrated mud suspension in standard consolidation columns. By simply following the settling interface, settling-consolidation curves are obtained, from which the following parameters can be derived:

- Settling velocity w_s and gelling concentration c_{gel} (Dankers and Winterwerp, 2007).
- Permeability K_k and fractal dimension D (Merckelbach & Kranenburg, 2004; Merckelbach, 2000; Winterwerp & van Kesteren, 2004).
- Effective stress coefficient K_p, only when final bed level height is achieved (Merckelbach and Kranenburg, 2004; Merckelbach, 2000).
- Consolidation coefficient, c_v, derived from a.o. K_k, D and K_p (see later).

The consolidation coefficient c_v is used to determine the erosion parameter M, which is used in the numerical model. Also the settling velocity is used to calibrate the numerical model.

The settling column is a cylindrical column with a height of 1 m and a diameter of 12.2 cm. Sub-samples are taken from the collected samples and diluted with synthetic saline water. The saline water is prepared by adding $NaCl$ to tap water until obtaining the proper salinity. The tests are done at different concentrations, i.e. 10 g/l, 30 g/l and 60 g/l (2 samples only). At the beginning of the experiment, the sediment-water mixture is gently stirred (to prevent breaking of the flocs) to get a uniform distribution over the settling column. Over time, the

sediments settle in the column and an interface between the water-sediment mixture and the clear water above becomes visible. In the meantime, a bed starts to form at the bottom of the column. This situation is referred to as the hindered settling phase. After a while, the interface between clear water and the water-sediment mixture merges with the bed and phase I starts. From here on, the bed starts to consolidate. A camera is used to take pictures of the column(s) at an increasing time interval, to be able to determine the position of the interface over time.

Figure 2.13 One of the pictures taken during the settling column experiment.

In the first phase of settling, before a consolidating bed is formed, sediments settle in the hindered settling regime. During this phase, the settling velocity and gelling concentration can be computed from the observations. When a consolidating bed is formed, the sediment / water interface coincides with the bed / water interface. Analysis of this interface allows the determination of consolidation parameters.

2.3.6.1 Hindered settling and gelling concentration

Consolidation of mud is preceded by a settling phase, sometimes in a hindered settling regime. Hindered settling of mud is caused by the influence of neighbouring particles on an individual particle within a suspension, which hinder (or decrease) the settling velocity. The larger the mud concentration in the suspension, the smaller the settling velocity. The end of hindered settling phase is characterized by the gelling concentration c_{gel} at which a space filling network develops, meaning that all particles are in contact with each other leaving no possibility for further settling. Consolidation starts immediately after this gelling concentration is achieved. The effective settling velocity w_{eff} can be calculated following the water / settling particles interface during the hindered settling regime. Figure 2.14 shows the evolution of the settling interface over the hindered settling regime from one of the conducted experiments. A linear relation between the height of the interface and the elapsed time can be found.

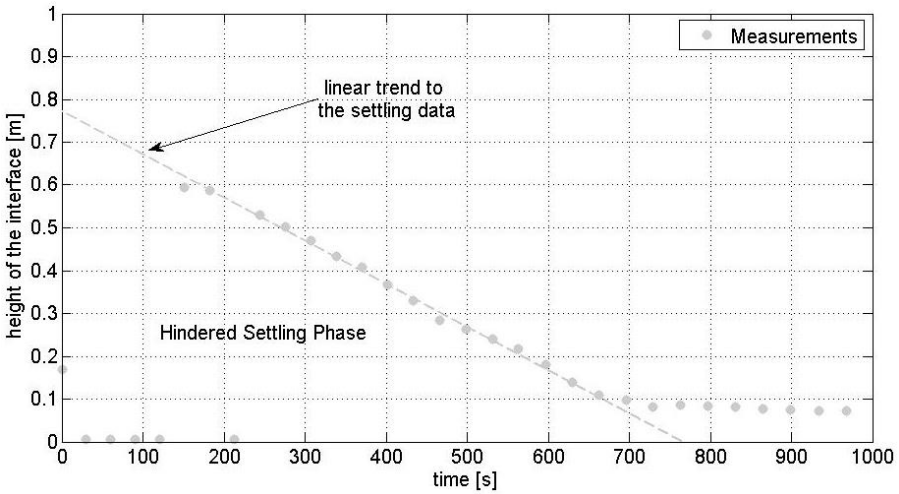

Figure 2.14 Evolution of settling interface during the hindered settling regime

Once the effective settling velocity w_{eff} is determined, the settling velocity of individual aggregates $w_{s,0}$ and the gelling concentration c_{gel} can be calculated. Dankers (2007) establishes a relationship between effective settling velocity w_{eff} and volumetric concentration of flocs ϕ:

$$w_{eff} = w_{s,0} \frac{(1-\phi)^m (1-\phi_p)}{1+2.5\phi}$$

With:

w_{eff}	effective settling velocity [m/s]
$w_{s,0}$	settling velocity of individual aggregates [m/s]
ϕ	volumetric concentration of flocs [-]
m	empirical parameter that accounts for effects of non-linearity, Dankers (2007) recommends a value of 2.
ϕ_p	volumetric concentration of the primary particles

The volumetric concentration of flocs ϕ and the volumetric concentration of the primary particles ϕ_p can be computed with:

$$\phi = \frac{c}{c_{gel}}$$

With:

ϕ	volumetric concentration of flocs [-]
c	mass concentration of mud [kg/m^3]
c_{gel}	gelling concentration [kg/m^3], obtained by fitting the experimental data

$$\phi_p = \frac{c}{\rho_s}$$

With:

ϕ_p	volumetric concentration of the primary particles [-]
c	mass concentration of mud [kg/m^3]
ρ_s	density of solids [kg/m^3], assumed to be 2650 kg/m^3 in this study

The mass concentration c at the settling interface is the initial mass concentration of mud (Dankers and Winterwerp, 2007), where the effective settling velocity w_{eff} of the settling interface is measured.

2.3.6.2 Phase I

When the gelling concentration c_{gel} is reached, the initial phase of consolidation starts (Phase I). This phase is governed by the permeability of the soil. From studying the variation of the mud-water interface as a function of time in Phase I, the fractal dimension n and permeability parameter K_k can be obtained (Merckelbach, 2000). The procedure is to plot the mud-water interface versus time on double logarithmic scales. For these curves, the fractal dimension n and the permeability parameter K_k can be obtained by fitting (Merckelbach and Kranenburg, 2004; Winterwerp and van Kesteren, 2004):

$$h(t) = \left(\frac{2-n}{1-n} \zeta_m \right)^{\frac{1-n}{2-n}} \left((n-2) K_k \frac{\rho_s - \rho_w}{\rho_w} \right)^{\frac{1}{2-n}} t^{\frac{1}{2-n}} + \zeta_s$$

With:

$h(t)$	height of the interface [m]
ζ_s	Gibson height for sand [m]
n	fractal dimension [-]
ζ_m	Gibson height for mud [m]
K_k	permeability coefficient [m/s]
ρ_s	density of solids [kg/m^3]
ρ_w	density of water [kg/m^3]
t	time [s]

2.3.6.3 Phase II

After Phase I is completed, the final phase of consolidation (Phase II) starts, where deformations are very small and effective stresses dominates the consolidation process. By measuring the final consolidation height at the end of Phase II, the effective stress coefficient K_p is determined (Merckelbach & Kranenburg, 2004).

$$h_\infty = \frac{n}{n-1} \frac{K_p}{g(\rho_s - \rho_w)} \left(\frac{g(\rho_s - \rho_w)}{K_p} \zeta_m \right)^{\frac{n-1}{n}}$$

With:

h_∞	final height of the bed [m]
n	fractal dimension [-]
K_p	effective stress coefficient [Pa]
g	gravitational acceleration [m/s^2]
ζ_m	Gibson height for mud [m]
ρ_s	density of solids [kg/m^3]
ρ_w	density of water [kg/m^3]
t	time [s]

Finally, the consolidation parameter c_v can be calculated from:

$$c_v = \frac{K_k K_p D}{g \rho_w}$$

With:

$$D = \frac{2}{3-n}$$

n	fractal dimension [-]
K_k	permeability coefficient [m/s]
K_p	effective stress coefficient [Pa]
g	gravitational acceleration [m/s^2]
ρ_w	density of water [kg/m^3]

Figure 2.15 shows the height of the interface over time for phase I and phase II, for one of the consolidation experiments. The solid blue line is obtained by fitting the equation from Winterwerp and van Kesteren (2004), which accounts for the sand content, whereas the dotted blue line is obtained by fitting the original equation from Merckelbach (2000). In this report, only the parameters obtained with the solid blue line are considered. Where the measurements start to deviate from the blue line, the transition from Phase I to Phase II is found. The final height of the bed is plotted with the black line.

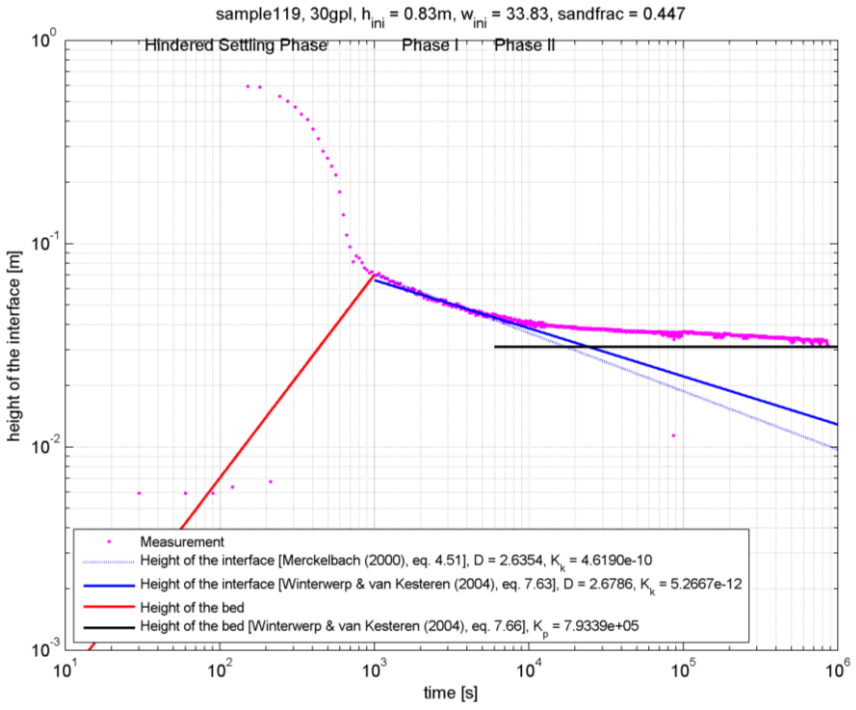

Figure 2.15 Example of a consolidation test, showing the measured height of the interface (pink dots) in time for sample 119 at 30 g/l plotted on double-logarithmic axes. See text for details.

2.3.7 Erosion parameters

Erosion and deposition of sediment determine morphological changes. For cohesive sediment, erosion of sediment is determined by the product of the erosion parameter M and the dimensionless excess bed shear stress. Deposition is governed by the sediment

concentration C and the settling velocity w_s. The resulting formulas for erosion and deposition, used in Delft3D, are:

$$E = M\left(\frac{\tau - \tau_{cr}}{\tau_{cr}}\right)^n$$

$$D = w_s C$$

With:

E	erosion [kg/m^2/s]
M	erosion parameter [kg/m^2/s]
τ	bed shear stress [Pa]
τ_{cr}	critical shear stress for erosion [Pa]
D	deposition [kg/m^2/s]
w_s	settling velocity [m/s]
C	sediment concentration [kg/m^3]
n	user defined power, generally between 1 and 1.5. (in the WED model, n = 1 for layer S1 and n = 1.5 for layer S2 – see report 5)

Three of the parameters are user-defined, being the settling velocity w_s (§2.3.6), the critical shear stress for erosion τ_{cr}, and the erosion parameter M.

The critical shear stress for erosion τ_{cr} is determined by sediment properties such as clay mineralogy, composition (sand/mud) and water content. Since the water bonding capacity of a mud is coupled to the water content, the Plasticity Index PI provides an indication of the critical shear stress for erosion τ_{cr}. Winterwerp et al. (2012) relate a range of Plasticity Indexes PI to critical shear stresses for erosion τ_{cr}, based on observations (Figure 2.16). This relation differs for cohesive sediment (PI > 7%) and low-cohesive sediment (PI < 7%). For PI > 7%, the critical shear stress for erosion τ_{cr} can be approximated with:

$$\tau_{cr} = \gamma_{cr} PI^{\beta} \qquad \text{(a)}$$

With:

τ_{cr}	critical shear stress for erosion [Pa]
γ_{cr}	empirical parameter [-]
β	empirical parameter [-]

For mud (PI > 7%) dominated by illite or kaolinite, the values for γ_{cr} and β are typically 0.7 (±factor 2) and 0.2, respectively.

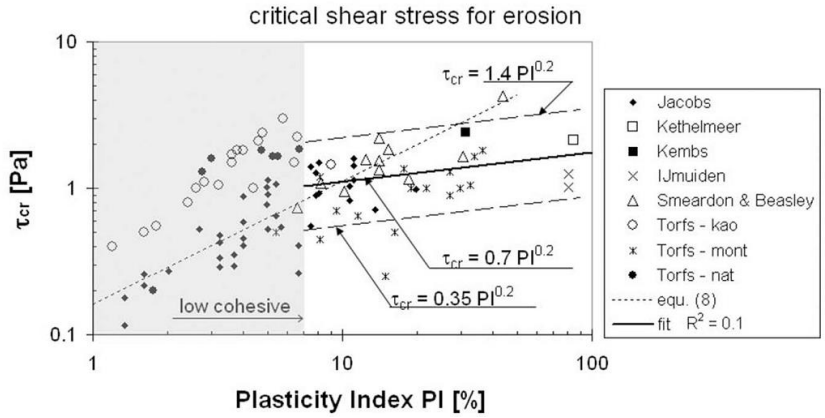

Figure 2.16 Relation between the Plasticity Index PI and the critical shear stress for erosion τ_{cr}, from Winterwerp et al. (2012).

The erosion parameter M can be derived from the measurements, using variables computed in different experiments. To compute this erosion parameter M, the approach by Winterwerp et al. (2012) is used. They use a slightly different formula for *E* compared to Delft3D, with Winterwerp's formulation given by:

$$E = M_E \left(\tau - \tau_{cr} \right)$$

With:

E	erosion [kg/m^2/s]
M_E	erosion parameter [s/m]
τ	bed shear stress [Pa]
τ_{cr}	critical shear stress for erosion [Pa]

To convert this parameter M_E to the parameter M used in Delft3D, the following conversion is applied:

$$M = M_E \tau_{cr}$$

With:

M	erosion parameter [kg/m^2/s]
M_E	erosion parameter [s/m]
τ_{cr}	critical shear stress for erosion [Pa]

A parameterisation for M_E can be derived by applying soil mechanical theories. Herein the erosion velocity of the bed is limited by the velocity V_s [m/s] at which the sediment bed can swell to a structure at which particles can be eroded. This velocity can be described with existing soil mechanical theories, and is determined by the consolidation coefficient c_v and the swelling depth δ_s. The consolidation coefficient has been determined through consolidation tests (§2.3.6) whereas the swelling depth relates to the median grain size d_{50}, the dry density ρ_{dry}, the mass concentration ϕ_s and the undrained shear strength c_u. An equation relating these parameters to an expression for the erosion parameter M_E has been established by Winterwerp and van Kesteren (2004):

$$M_E = \frac{c_v \phi_s \rho_{dry}}{10 d_{50} c_u}$$

With:

M_E	erosion parameter [s/m]
c_v	consolidation coefficient [m^2/s]
ϕ_s	mass concentration [-]
ρ_{dry}	dry density [kg/m^3]
d_{50}	median grain size [m]
c_u	undrained shear strength [Pa]

The mass concentration is defined as:

$$\phi_s = \frac{M_{s,dry} / \rho_s}{\frac{M_w}{\rho_w} + \frac{M_{s,dry}}{\rho_s}} = \frac{\rho_{dry}}{\rho_s}$$

With:

ρ_{dry}	dry density [kg/m^3]
ρ_s	density of solids [kg/m^3]

Where ρ_{dry} is determined from the bulk measurements (§2.3.1). A comparison of this equation to observed values for M_E is provided in Figure 2.17.

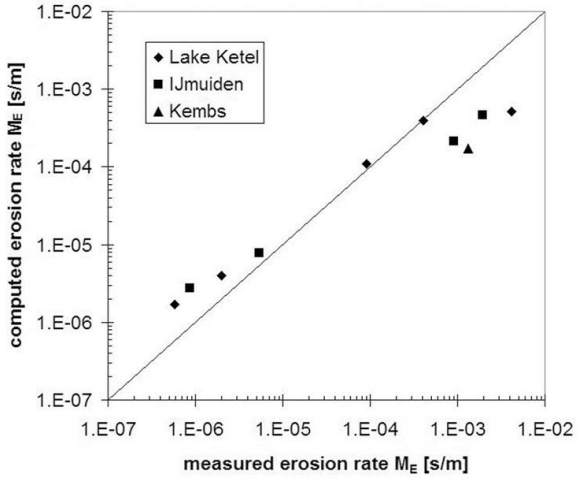

Figure 2.17 Measured and observed values for M_E. Taken from Winterwerp et al. (2012).

3 Results

3.1 Water content, dry density and organic content

The spatial distribution of the water content W is given in Figure 3.1. In muddy areas (the Dollard Bay, the Ems River) the water content W is typically larger than in sandy areas.

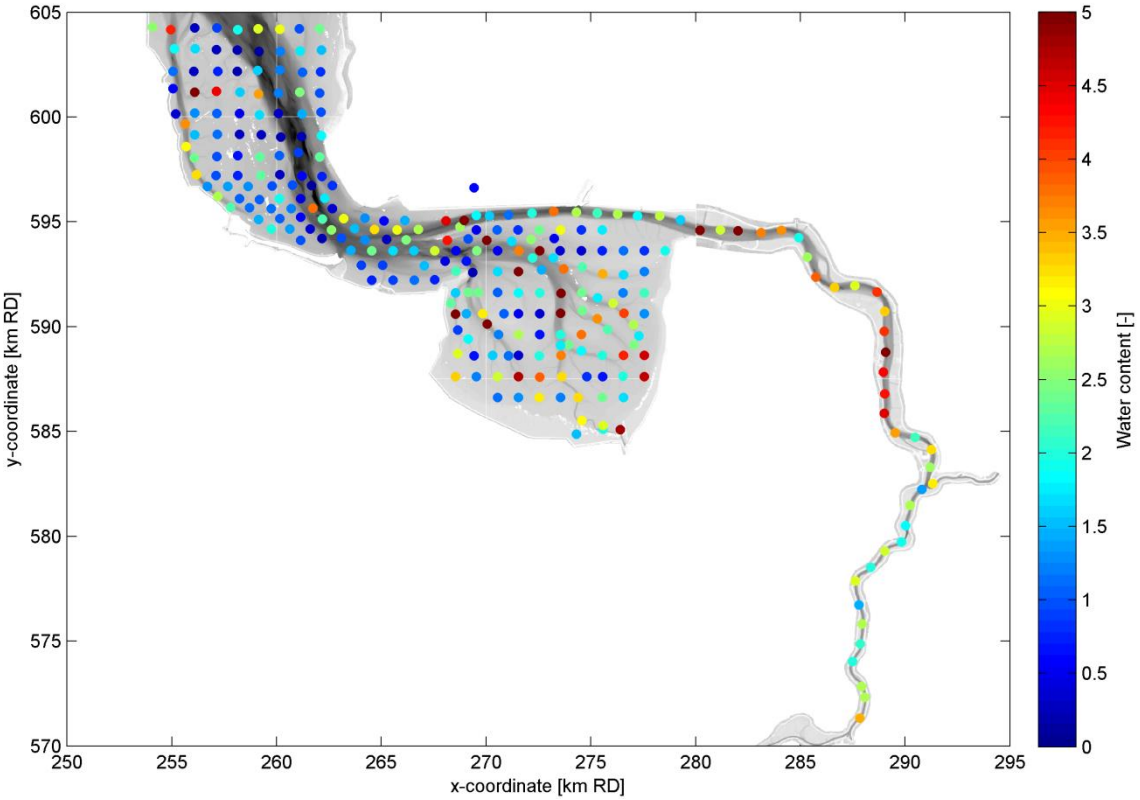

Figure 3.1 Water content W

The dry density ρ_{dry} is strongly related to the water content, and is shown in Figure 3.2. Sandier sediment (with a lower water content) has a higher density. Although it is based on the same measurement as the water content, the dry density ρ_{dry} more clearly distinguishes the sediments of the Friesche Gaatje, in which the dry density ρ_{dry} is larger. Typical values for the dry density of mixed tidal flats in the Wadden Sea is 400 kg/m^3 (Delwig et al., 2000); the density in the Dollard is lower. This is mainly because of the relatively large mud content in the Dollard flats (see section 3.2.3). The mud content of the samples collected in the lower Ems River is below 200 kg/m^3, in agreement with Papenmeijer et al., 2013.

The organic content is given in Figure 3.3. The organic content tends to increase towards fresh water sources (the Ems River, Nieuwe Statenzijl), but this pattern is not very clear. There appears to be a relation between the water content and the organic content with depth, with slightly larger organic and water content in shallow water (Figure 3.4).

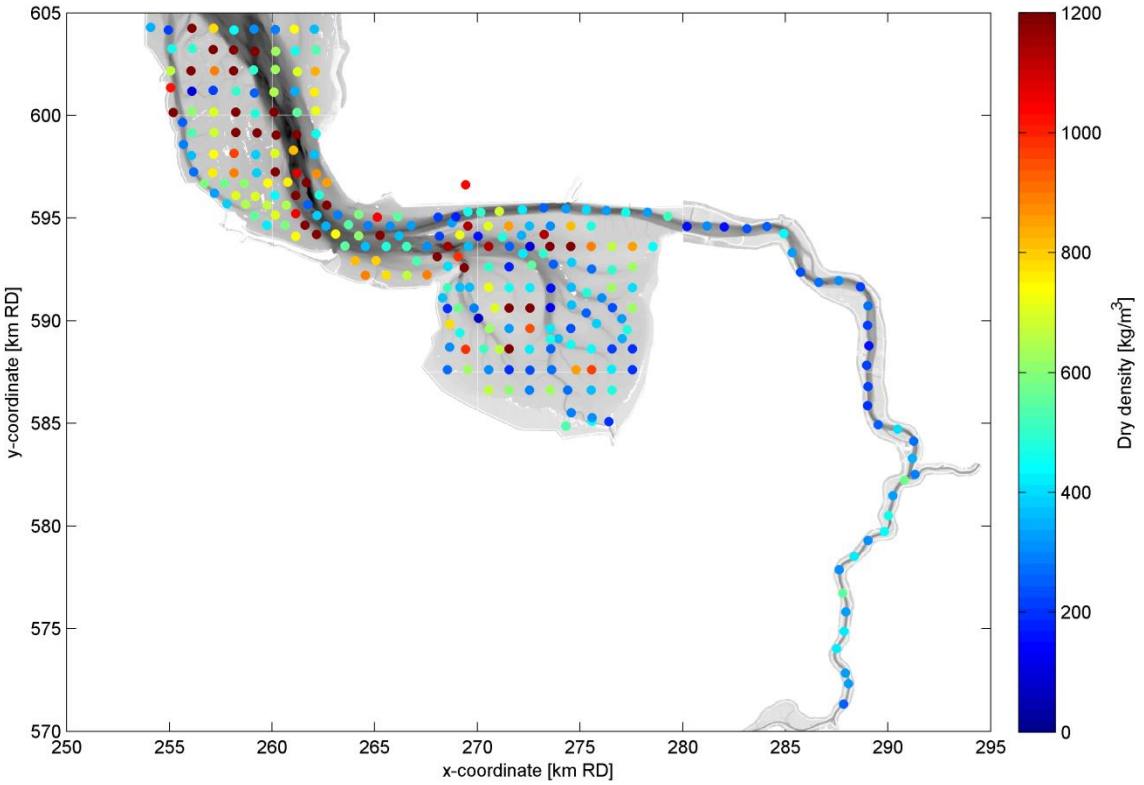

Figure 3.2 Dry density ρ_{dry}

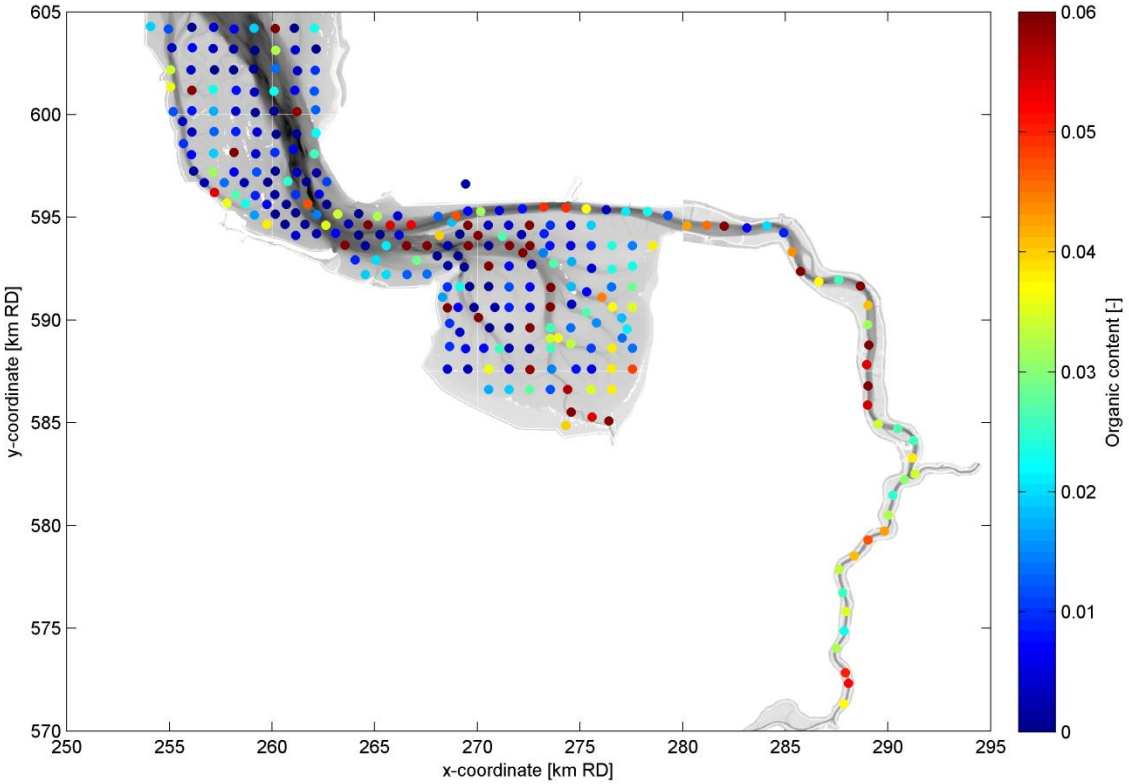

Figure 3.3 Organic content

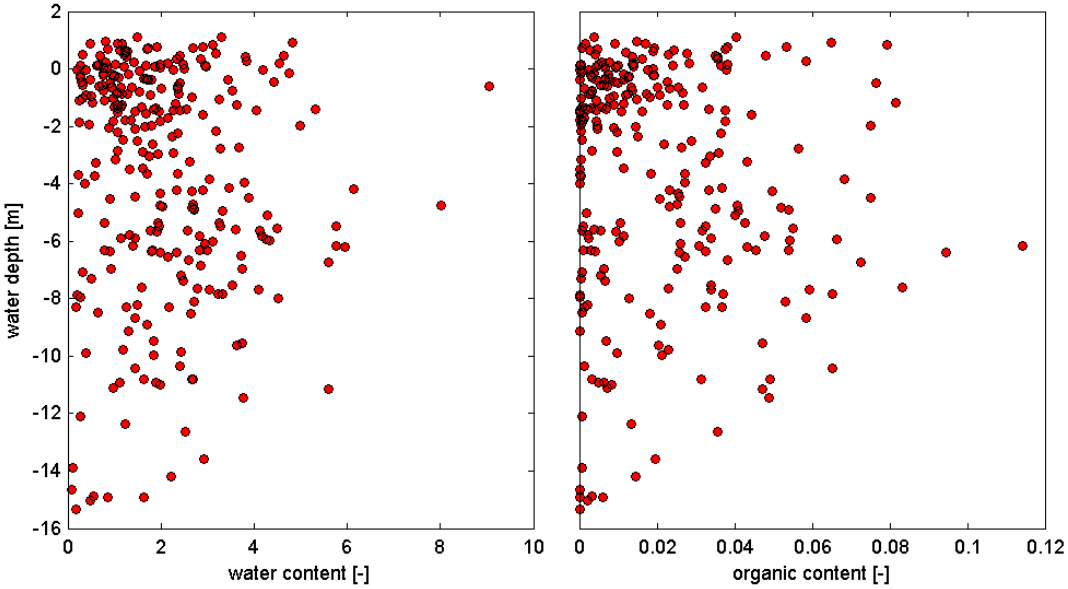

Figure 3.4 Variation of water content and organic content over the water depth.

3.2 Particle size distribution

3.2.1 Influence of the measuring method

The particle size distribution has been determined with the Malvern (all samples) and the Sedigraph (selection, see appendix B). These instruments give different results, especially for the finer fractions. An example of a particle size distribution determined with the Malvern and the Sedigraph is shown in Figure 3.5.

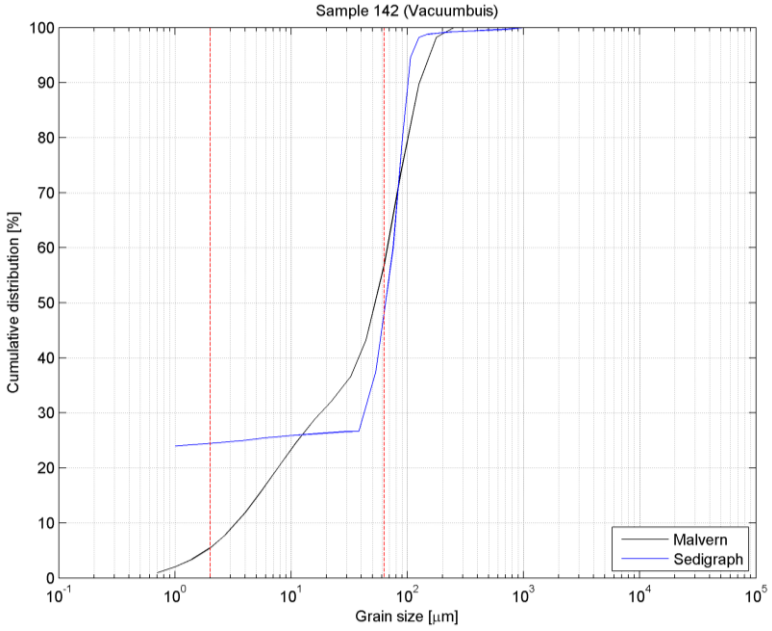

Figure 3.5 Particle size distribution for sample 142 as determined with Malvern (black) and Sedigraph (blue). Red lines indicate clay (d < 2 µm) and mud (d < 63 µm) limit.

A number of differences can be observed in Figure 3.5. The most striking difference is in the silt and clay range. The Sedigraph classifies almost all of the material inserted into the instrument (part of the sample with d < 38 µm) as clay; 27% of the total sample has a grain size less than 38 µm, and this consists for >90% of clay. The clay content measured with the Malvern, however, never exceeds ~12% (for all samples), see the left panel of Figure 3.7. For some of the samples, the difference for the coarser particles is also larger. This is visualised in the right panel of Figure 3.7. The Malvern overestimates the mud content (d < 63 µm) compared to the Sedigraph, and the overestimation is larger when the mud content is lower. The Sedigraph shows low silt content, see Figure 3.6, especially when compared to the clay content. This seems unrealistic.

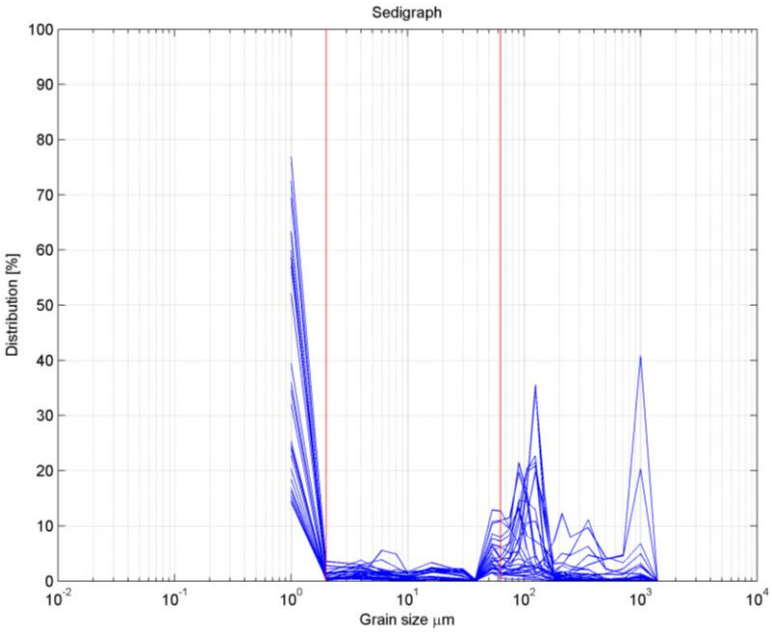

Figure 3.6 Particle Size Distribution determined with Sedigraph. Red lines indicate the silt range.

From literature is also known that the PSD is dependent on the measuring device. There are several instruments which use laser diffraction to measure the size of particles (e.g. Malvern Laser Sizer, Coulter LS). By measuring the intensity of light scattered as a laser beam passes through a dispersed particulate sample, the size of the particles that created the scattering pattern can be calculated. The conversion of the scattered pattern to a particle size distribution is influenced by the particle mineralogy (optical properties) and shape over the grain-size classes (spherical or plate-like) and the procedure used for the inversion. Plate-shaped particles have an average optical diameter which is larger than their equivalent spherical diameter. It is commonly known that using laser diffraction, the clay content (d < 2 µm) of a sample is underestimated (Beuselinck et al., 1998; Konert & Vandenberghe, 1997; McCave et al., 2006; Vdovic et al., 2010). In Zwarts (2004) a comparison between the mud content determined with the ‘afslibmethode’ (based on settling velocity) and the Malvern has been made for the 1989/1991 samples in the Ems-Dollard estuary and the Wadden Sea. The mud content in Zwarts (2004) is defined as the fraction smaller than 16 µm. In this case the mud content determined with the Malvern was ~3 times higher than the mud content determined with the ‘afslibmethode’. This underlines the difference between the analysis methods.

Hence, both the Malvern and the Sedigraph have their shortcomings. The Malvern is likely to shift some of the finer fraction (clay and fine silt) to the larger fraction (coarser silt and maybe

even sand). The Sedigraph overestimates the clay content and underestimates the silt content (see section 2.3.1.3). However, the mud content (clay plus silt; d < 63 µm) of the Malvern and the Sedigraph have a better correlation (R^2 = 0.55), as confirmed by the right panel of Figure 3.7. There is a clear correlation, although a substantial amount of scatter remains.

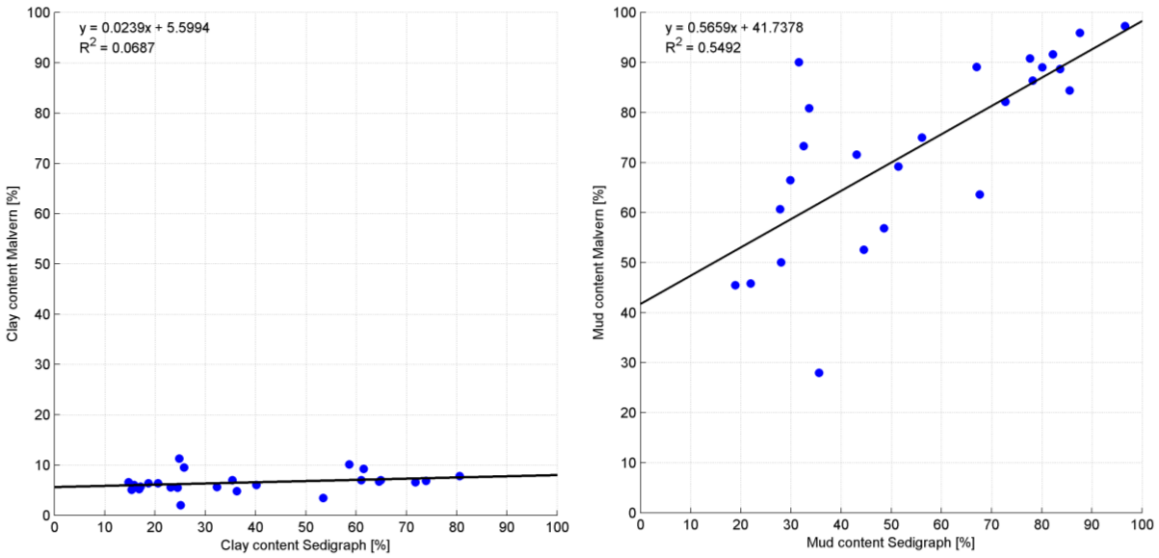

Figure 3.7 Correlation clay content (left) and mud content (right) measured with Malvern and Sedigraph

The clay content, however, is crucial for a number of analyses. In section 3.3 it is argued that the clay content (d < 2 µm) determined by the Malvern is theoretically not correct. Therefore, in order to better understand which methodology is more accurate, the measured grain size distribution is compared with additional soil mechanical analysis performed in sections 3.3 and 3.5.

3.2.2 Influence of sampling method

Differences in particle size distribution between 1989 and 2013 can be due to different sampling instrument, but also because of the exact position. It is likely that the sediment type actually sampled in 2013 is different compared to 2013, because of

- resulting from small-scale variations in sediment type (bedforms),
- morphological changes (channel migration)
- the offset of 130 m in the location of 2013 compared to 1989

However, it is not expected that the offset of 130 significantly influences the comparison, because:

- Except for the sharp transitions in-between channels and shoals, a difference in 130 m will not lead to large differences. But especially near the channels, using the exact same locations would also have introduced uncertainties because the tidal channels themselves migrate. A location which used to be a tidal channel may have shifted to flat, or vice versa.
- The small-scale (several m) variation in sediment distribution is, in environments such as the Ems Estuary, considerable, largely because of bed forms. The variation over 1 m may be as large as over 130 m, introducing an uncertainty which will not or marginally increase because of the 130 m difference.
- The uncertainty in positioning in 1989 was much larger than 2013.

The influence of the sampling instrument (van Veen grab versus Box corer/Vacuum tube) on the sand, silt and mud content is shown in Figure 3.8. The colours in Figure 3.8 indicate the number of the sample, a pair with the same colour means that the sample has been collected on the same location. The symbol indicates the sampling instrument. Since it is difficult to visualise the difference in clay, silt and mud content in one graph (as in Figure 3.8), a 1:1 comparison of the mud content is given in Figure 3.9.

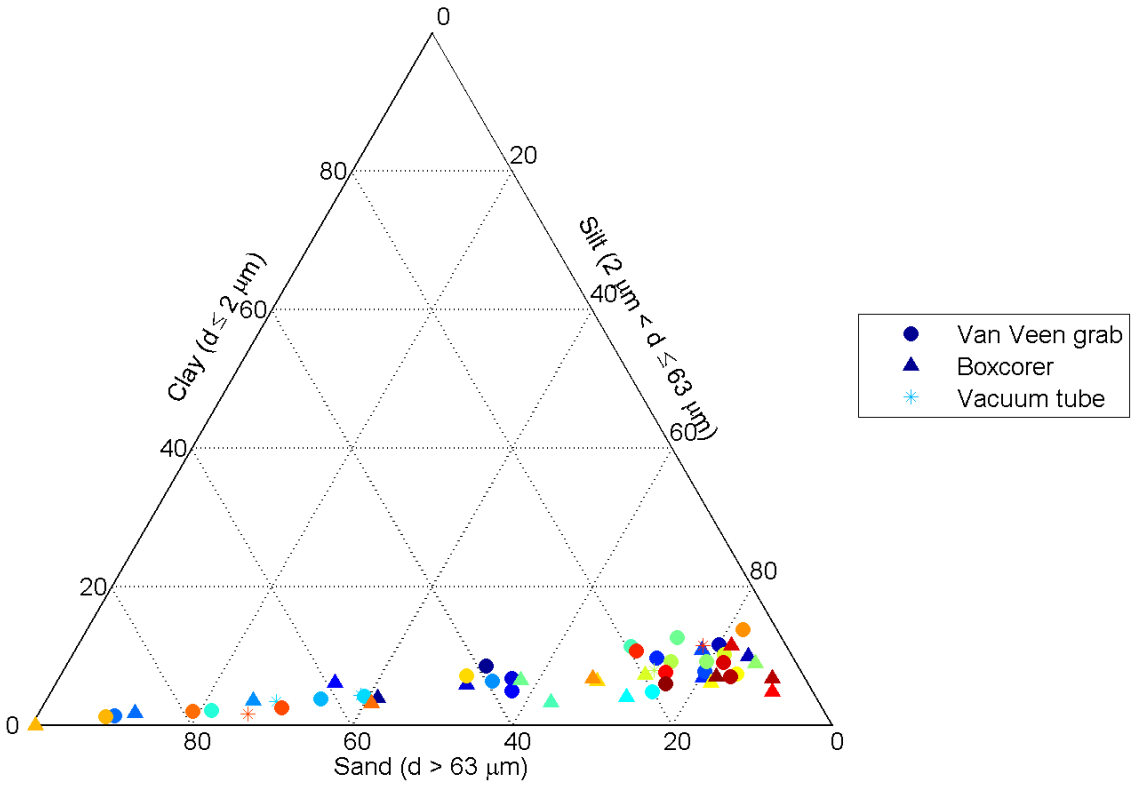

Figure 3.8 Influence of sampling instrument on clay, silt and sand content. Same colour indicates same sample number/location. Type of sampling instrument is indicated by symbol, van Veen grab (o), Box corer (Δ) and vacuum tube (*). Results from measurements in the Malvern.

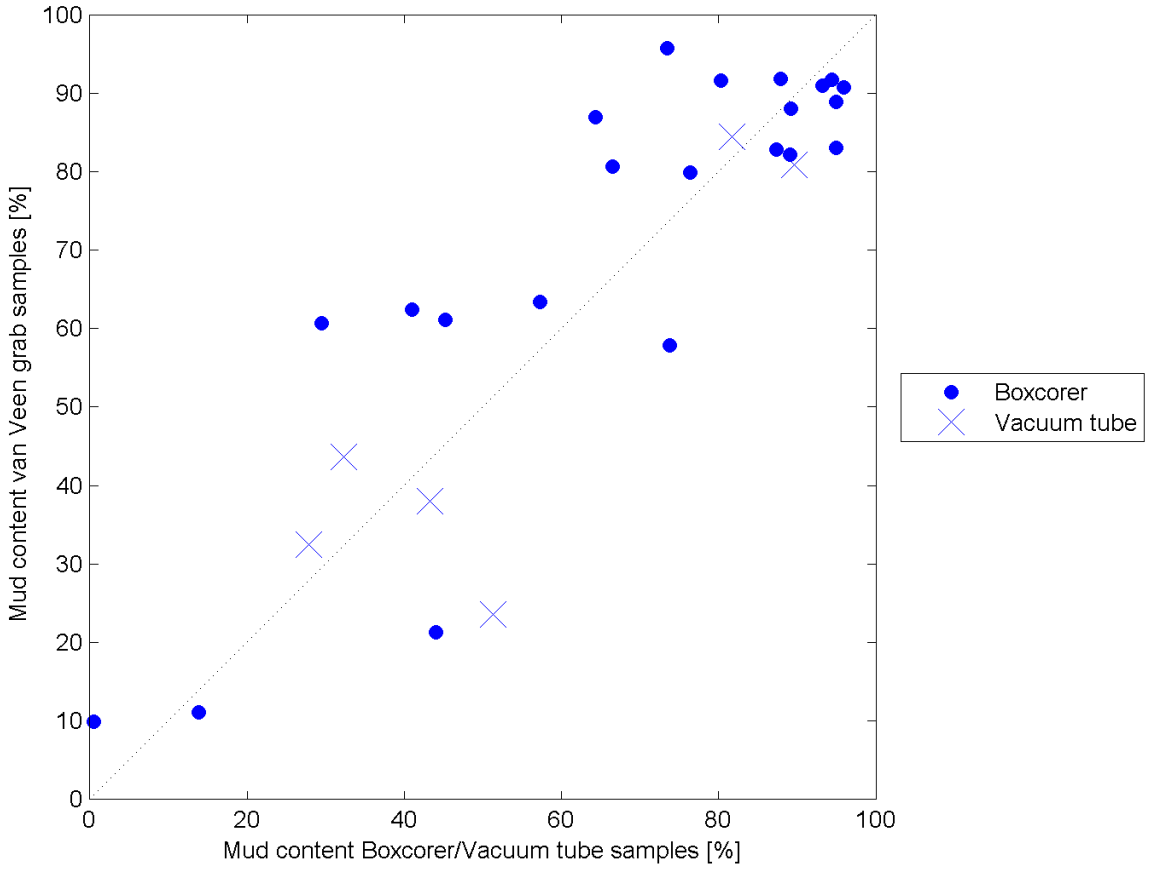

Figure 3.9 Mud content from sample taken by van Veen grab (vertical axis) plotted against mud content of same sample taken with a Box corer (o) or Vacuum tube (x), (horizontal axis).Results from measurements in the Malvern.

From a comparison between the particle size distributions of the samples collected by a Box corer or vacuum tube and a van Veen grab no clear trends are visible. Some distributions compare well, others are quite different. The difference does not point at a consistent over- or underestimation by the Box corer or the van Veen grab, nor at an over- or underestimation of coarse or fine fractions. This is confirmed by Figure 3.9, where the mud contents of the samples collected with the van Veen grab are plotted against samples taken by the Box corer or Vacuum tube.

Any impact of methodology will probably introduce a systematic difference. The observation that there is a random difference may be largely the result of not sampling on the exact same location. It is therefore concluded that the sampling methodology does not introduce a systematic difference, and that the 1989 van Veen samples can be compared with the 2013 boxcore measurements.

3.2.3 Mud content in the Ems estuary

The mud content of the samples is defined as the percentage of material with a grain size smaller than 63 µm. Figure 3.10 shows the mud content as measured in 2013 with the Malvern. The observed mud content is relatively high in

- The tidal flats of the Dollard(typical mud content is >70%)

- The main channel of the Dollard (the Groote Gat, see Figure 1.1 for location). This difference is most pronounced when comparing the mud content in the Groote Gat with the Heeringsplaat located southwest of the Groote Gat
- The lower Ems River and the Emden navigation channel

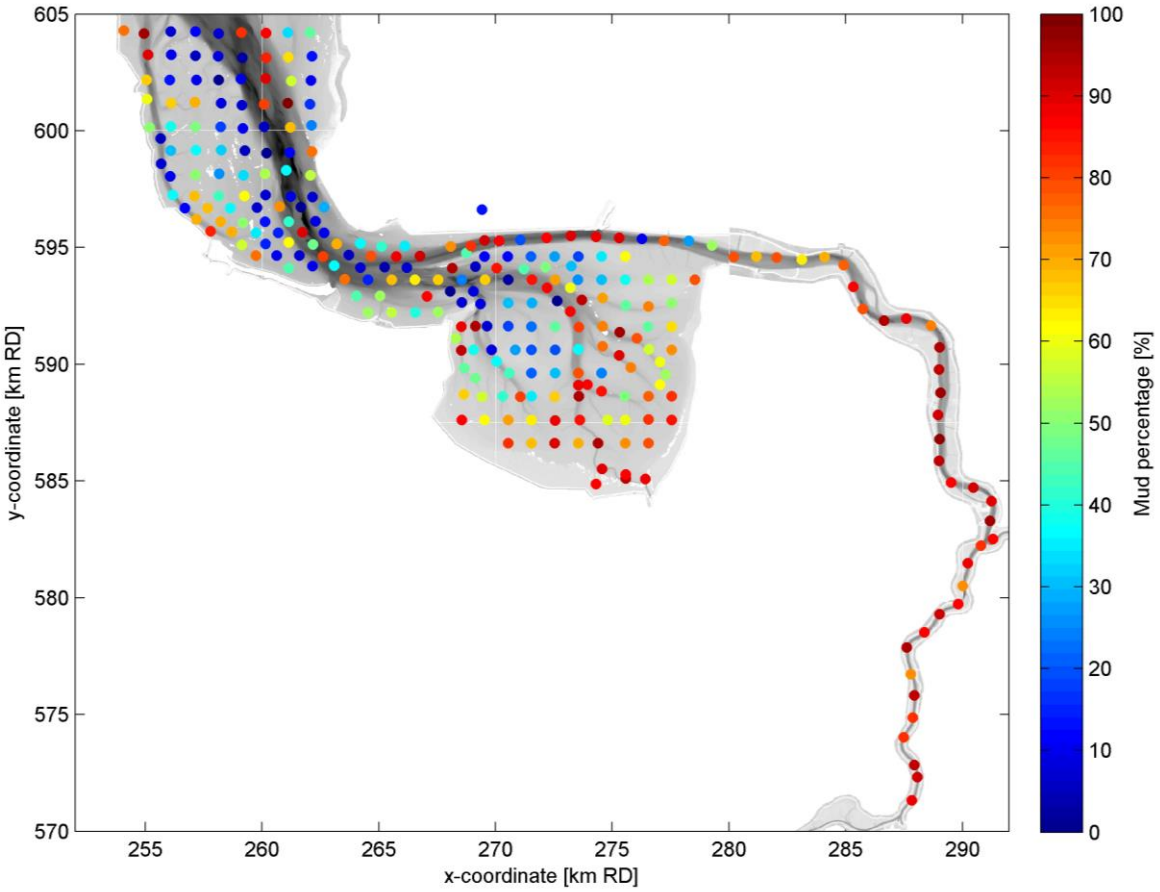

Figure 3.10 Mud content, defined as the percentage of material with a d < 63 µm, as derived with the Malvern from the samples collected in summer 2013.

When the PSD is plotted per subarea (see Figure 3.11), it is clearly visible that in the Ems-Dollard estuary both finer material and coarser material is present (two peaks, around 10 µm and 100 µm). In Figure 3.11 line colours indicate the depth at which the bed samples have been taken. In the Knock-Eemshaven section, the median grain size is larger in the deeper areas (blue lines). In the Dollard and the lower Ems River this difference is less pronounced.

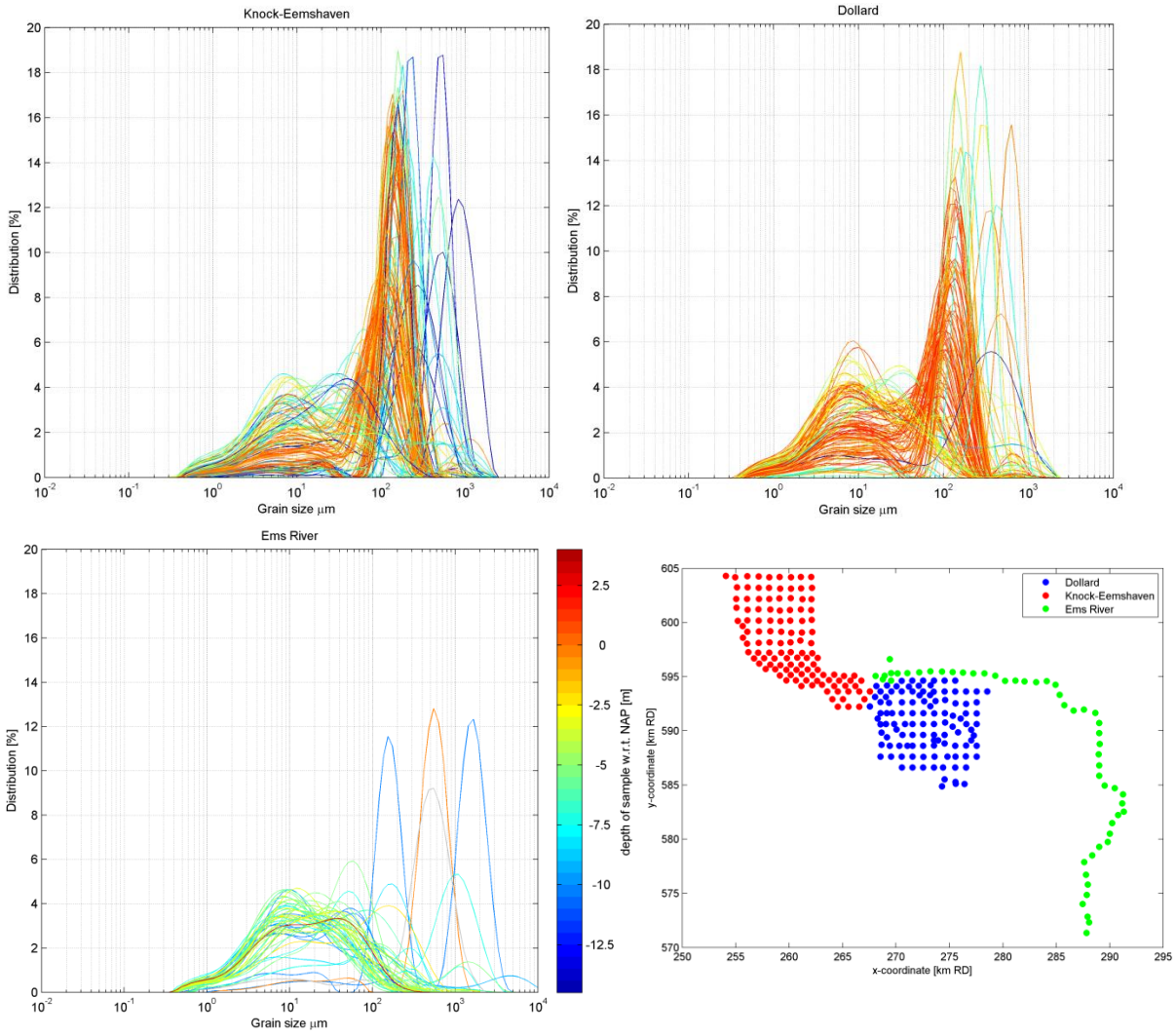

Figure 3.11 Particle size distribution dependent on bathymetry per area: Knock-Eemshaven (upper left), Dollard (upper right) and Ems River (lower left). Areas indicated in lower right panel. Line colour defined in the colour bar in the lower left panel.

3.3 Atterberg Limits

The plasticity chart indicates which types of clay are present in the samples. The samples in the Ems estuary are typical for non-swelling clays, illite or kaolinite, see Figure 3.12.

The activity chart of sediments from the Ems estuary is plotted using the clay content ξ^{cl} from the Sedigraph (Figure 3.13). The activity chart using the clay content ξ^{cl} computed with the Malvern data (Figure 3.14) is not realistic. The relation between ξ^{cl} and PI is poor, and the activity is unrealistically high because of underestimation of clay content by the Malvern. This strongly suggests that ξ^{cl} measured with the Malvern cannot be used to relate the Malvern PSD with the PI.

The activity chart (based on the Sedigraph clay content) is typical for illite (activity around 1.2). An activity of 1.2 is in line with expectations, because many natural systems are dominated by illite.

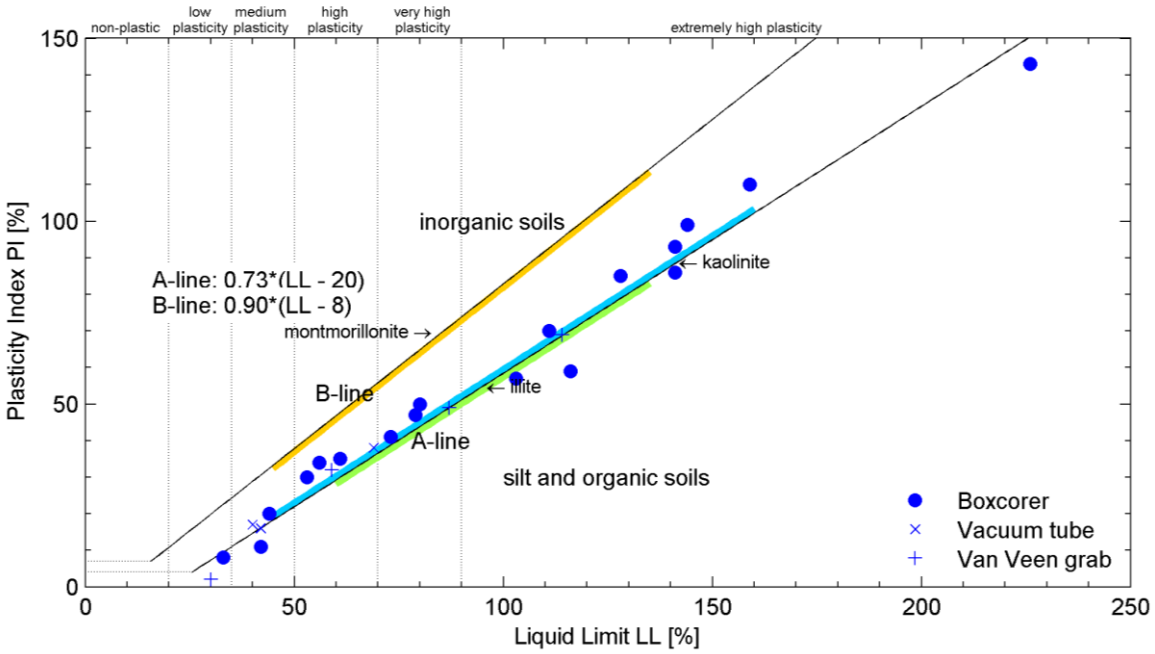

Figure 3.12 Plasticity chart of Ems-Dollard sediments. The A-line separates inorganic clays from organic soils, and the B-line is an upper limit of sediments found in nature. The green, blue and yellow lines are relations between LL and PI for the clay minerals Illite, Kaolinite, and Montmorillonite (resp.). Symbols indicate the sampling instrument.

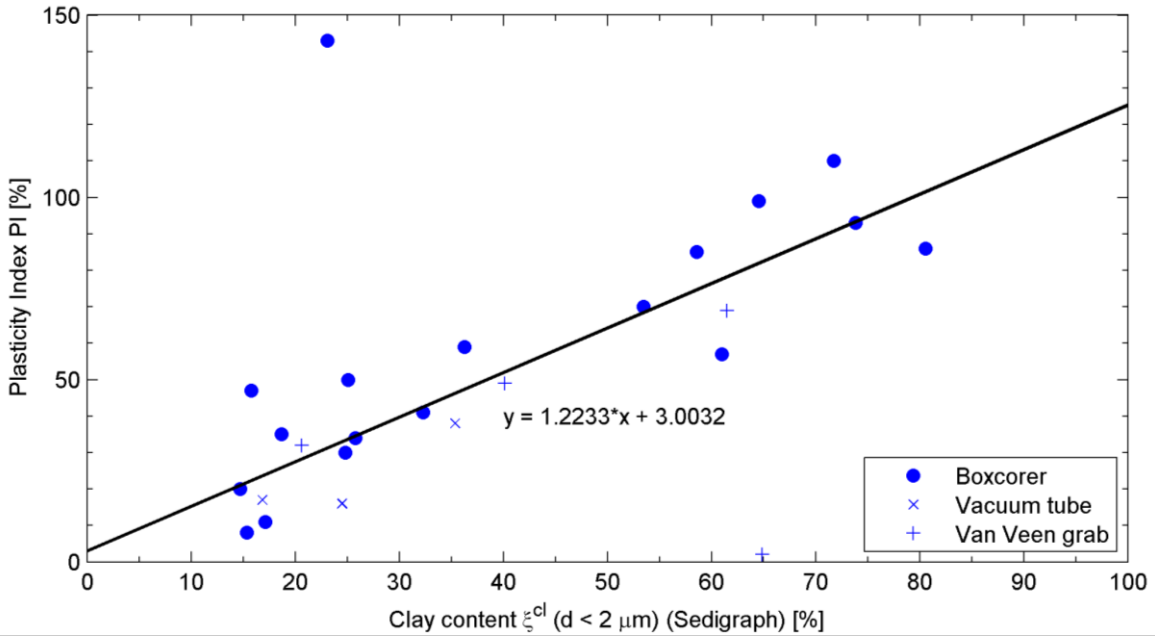

Figure 3.13 Activity chart of Ems-Dollard sediments. Clay content measured with Sedigraph. Symbols indicate the sampling instrument. Samples with $PI > 120$ and $PI < 2$ are not included in linear regression. $R^2 = 0.8216$.

Because the Sedigraph analysis was carried out on limited amount of samples, in order to combine the PI with all sediment samples, the PI needs to be related to the Malvern results as well, which are available for all samples. The relation between the mud content (d < 63 µm) measured by the Malvern and the Sedigraph correlates much better than the clay content (d < 2 µm). Therefore the PI is also related to the mud content (d < 63 µm) measured with the

Malvern (Figure 3.15). This relation cannot be used for a physical interpretation of sediment type (such as the activity of the clay), but it can be used to estimate PI values for all Malvern samples based on the mud content.

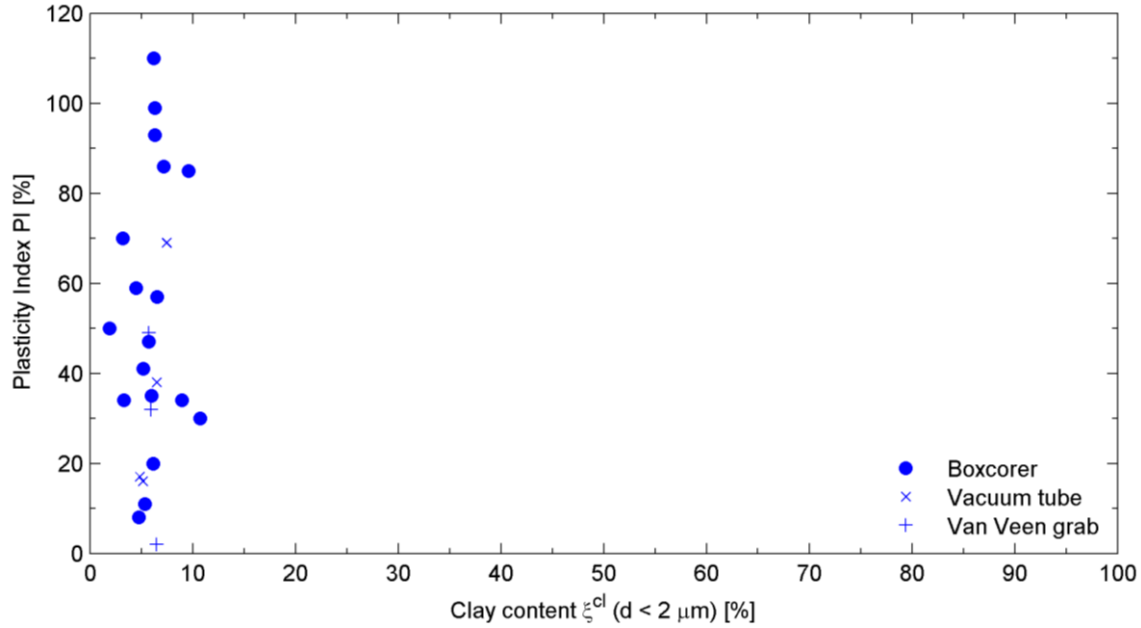

Figure 3.14 (Erroneous) activity chart of Ems-Dollard sediments. Clay content measured with the Malvern.

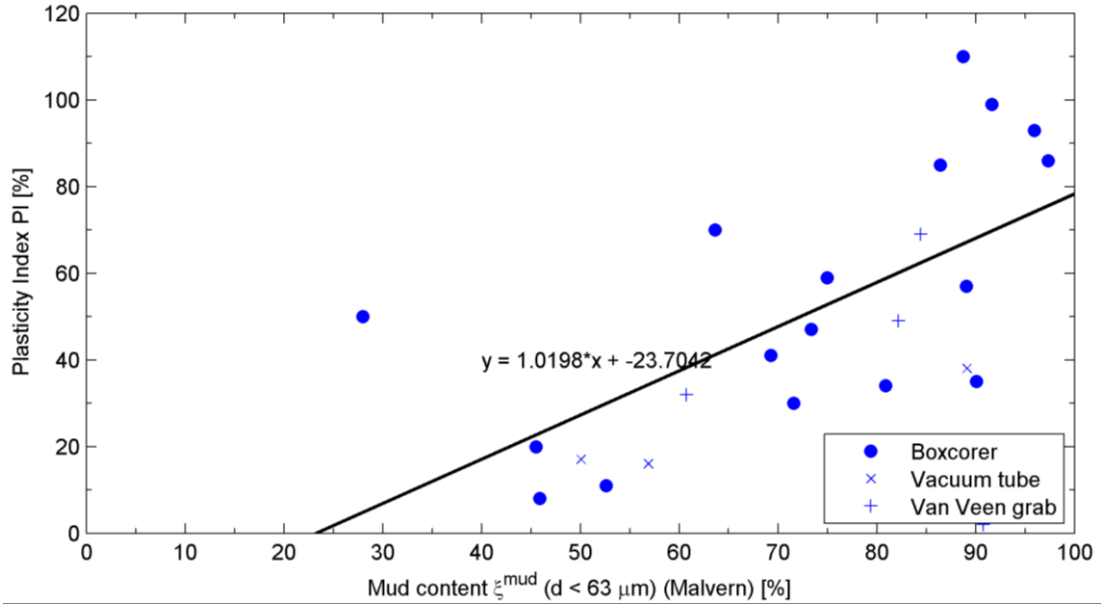

Figure 3.15 Activity chart of Ems-Dollard sediments using the mud content of the Malvern, instead of the clay content. Samples with PI > 120 and PI < 2 are not included in linear regression. R^2 = 0.4325.

The linear relation between the Plasticity Index PI and the mud content determined with the Malvern ($PI = 1.0198 \cdot \xi^{mud} - 23.7042$) is used to compute the Plasticity Index PI for all other samples. The result is shown in Figure 3.16. The Plasticity Index PI in the Ems River is higher, because the mud content is also higher. This map of the Plasticity Index PI is used in §4.4 to derived a value for the critical shear stress for erosion τ_{cr}.

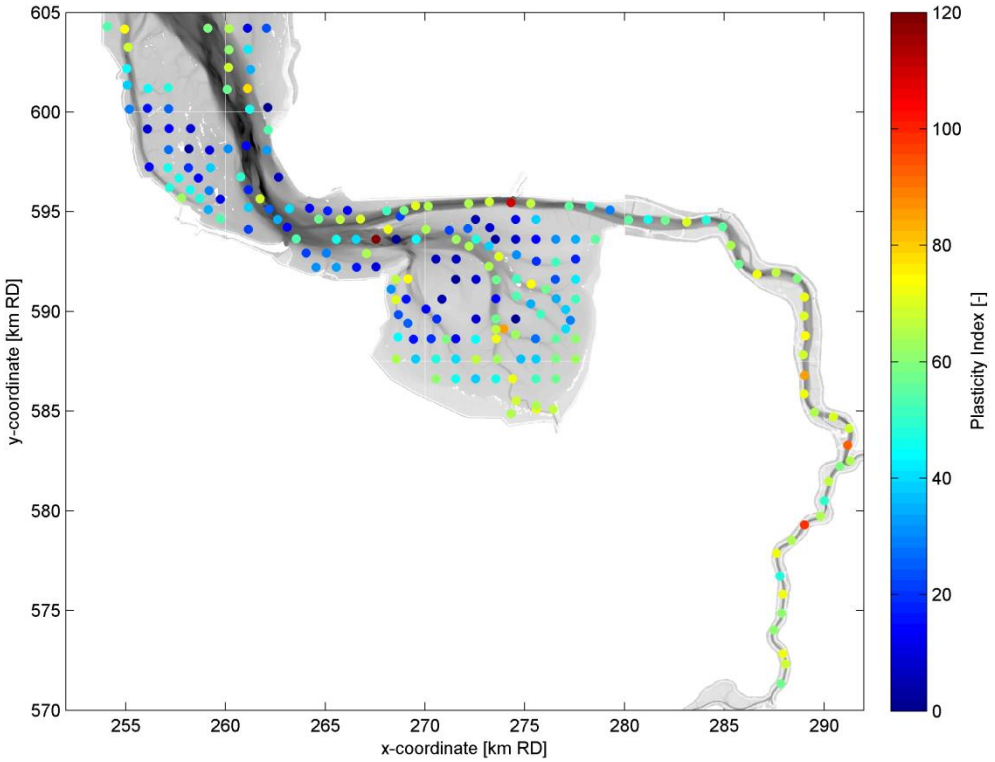

Figure 3.16 Spatial distribution of the PI, based on linear relation between PI and mud content.

3.4 Strength

The strength of the soil in the Ems-Dollard estuary resulting from the linear relation between void ratio and strength (see §2.3.3) is shown in Figure 3.17. In general, the strength of a soil close to the LL (Liquid Limit) is 1 kPa, the strength of a soil close to the PL (Plastic Limit) is 100 kPa (Winterwerp and van Kesteren, 2004). The LL corresponds to a water content in which a groove inserted in the sample fills in by fluidisation. The PL corresponds to the water content above which the sample easily crumbles. Most samples have a strength below 1 kPa, i.e. the samples are mostly fluid. The strength of the soil is higher at locations were the soil is more compacted and the water content W in the soil is lower. On the flats in the Dollard Bay and in the Ems River, the strength of the soil is low.

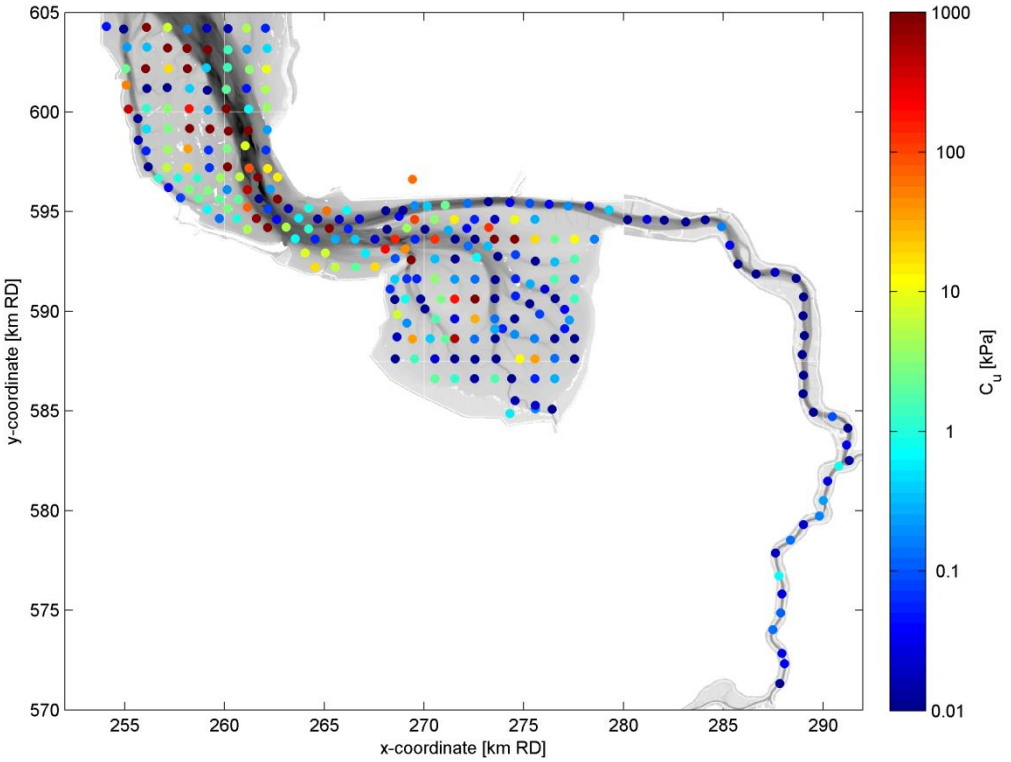

Figure 3.17 Spatial distribution of undrained shear strength c_u based on general relation of Winterwerp et al. (2012).

3.5 Zeta Potential

Figure 4.19 shows measurements of the ζ-potential of Ems-Dollard sediments at a pH of 3, 4, 6, 8 and around 9. The samples with a pH of 8 and 9 are natural, i.e. without a lower pH. Samples for which the ζ-potential is smaller than 30 mV in absolute value will flocculate. Since all natural samples for which the ζ-potential is measured have values below 30 mV, the natural sediment is likely to flocculate for the environmental conditions encountered during the field experiments. In order to expand the range of conditions, ζ-potential was also measured for different pH values. During these measurements, the ionic strength was not maintained constant, resulting in a salinity varying between 0 and 2.5 ppt. These conditions may not reflect conditions that may actually occur in the Dollard because the salinity is higher: in reality the sediment will flocculate even more easily.

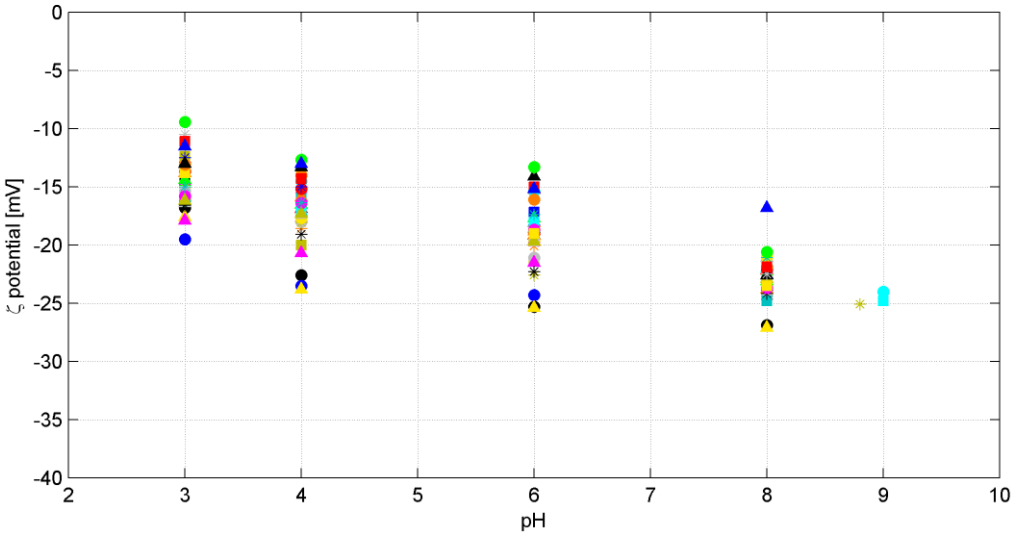

Figure 3.18 Zeta potential as a function of acidity (pH). Samples with ζ-potential >-30 mV will probably flocculate.

3.6 CST

The results of the CST test are used to determine the Gibson coefficient, which is similar to the consolidation coefficient from the settling column test. In this way, an independent check of the consolidation coefficient is obtained.

The CST is determined for three samples (sample 27, 173 and 5726) at different void ratios, see Figure 3.19. The void ratio is decreased by compressing the sample. The linear relation between the void ratio and the CST is met for all three samples, which gives confidence in the results. The resulting Gibson coefficient, determined using the formula in §2.3.5, is listed in Table 3.1. The Gibson coefficient for the three samples varies with a maximum of a factor 2, which is sufficiently close to compute an average value (see Table 3.1). Note that the results on the Gibson coefficient are later used for evaluating the quality of the data obtained from the settling column/consolidation tests in §3.7.

Table 3.1 Gibson coefficient determined from CST.

Sample #	C_{gib} [m^2/s]
27	$7.73 * 10^{-10}$
173	$8.21 * 10^{-10}$
5726	$1.63 * 10^{-9}$
average	$1.07 * 10^{-9}$

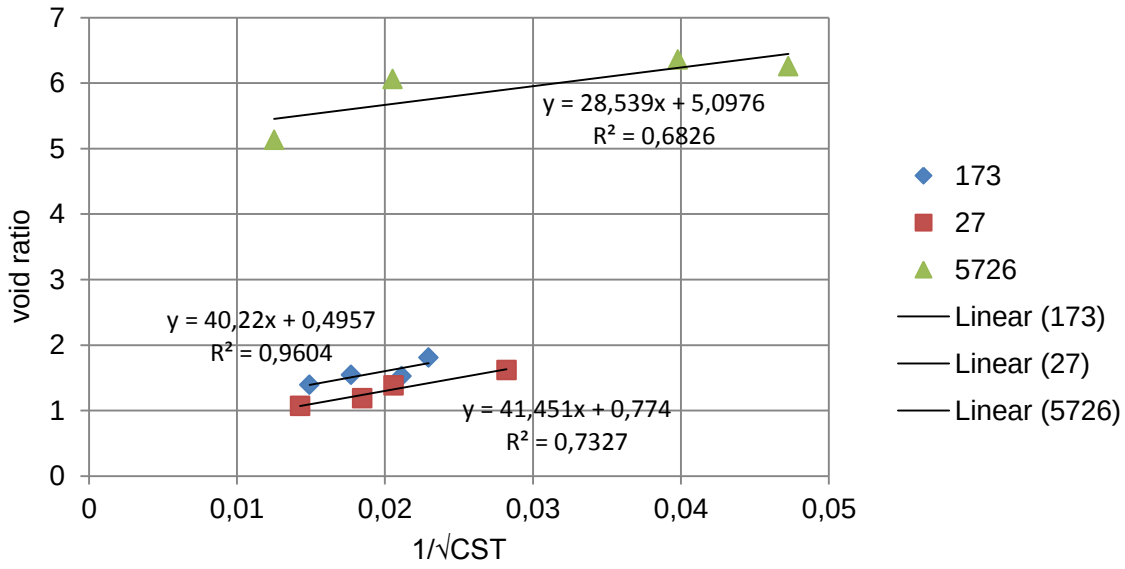

Figure 3.19 Results of the CST test for sample 27 (69% mud), sample 173 (90% mud) and sample 5726 (97% mud).

3.7 Settling column / Consolidation test

The consolidation test is applied to a couple of samples, following the procedure described in §2.3.6. An overview of the samples analysed for their settling and consolidation behaviour is shown in Table 3.2, together with the result of the hindered settling phase: the observed effective settling velocities. The effective settling velocity is obtained by fitting a linear line through the points indicating the height of the interface in time, during the hindered settling regime (Figure 2.14). Measurement errors (malfunctioning camera) during the experiments on sample 5734 did not allow for the identification of the settling interface during the hindered settling regime, and therefore it was not possible to determine w_{eff} for this sample.

Table 3.2 Overview of observed effective settling velocities derived from the hindered settling phase of the conducted settling-consolidation experiments

Sample #	sand content [-]	concentration (sand + mud) (g/l)	mud concentration c (g/l)	Effective settling velocity w_{eff} (m/s)
49	0.15	10	8.43	0,0010
135	0.11	10	8.81	0,0009
119	0.44	10	5.53	0,0011
5734	0.27	10	7.28	-
49	0.15	30	25.29	0,0007
119	0.44	30	16.59	0,0010
135	0.11	30	26.43	0,00065
5734	0.27	30	21.84	-
119	0.47	60	31.38	0,0007
5734	0.27	60	43.68	-

The clear water settling velocity $w_{s,0}$ and the gelling concentration c_{gel} can be computed using the results from the effective settling velocity and the formula in §2.3.6. Fitting this equation to the data obtained from all the conducted experiments results in the values of $w_{s,0}$ and c_{gel} indicated in Figure 3.20. Clustering the measurements from all samples to obtain $w_{s,0}$ and c_{gel}

is possible by assuming that the mud present in all samples is similar and will therefore show the same settling behaviour, and will start consolidation at the same concentration. Another possible approach would be to fit the equation only to data produced from the study of one sample. This is also done. The results of the two possible approaches are shown in Table 3.3.

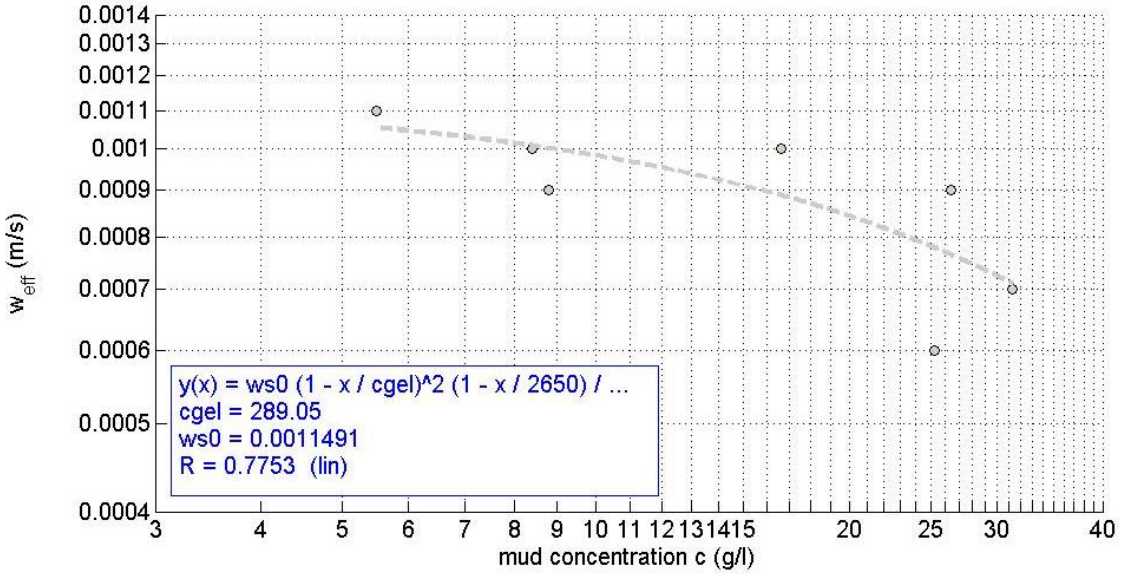

Figure 3.20 Tested mass concentration against observed effective settling velocities. The equation above is fitted in the data to obtain the indicated values of c_{gel} and $w_{s,0}$.

Table 3.3 Results of c_{gel} and $w_{s,0}$

sample #	c_{gel} (g/l)	$w_{s,0}$ (mm/s)
all (49, 119, 135)	289	1.1
49	205	1.2
119	236	1.0
135	202	1.1

In all cases, the clear water settling velocity $w_{s,0}$ varies between 1 and 1.2 mm/s. This settling velocity can be used to re-calibrate the numerical model. The gelling concentration c_{gel} exhibits a larger variation, ranging between 205 and 290 g/l. The gelling concentration c_{gel} is not used in the numerical modelling.

To determine the consolidation coefficient, the parameters derived from phase I and II are used. In appendix C the height of the interface in time is plotted with double logarithmic axes. The formulas listed in §2.3.6 are fitted through the data, and the values for the parameters D, K_k and K_p are obtained. These parameters are summarised in Table 3.4. The results show consistent values for K_k and D for every set of measurements within one sample, as well as overall. The average value of the consolidation coefficient c_v matches well with the Gibson coefficient, which increases the reliability of the data.

Table 3.4 Constants derived from phase I and II of the settling column tests.

Sample #	conc [g/l]	Water level [m]	Sand fraction [-]	ρ_s [kg/m^3]	ρ_w [kg/m^3]	Initial water content [-]	D [-]	K_k [m/s]	K_p [Pa]	c_v [m^2/s]
49	10	0,82	0,157	2650	1015	101,5	2,67	5,6E-12	4,5E+5	1,5E-09
49	30	0,82		2650	1015	33,8333	2,68	8,3E-12	8,3E+5	4,3E-09
119	10	0,81	0,447	2650	1015	101,5	2,7	1,2E-12	5,0E+5	4,0E-10
119	30	0,83		2650	1015	33,8333	2,68	5,3E-12	7,9E+5	2,6E-09
119	60	0,8		2650	1015	16,9167	2,69	1,5E-12	2,0E+6	1,9E-09
135	10	0,81	0,119	2650	1015	101,5	2,74	2,9E-12	3,2E+5	7,2E-10
135	30	0,83		2650	1015	33,8333	2,77	1,8E-12	1,5E+6	2,4E-09
5734	10	0,8	0,272	2650	1001	100,1	-	-	-	-
5734	30	0,84		2650	1001	33,3667	2,71	4,2E-12	1,8E+5	5,3E-10
5734	60	0,81		2650	1001	16,6833	2,74	4,0E-12	2,7E+6	8,5E-09
average										2,3E-09

4 Interpretation

The results of the laboratory and data analysis are interpret in order to (1) increase insight in the mud dynamics in the Ems-Dollard, (2) obtain parameters for input and calibration of the numerical models, and (3) to determine changes in the mud content with respect to 1989. This chapter starts with a general interpretation of all results.

4.1 Laboratory and data analyses

A total of 274 undisturbed sediment samples were collected during a 3-month measurement campaign in the Ems Estuary in 2013, using a Box corer (deep water) or vacuum tube (shallow water). To compare undisturbed samples with the van Veen grab samples taken in 1989, 28 additional grab samples were collected. Five samples were taken by hand, because the water depth was too shallow. All 307 samples were analysed for a number of bulk properties (grain size distribution, dry density, carbon content). More complex analysis techniques were applied on a limited number of samples.

The most important bulk parameter is the grain size distribution. Both the pre-treatment and analysis of the samples were done with the closest possible similarity to the 1989 measurements. In both measurements, a Malvern instrument was used. However, a comparison with a second settling velocity instrument (the Sedigraph) and a comparison with soil mechanical properties revealed that the clay content (d < 2 µm) of the Malvern instrument should be carefully interpreted. The mud content (d < 63 µm) seems to be more realistic than the clay content, and therefore only the mud content (d < 63 µm) measured with the Malvern is used for further analysis.

The activity plot suggests that the dominant clay type is illite with a bit of kaolinite, which are non-swelling clays. The bulk density non-swelling clay deposits increase more rapidly upon deposition compared to that of swelling clays, resulting in larger shear strength (Warkentin and Yong, 1962) and hence resistance against erosion. The amount of clay within the samples was strongly dependent of the type of analysis method, where the Sedigraph produced much larger clay contents than the Malvern measurements. The Sedigraph results correlate well with other soil-mechanical parameters, notably the Plasticity Index PI. Based on the PI-relation, it is concluded that the Sedigraph measurements are more accurate than the Malvern measurements for the clay content (d < 2 µm), and that the clay content of the Malvern cannot be used. As an alternative, we have related the PI to the mud content (d < 63 µm) measured by the Malvern, which is in agreement with Sedigraph measurements. The mud content of the Malvern is more reliable, because the main error arises from the clay fraction being added to the silt fraction.

To estimate a value for the undrained shear strength c_u, the relation of Winterwerp et al. (2012) between the void ratio e_i and the undrained shear strength c_u (a measure for the density of the deposit) was used.

The settling column test measured a settling velocity between 1 and 1.2 mm/s, and an average consolidation parameter c_v of 2.3 10^{-9} m^2/s. The related Gibson coefficient C_{gib}, measured with CST tests is 1.1 10^{-9} m^2/s. Although the two parameters vary by a factor two, for soil mechanical parameters this is a fairly good correspondence. The average value of the c_v will be used to determine the erosion parameter M, using the equation in § 2.3.7.

4.2 Changes in mud content with respect to 1989

The sampling methodology was different in 1989 compared to 2013, but a test on the effect of sampling revealed that although there is a deviation, there is no systematic difference. The deviation is random, and probably caused by natural small-scale variations in sediment size and morphological changes. During both field campaigns the pre-treatment of samples, which strongly influences the measured PSD of fine sediments, was the same.

In the previous chapter the shortcomings of the Malvern measurements were discussed, mainly focussing on the clay content (d < 2 µm). The low clay content as determined by the Malvern is also confirmed in literature (Beuselinck et al., 1998; Konert & Vandenberghe, 1997; McCave et al., 2006; Vdovic et al., 2010). From the analysis of the Atterberg Limits (§3.3) a reasonable correlation between the mud content (d < 63 µm) as determined by the Malvern and the Plasticity Index PI is obtained. This increases the confidence in the Malvern results for the mud content, and enables a conversion from mud content to Plasticity Index. Besides, the 1989 measurements were also analysed with a Malvern device. Although the specifications of the two devices may be different, the theory and principles used to determine the PSD are equal and hence the same shortcomings may apply to the 'old' Malvern device. In addition, mud content (clay + silt) measurements appear to be reliable (§3.2.3). Therefore a comparison between the mud content of 2013 measurements and the 1989 measurements can be made.

The 1989 samples (Figure 2.2) are subtracted from the 2013 samples (Figure 3.10) to obtain the spatial distribution of the change in mud content (d < 63 µm) (Figure 4.1). The comparison reveals a large spatial variation. Around the harbour entrance of Delfzijl, in the majority of the Ems River, and at the mouth of the Ems River (in the Ems Estuary), the mud content seems to have increased. The Groote Gat (see Figure 1.1 for name and location) also seems to have become muddier. In general, it seems that the mud content on the bed of deeper areas has increased.

Strikingly, the mud content in the shallow parts of the Dollard has decreased from 1989 to 2013. This change can be real or methodological. A methodological explanation is that the 1989 methodology overestimated the mud content (relative to 2013). Possibly, the mud content remained constant but simply appears to increase by use of a different instrument. This would imply that the increase in mud content in some areas is in reality larger than Figure 4.1 suggests. A comparison of the 1989 and 2013 data in a ternary diagram (Figure 4.2) reveals that the clay content was systematically higher in 2013 compared to 1989. However, a mud content exceeding 90% was common in 1989, but not observed in 2013. This supports the hypothesis above that the 1989 measurements overestimated the mud content of samples relative to 2013. As such, it is not possible to determine sufficiently accurate whether the decrease in mud content in the Dollard is realistic or not.

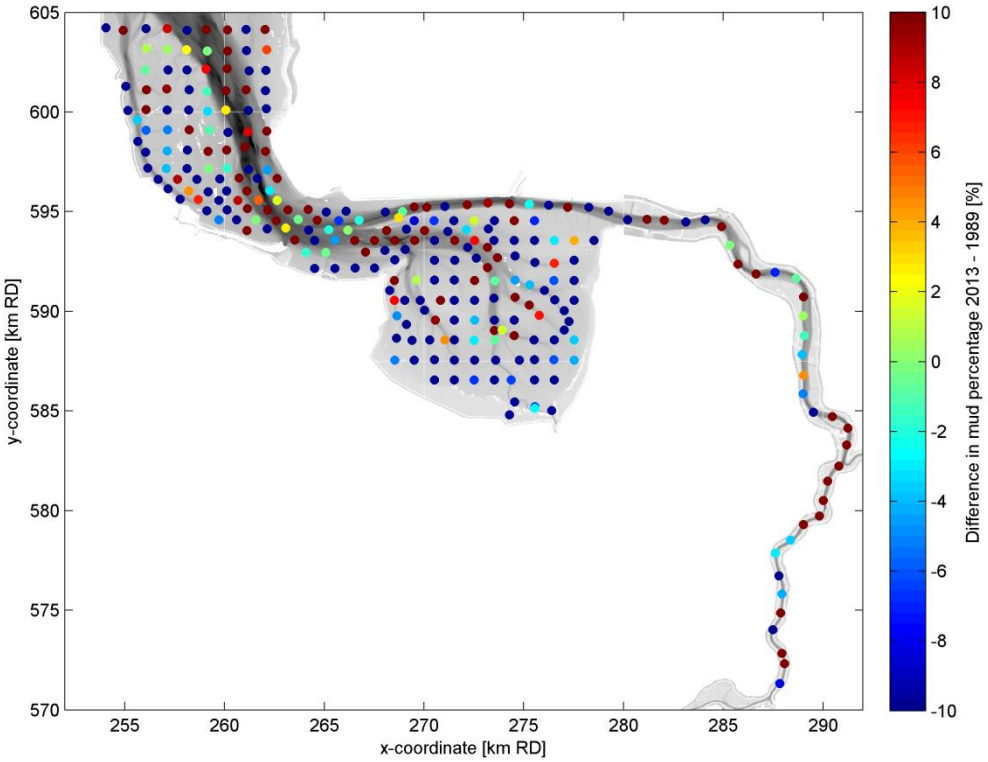

Figure 4.1 Difference in mud percentage (d < 63 µm) between 2013 and 1989.

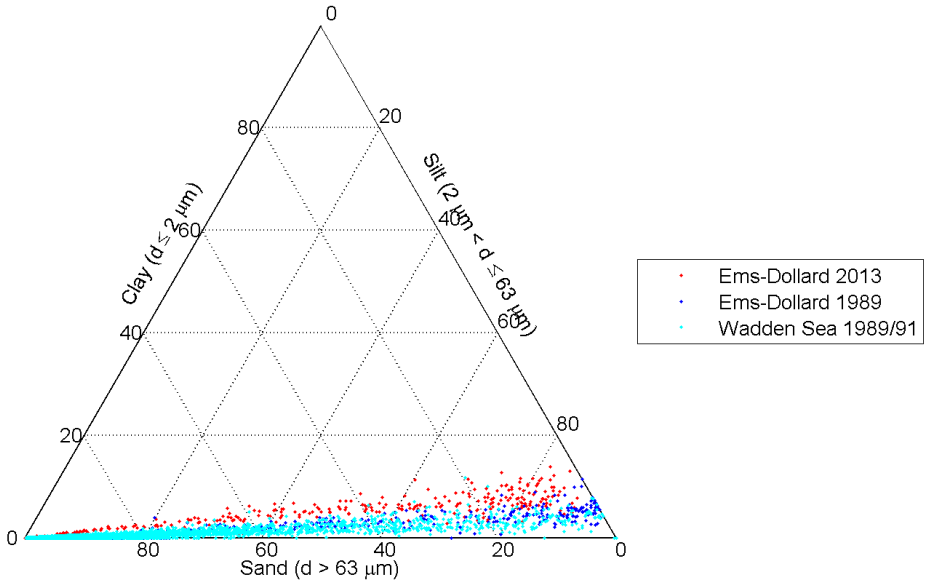

Figure 4.2 Ternary diagram of sand, silt, and clay, for measurements in the Ems-Dollard in 1989 and 2013, and the Wadden Sea in 1989/1991.Results from measurements in the Malvern.

4.3 System understanding

The mud content in the channels increased, in the Groote Gat and in the lower Ems River. The change in the lower Ems River is in line with earlier observations related to the increase in fluid mud in the lower Ems River. An increase in the Groote Gat channel, as suggested by

Figure 4.1, has not been previously documented. Although this increase may be related to the period of sampling (sampling shortly after a storm will probably result in lower mud contents), the systematic increase suggests an actual change in the bed sediment. Even more, the observation of a larger mud content in the tidal channels compared to the tidal flat is different from other parts of the Wadden Sea and the Western Scheldt, where tidal channels are typically more sandy compared to the tidal flats. This may be caused by a balance of wave reworking of the flats and supply by tidal currents. This is explained below.

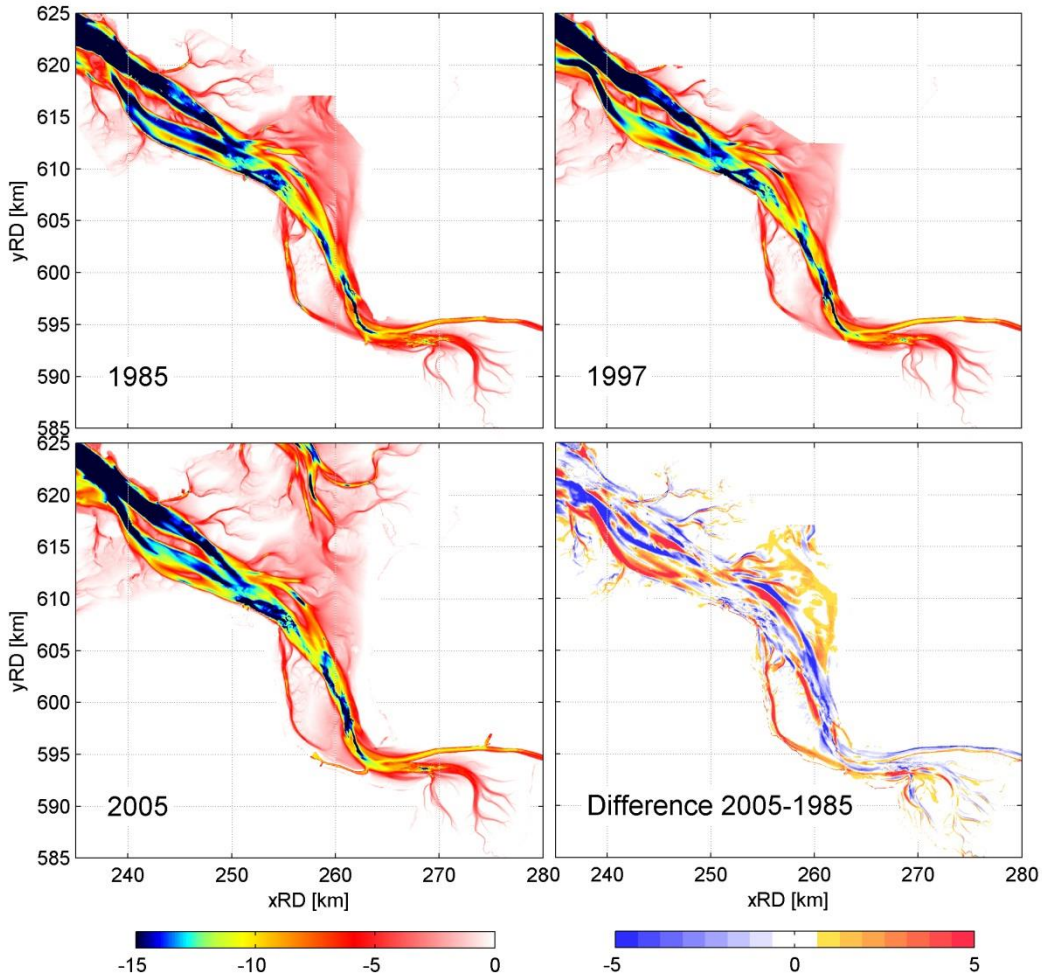

Figure 4.3 Bathymetry in 1985, 1997, 2005 (depth relative to NAP), and the difference between 2005 and 1985

A large amount of sediment is annually transported into the Ems estuary by a combination of tidal asymmetry, density-driven flows, and settling and scour lags. For accreting tidal flats (which are observed in many parts of the Wadden Sea and the Western Scheldt), the sediment transported up-estuary is deposited on the flats. However, the tidal flats in the Dollard are probably not accreting (see Figure 4.3): the tidal flats of the Dollard are probably the least dynamic part of the Ems estuary in terms of long-term bed level change. The low dry bulk density of the flats (Figure 3.2) however, suggests that the sediment is poorly consolidated. A likely explanation for this low consolidation degree is regular resuspension. Probably, the tidal flats in the Dollard have reached a critical bed level at which all sediment exceeding the height is eroded by wave action, and transported back to the tidal channel. In the Groote Gat, sediment eroded from the flats and sediment transported up-estuary

therefore accumulates. The amount of mud on the bed of the Groote Gat has apparently increased since 1989, in addition to the increase in suspended sediment concluded earlier (report 3). During periods of low wave activity, sediment is transported back towards the tidal flats, where it slowly consolidates.

4.4 Parameters for numerical model input and calibration

Three of the variables used in the numerical modelling, can be calibrated using the results of the measurements. These variables are the critical shear stress for erosion τ_{cr}, the erosion parameter M and the settling velocity w_s. For the settling velocity w_s, a uniform value for the entire estuary is derived from the settling column tests. Note that despite of the high sediment concentrations at which these tests are performed, the results represent a situation in which sediment settle freely, and not affected by the other particles in suspension. For the critical shear stress for erosion τ_{cr} and the erosion parameter M, spatial varying values are derived from the measurements. The maps showing this spatial variation are described in the next two sections.

4.4.1 The critical shear stress for erosion τ_{cr}

The critical shear stress for erosion τ_{cr} can be determined based on the (spatially varying) Plasticity Index PI (Figure 3.16). For γ_{cr} a value of 0.7 is chosen, being the average in Winterwerp et al. (2012). The resulting spatial distribution of the critical shear stress for erosion τ_{cr} is shown in Figure 4.4. In some areas no value for the critical shear stress for erosion τ_{cr} is computed, because the formula is only valid for sediments with a Plasticity Index PI larger than 7%. For very sandy sediments, the Plasticity Index PI is smaller than 7%.

Typically, the highest values for the critical shear stress for erosion τ_{cr} are found for in the most muddy parts of the estuary (the Dollard basin and the lower Ems River), with values of typically 1.5 Pa. Several uncertainties exist in the determination of τ_{cr}:

- The value of γ_{cr} varies between 0.35 and 1.4, and therefore the values of τ_{cr} can be a factor 2 higher or lower.
- The relation between the grain size distribution and the *PI* is not done with the clay content (which is the conventional approach), but with the mud content (which is more accurately determined with the Malvern). This difference will lead to more scatter in the computed values for τ_{cr}, but probably not so much the absolute value.
- The relationship between τ_{cr} and *PI* is derived for consolidated sediment, and therefore does not account for the state of consolidation of the material. However, observations of the water content W (Figure 3.1) reveal that the sediment is not fully consolidated (especially in the lower Ems River). Therefore the computed values for τ_{cr} are probably an overestimation.
- The number of samples used to relate τ_{cr} and *PI.* The accuracy of the fit will increase with the number of samples. Given the relatively good relation (Figure 3.13 and Figure 3.15), however, this source of uncertainty is probably much lower than the uncertainties mentioned above.

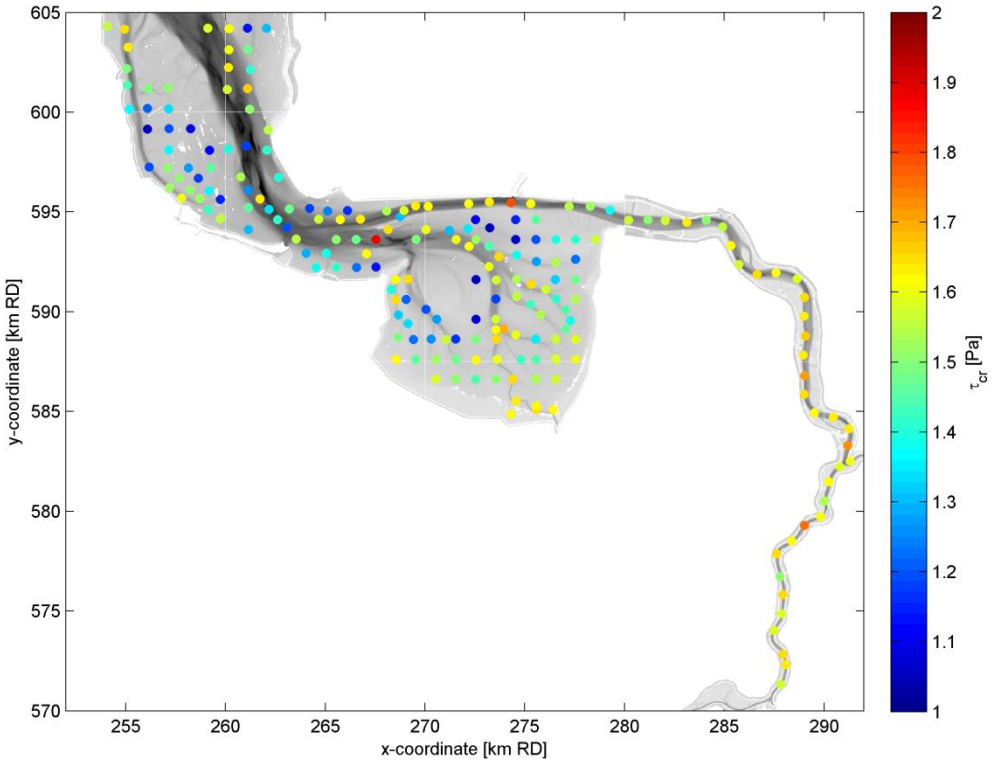

Figure 4.4 Spatial distribution of critical shear stress for erosion τ_{cr}, relating Figure 2.16 to Figure 3.16.

4.4.2 The erosion parameter

A spatial distribution map of M_E can be constructed using the consolidation coefficient c_v from the settling column test, the dry density ρ_{dry}, the median grain size d_{50} and the undrained shear strength c_u, which is related to the void ratio e_i (water content). The result is shown in Figure 4.5. In the numerical model, the erosion parameter M is used, which is determined by multiplying M_E (Figure 4.5) with the critical shear stress for erosion τ_{cr} (Figure 4.4). For the deeper layer (S2) of the WED model, the excess bed shear stress (τ - τ_{cr})/ τ_{cr} is raised to the power 1.5, and therefore the power *M* computed here does not exactly correspond to the power *M* in the sediment transport model. The spatially varying distribution of the erosion parameter M is shown in Figure 4.6.

The value for M is highest (i.e. bed sediment can be most easily eroded) in the lower Ems River and in the Dollard, where the clay content and void ratio are largest. The strongest contribution to the spatial variation in *M* is by the void ratio, which is related non-linearly to the undrained shear strength (see the relationship in section 3.4, resulting in Figure 3.17). The erosion parameter is large (because of the large void ratio) in area where τ_{cr} is also large (because of the large clay content). The method to compute τ_{cr} does not account for the dry bed density (as explained above), and therefore overestimates τ_{cr} for unconsolidated mud deposits.

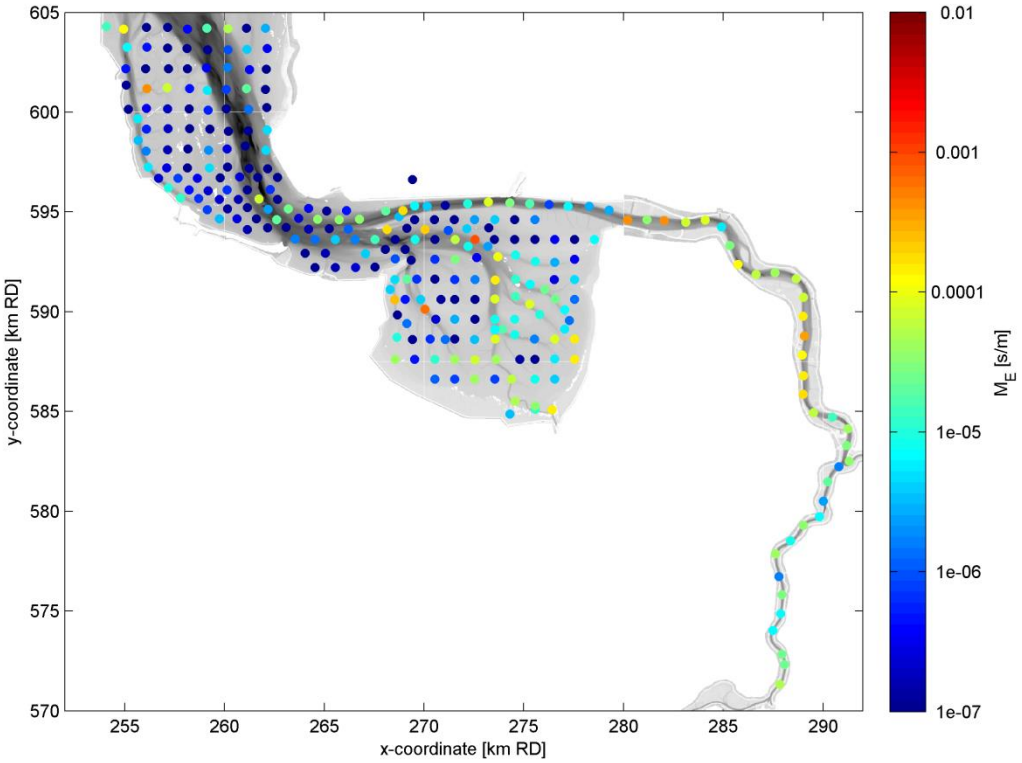

Figure 4.5 Spatial distribution of M_E.

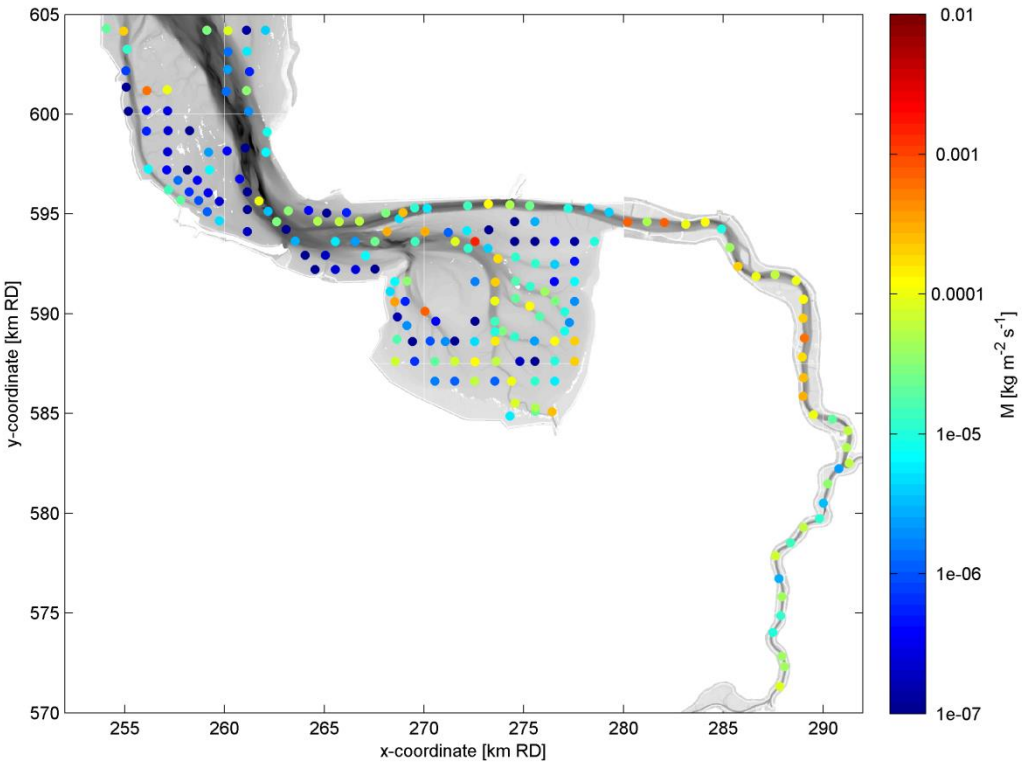

Figure 4.6 Spatial distribution of M, obtained by multiplying Figure 4.4 with Figure 4.5.

4.4.3 Implications for numerical model setup

The variables used for the numerical modelling can be better estimated with the results of the soil sampling analysis. In this section, the recommended values for the settling velocity w_s, the critical shear stress for erosion τ_{cr} and the erosion parameter M based on the measurement results are compared with the model setup and sensitivity analysis described in the draft report of the sediment transport model setup (report 5).

Settling velocity

The analysis in this report suggests a typical value for the clear water settling velocity $w_{s,0}$ of 1 to 1.2 mm/s (§3.7). Note that $w_{s,0}$ represents the bulk settling velocity of the sediments. However, visual observation during the tests confirmed that the very fine fraction settles with quite some delay with respect to the bulk sediments, and therefore $w_{s,0}$ does not account for the finest fraction. In the numerical sediment transport model (report 5) two sediment fractions are used: one fast-settling fraction, and one more slowly-settling fraction. The bulk settling fraction computed here is a first approximation of the faster settling fraction.

Critical shear stress for erosion

The analysis in this report suggests a critical shear stress for erosion τ_{cr} between 1 and 2 Pa (Figure 4.4). However, the formula used in the analysis is only valid for consolidated sediment. In the Ems-Dollard estuary, this may not always be the case. Especially the high critical shear stress for erosion τ_{cr} in the Ems River is not realistic, because the high water content in these sediments implies that they have not consolidated. This may also be the case in the more muddy parts of the Dollard Bay. Therefore the computed values for the critical shear stress for erosion τ_{cr} in Figure 4.4 provide an upper limit. Values around 1 Pa are possibly more in agreement with the consolidation state of the sediments. The effect of the degree of consolidation has a larger uncertainty for determining τ_{cr} than the uncertainty arising from determining the clay content of the the sediment.

The numerical model has two bed layers, each with different values for the critical shear stress for erosion τ_{cr}. The upper fluff layer of the model (S1) has a very low critical shear stress for erosion τ_{cr}. This sediment is unconsolidated, and is easily resuspended. Its thickness is typically several millimetres, and is therefore not explicitly part of the sampling campaign. The soil sample analysis can therefore not be used to improve the critical shear stress for erosion τ_{cr} of the upper layer.

Erosion parameter

The computed erosion parameter *M* is more difficult to relate to model input. The erosion and deposition fluxes are more complex compared to the basic equations described above (including multiple layers and fractions). Therefore the erosion parameter *M* is still used as a calibration parameter, optimizing the correlation between computed parameters (such as the sediment concentration) with observed parameters.

5 Conclusions and recommendations

5.1 Conclusions

The aims of this study were threefold, being to

1. Determine changes in the mud content with respect to 1989.
2. Increase the insight in the mud dynamics in the Ems-Dollard (transport and segregation).
3. Obtain parameters for input and calibration of the numerical models (typical values for settling velocity w_s and critical shear stress for erosion τ_{cr}).

With respect to aim 1) the 1989 and 2013 samples have been taken with different devices (van Veen grab in 1989, mainly boxcore in 2013), pre-processed in an identical way, and analysed for the PSD in different versions of a Malvern Mastersizer. Concerning the bed sampling methodology it is safe to assume that this does not introduce a systematic difference, not in mud content or clay content. This is supported by the fact that the sampling instrument (Box corer / Vacuum tube / van Veen grab) results in randomly differing grain size distributions, but not in a systematic under- or overestimation of the mud content.

Concerning the PSD analysis method it appears that the clay content (<2µm) measured with the Sedigraph differs so much from the Malvern clay content, that the clay content measured with the Malvern cannot be used for further analysis. The mud content (<63µm) determined with the Sedigraph shows better agreement with the Malvern measurements. Therefore the changes between 1989 and 2013 are only evaluated for the mud content, not the clay content. Because of methodological differences between 1989 and 2013, the mud content is systematically lower in 1989. This systematic change cannot be quantified, and therefore the changes in mud content from 1989 to 2013 are evaluated qualitatively. The changes summarised hereafter are compensated (qualitatively) for the overall increase in the mud content from 1989 to 2013. This qualitative comparison of the mud content of 1989 with the mud content of 2013 reveals the following:

- The mud content on the tidal flats of the Dollard Bay seems to have decreased.
- The bed of the main tidal channel in the Dollard (the Groote Gat) appears to have become muddier.
- Most of the lower Ems River shows an increase in mud content.

Seasonal variations in the mud content have not been taken into account. The mud content in estuaries such as the Ems estuary and the Dollard basin varies seasonally, typically with the highest mud content on the flats at the end of summer. Even though the 1989 and 2013 samples were collected in a similar period (August to October 2013 and September to December 1989) some of the observed changes (between 1989 and 2013) may be attributed to seasonal fluctuations.

With respect to aim 2) the conclusions are that

- The Atterberg limits indicate that the dominant clay mineral is probably illite, possibly with some kaolinite. These clay minerals form compacter sediment beds with a larger resistance against erosion compared to other clay minerals.
- The bed sediment in the Ems River is muddy and has a low bulk density. This represents regularly resuspended, poorly consolidated sediment.
- The tidal flat Hond-Paap and the seaward tidal flat of the Dollard are relatively sandy. The mud content increases deeper into the Dollard, peaking in the upper intertidal area. The main channel of the Dollard (the Groote Gat) is also very muddy.

- The observations in the Dollard may be explained as follows. The tidal flats in the Dollard have reached a critical bed level at which all sediment exceeding the height, is eroded by wave action and transported back to the tidal channel (resulting in low bed level changes). In the Groote Gat channel, sediment previously eroded from the flats and sediment that is transported up-estuary therefore accumulates (resulting in muddy bed sediment). During periods of low wave activity (summer), sediment is transported back towards the tidal flats, where it slowly consolidates.

With respect to aim 3) the conclusions are that

- A settling velocity $w_{s,0}$ of 1 to 1.2 mm/s is derived from consolidation tests. The upper value (1.2 mm/s) is used in the numerical model (report 5) for the fast settling fraction.
- The mud content is used to determine the *PI*, which is in turn used to determine the critical shear stress for erosion τ_{cr}. Preferably, the *PI* is determined using the clay content, and the *PI* has a clear relation with the clay content measured with the sedigraph. However, the clay content could not be determined for all samples because of earlier addressed methodological reasons. Therefor the mud content (measured with the Malvern) has been used to determine the *PI*. Because no relationship between the clay and mud content could be established, the accuracy of the *PI* and hence the τ_{cr} is probably affected.
- The critical shear stress for erosion τ_{cr} varies between 1 and 1.6 Pa, assuming the sediments to be well consolidated. The large water content in the top layer in the Ems River and the Dollard Bay suggests that the critical shear stress for erosion is lower, and therefore the most realistic assumption to be made is closer to 1 than 1.6 Pa.
- The measurement campaign has provided a well-documented dataset in the Ems Estuary for the mud content <63µm and other parameters.
- The map of distribution of mud content is used as validation material for models.

5.2 Recommendations

- The results from the Malvern and Sedigraph show a large difference in the particle size distribution. We recommend analysing the differences in more detail. The influence of different settings of the Malvern can be studied in more detail, as well as the effect of particle size varying density on the PSD. The low silt content (<16µm) in the Sedigraph results should be investigated as well.
- The old (1989) and new (2013) samples can be compared in a better way, if the old samples are re-analysed with the new Malvern device (the same as is used for the present study). Comparison of a subset of samples can already give insight in the order of magnitude of differences between the different Malvern devices and hence the difference between all old and new samples. The old samples have been frozen at TNO, which does not influence the PSD. Therefore determination of the size distribution is still feasible.
- In addition to the type of instrument used to determine the PSD, also the pre-treatment of samples and settings of the instrument influence the outcome. The used methodology information should therefore always be reported. The pre-treatment determines whether the primary particles or coagulates representing in situ conditions are measured. For the settling velocity, only the in situ conditions are relevant. However, to relate the grain size distribution to other soil mechanical parameters (using existing relationships from literature) the conventions used in these relationships should be followed. Often, these are based on primary particles (i.e. non-flocculated sediment).
- Procedural improvements include:

- Use of the Malvern: follow-up research at the Deltares laboratory (not reported here) suggest that sediment larger than 16 µm should be analysed separately from the smaller fraction. This should be further explored, and in the future analyses should be performed accordingly.
- The zeta potential measurements should have been carried out at more realistic salinity values and at constant ionic strength

6 References

Beuselinck, L., Govers, G., Poesen, J., Degraer, G. and Froyen, L. (1998), Grain-size analysis by laser diffractometry: comparison with the sieve-pipette method. Catena 32, pp. 193-208.

Blok. B. and Arentz. L. (2012). Bodemmonster Analyse Egmond. Deltares report 1205620.

Chassagne, C. (2012). Personal communication.

Cleveringa, J. (2008). Ontwikkeling sedimentvolume Eems-Dollard en het Groninger wad: Overzicht van de beschikbare kennis en gegevens. rapport A2269. Alkyon, Marknesse. 47 pp.

Cornelisse, J.M. (2011), Rotovisco meter Haake M1500, Standard operation protocol. Draft report Deltares.

Dankers, P. and Winterwerp, J., 2007. Hindered settling of mud flocs: Theory and validation. Continental shelf research, 27(14): 1893-1907.

Dellwig, O., J. Hinrichs, A. Hild, H.-J. Brumsack (2000). Changing sedimentation in tidal flat sediments of the southern North Sea from the Holocene to the present: a geochemical approach. Journal of Sea Research, 44, pp. 195–208

Huisman, M. and van Kesteren, W.G.M. (1998). Consolidation theory applied to the capillary suction time (CST) apparatus. Wat. Sci. Tech. Vol. 37, no. 6-7, pp. 117-124.

Konert, M. and Vandenberghe, J. (1997), Comparison of laser grain size analysis with pipette and sieve analysis: a solution for the underestimation of the clay fraction. Sedimentology 44, pp. 523-535.

McCave, I.N., Hall, I.R. and Bianchi, G.G. (2006), Laser vs. settling velocity differences in silt grainsize measurements: estimation of palaeocurrent vigour. Sedimentology 53, pp. 919-928.

McLaren, P., Stayaert, F. and Powys, R. (1998), Sediment Transport Studies in the Tidal Basins of the Dutch Waddenzee. Senckenbergiana.maritima 29, pp. 53-61.

Merckelbach, L. and Kranenburg, C., 2004. Determining effective stress and permeability equations for soft mud from simple laboratory experiments. Géotechnique, 54(9): 581-591.

Merckelbach, L.M., 2000. Consolidation and strength evolution of soft mud layers.

Van Heuvel, T. (1991). Sedimenttransport in het Eems-Dollard estuarium, volgens de method McLaren. Rijkswaterstaat, dienst Getijdewateren. Nota GWWS-91.002.

Van Maren, D.S. (2013). Meetplan Eems-Dollard, slibverspreiding en eigenschappen. Deltares report 1205711-001.

Papenmeier, S., Schrottke, K., Bartholoma, and Flemming, B.W. (2013). Sedimentological and Rheological Properties of the Water–Solid Bed Interface in the Weser and Ems Estuaries, North Sea, Germany: Implications for Fluid Mud Classification. Journal of Coastal Research, in press, doi:10.2112/JCOASTRES-D-11-00144.1

Rijkswaterstaat, 2009. Programma Rijkswateren 2010-2015 Uitwerking Waterbeheer 21e eeuw, Kaderrichtlijn Water en Natura 2000 Beheer- en Ontwikkelplan voor de Rijkswateren 2010-2015 (366 p.)

Vdovic, N., Obhodas,J. and Pikelj, K. (2010). Revisiting the particle-size distribution of soils: comparison of different methods and sample pre-treatments. European Journal of Soil Science, December 2010, 61, 854-864.

Warkentin, B. P. and Yong, R. N. (1962). Shear strength of montmorillonite and Kaolinite related to interparticle forces. Clays and Clay Minerals 9, p. 210-218.

Winterwerp, J.C. and van Kesteren, W.G.M. (2004). Introduction to the physics of cohesive sediment in the marine environment. Elsevier, Developments in Sedimentology 56.

Winterwerp, J.C., van Kesteren, W.G.M., van Prooijen, B., and Jacobs, W. (2012). A conceptual framework for shear flow-induced erosion of soft cohesive sediment beds. Journal of Geophysical Research 117.

Zwarts, L. (2004). Bodemgesteldheid en mechanische kokkelvisserij in de Waddenzee. RIZA-Rapport, 2004.028.

A Bulk properties of samples

no	Instr	X (RD) [m]	Y (RD) [m]	Z [m]	sand [%]	mud [%]	clay [%]	d_{50} [µm]	ρ_{bulk} [kg/m^3]	ρ_{dry} [kg/m^3]	W [-]	e_i [-]	OC [%]	pH [-]	sal [psu]
6	B	261138.8	594125.2	-1.8	54.8	45.2	3.9	69	1474	743	0.98	2.57	0.4	7.5	23.4
6	VV	261138.8	594125.2	-1.8	38.9	61.1	8.6	29					0.0		
7	B	262157.2	594202.2	-5.0	89.8	10.2	0.7	162	2039	1660	0.23	0.60	0.2		
8	B	263082.6	594240.3	-11.1	62.9	37.1	5.8	102	1474	744	0.98	2.56	0.7	7.9	24.2
9	B	264222.1	594135.4	-9.1	93.0	7.0	0.8	163	1389	605	1.29	3.38	0.0	7.8	22.9
10	B	265247.7	594159.7	-8.0	96.4	3.6	0.4	280	1978	1560	0.27	0.70	0.0	7.8	24.6
11	B	266190.1	594142.4	-7.2	93.0	7.0	0.6	192	1238	362	2.42	6.33	0.5	7.6	22.7
12	B	268149.1	594127.9	-5.1	5.6	94.4	10.0	8	1149	217	4.29	11.21	4.0	8.1	23.4
12	VV	268149.1	594127.9	-5.1	8.3	91.7	11.6	10					0.0		
13	B	269141.9	594185.4	-3.2	94.4	5.6	0.5	268	1465	729	1.01	2.64	0.0	7.9	22.6
14	B	270035.8	594112.0	-4.2	14.1	85.9	3.2	21	1111	156	6.13	16.00	24.4	7.9	22.3
15	B	271211.2	594077.1	-3.7	55.2	44.8	5.3	78	1314	485	1.71	4.46	2.7	7.8	19.8
16	B	272136.4	594166.3	-1.4	51.1	48.9	6.8	66	1229	347	2.54	6.64	0.2	8.0	23.1
17	B	264666.9	594638.2	-7.9	20.9	79.1	5.4	17	1189	282	3.22	8.40	6.5	7.6	22.9
18	B	263718.2	594690.4	-8.2	94.1	5.9	0.4	187	1348	540	1.50	3.91	0.2	7.9	21.1
19	B	262622.0	594620.3	-12.6	19.1	80.9	9.5	12	1230	349	2.53	6.60	3.6	7.6	20.0
20	B	261607.2	594665.6	-4.0	93.2	6.8	0.7	157	1865	1377	0.35	0.92	0.0		
21	B	260631.8	594654.2	-1.8	90.0	10.0	1.3	118	1379	589	1.34	3.50	0.0	8.0	23.3
22	B	259749.2	594652.2	-1.8	24.7	75.3	7.1	33	1280	430	1.98	5.17	3.8	8.1	22.5
23	B	259139.3	595120.1	-1.5	42.7	57.3	5.9	53	1356	552	1.45	3.80	1.6	7.7	23.5
23	VV	259139.3	595120.1	-1.5	36.6	63.4	6.8	43					0.0		
24	B	260146.6	595161.2	-1.5	84.8	15.2	2.3	107	1446	698	1.07	2.79	0.0	7.7	22.9
25	B	261153.9	595230.1	-3.7	38.3	61.7	6.5	21	1674	1068	0.57	1.48	0.0	7.8	22.5
26	B	262178.3	595143.7	-14.2	51.6	48.4	4.0	71	1256	390	2.22	5.79	1.5	7.6	22.0
27	B	263194.4	595163.2	-7.7	30.7	69.3	5.6	18	1198	297	3.04	7.92	3.4	7.7	20.2
28	B	264211.1	595189.6	-3.5	63.2	36.8	3.4	86	1381	593	1.33	3.47	0.0	8.4	23.7
29	B	265127.6	595053.0	-3.3	59.0	41.0	6.1	94	1654	1036	0.60	1.56	3.3	7.2	22.9
29	VV	265127.6	595053.0	-3.3	37.5	62.5	5.0	35					0.0		
30	B	266108.6	595082.9	-2.1	64.6	35.4	3.2	91	1356	552	1.45	3.80	0.5	7.8	22.0
31	B	269532.8	595316.4	-9.5	7.8	92.2	6.5	12	1298	458	1.83	4.78	0.7	7.7	
32	B	268084.8	595059.0	-8.0	26.6	73.4	6.7	79	1143	207	4.53	11.82	1.3	7.8	18.2
33	B	268942.1	595075.9	-11.2	17.9	82.1	6.6	20	1120	170	5.59	14.61	4.7	7.7	23.7
34	B	270152.8	595291.7	-10.8	12.6	87.4	6.9	16	1327	506	1.62	4.24	3.1	7.7	20.3
34	VV	270152.8	595291.7	-10.8	17.1	82.9	9.7	16					0.0		
35	B	271055.0	595336.4	-10.9	80.4	19.6	2.3	133	1432	676	1.12	2.92	0.5	7.9	18.6
36	B	272185.0	595408.9	-11.0	12.9	87.1	9.4	12	1279	427	1.99	5.20	0.8	7.9	18.6
37	B	273224.1	595498.6	-11.5	10.2	89.8	8.8	11	1166	245	3.77	9.84	4.9	7.8	17.8
38	B	274293.3	595466.9	-10.8	11.3	88.7	6.6	11	1219	330	2.69	7.03	4.9	7.8	17.8
39	B	275291.9	595429.0	-8.3	10.8	89.2	10.9	10	1259	396	2.18	5.70	3.7	8.1	21.1
39	VV	275291.9	595429.0	-8.3	12.0	88.0	7.9	13					0.0		
40	B	276271.6	595384.9	-10.8	90.2	9.8	0.5	347	1221	333	2.66	6.95	0.3	8.4	21.9
41	B	277224.4	595293.1	-10.0	22.8	77.2	8.7	14	1295	454	1.85	4.83	2.1	8.0	20.9
42	B	278270.9	595291.9	-7.6	72.0	28.0	2.0	119	1212	320	2.79	7.29	2.3	7.9	20.1
44	B	262663.7	595624.3	-7.1	89.9	10.1	1.3	131	1907	1445	0.32	0.83	0.1		
45	B	261726.4	595649.7	-9.5	9.9	90.1	10.2	14	1166	245	3.75	9.80	4.7	8.1	22.0
46	B	260691.5	595625.0	-2.5	84.7	15.3	1.8	133	1416	650	1.18	3.07	0.1	7.9	24.0
47	B	259742.4	595636.9	-1.3	65.2	34.8	3.5	84	1425	665	1.14	2.99	0.6	7.8	23.0
48	B	258702.3	595680.1	-1.3	29.9	70.1	6.4	30	1419	654	1.17	3.05	2.3	7.7	23.2
49	B	257793.2	595704.3	-2.9	15.7	84.3	7.4	15	1252	383	2.26	5.91	3.6	7.7	24.2
50	B	258227.4	596101.3	-0.8	30.9	69.1	5.2	30	1445	697	1.07	2.80	2.7	7.8	26.4
51	B	259188.2	596065.2	-1.3	48.8	51.2	5.1	61	1447	700	1.07	2.78	0.9	7.8	22.8
52	B	260137.7	596111.4	-1.4	86.1	13.9	1.8	138	1291	448	1.88	4.91	0.1	7.7	23.6
52	VV	260137.7	596111.4	-1.4	89.0	11.0	1.4	121					0.0		
53	B	261149.3	596117.2	-9.9	58.5	41.5	5.4	189	1824	1312	0.39	1.02	1.0		
54.1	B	262288.2	596131.5	-5.6	90.7	9.3	1.1	115	1305	471	1.77	4.63	0.6		
54.2	B	262288.2	596131.5	-5.6	99.5	0.5	0.1	149	1226	343	2.58	6.73	0.1		
55	B	262666.0	596731.6	-5.4	70.6	29.4	3.5	101	1546	861	0.80	2.08	1.0	7.5	27.0
55	VV	262666.0	596731.6	-5.4	39.3	60.7	6.4	30					0.0		
56	B	261658.0	596727.3	-13.9	100.0	0.0	0.0	491	2293	2071	0.11	0.28	0.1		
57	B	260754.4	596747.6	-7.0	27.4	72.6	6.1	38	1489	768	0.94	2.45	2.5	8.4	25.6
58	B	259787.2	596713.2	-1.3	92.9	7.1	0.9	129	1469	735	1.00	2.60	0.1	7.8	23.9
59	B	258632.6	596685.5	-0.9	63.6	36.4	4.0	86	1391	610	1.28	3.34	0.3	7.8	22.5
60	VT	257659.8	596697.7	-0.6	31.9	68.1	5.8	38	1374	581	1.36	3.56	1.3	8.0	25.9
61	B	257188.3	596216.2	-4.9	30.0	70.0	6.3	34	1218	329	2.70	7.05	5.4	7.9	23.7
62	B	256701.8	596685.8	-5.8	87.6	12.4	1.5	126	1383	596	1.32	3.45	0.2	8.0	27.0

no	Instr	X (RD) [m]	Y (RD) [m]	Z [m]	sand [%]	mud [%]	clay [%]	d_{50} [µm]	ρ_{bulk} [kg/m^3]	ρ_{dry} [kg/m^3]	W [-]	e_i [-]	OC [%]	pH [-]	sal [psu]
63	VT	257109.0	597221.0	-0.7	31.7	68.3	6.6	35	1486	763	0.95	2.47	3.2	7.8	
64	VT	258141.7	597221.5	-0.6	56.7	43.3	4.4	73	1570	900	0.74	1.94	0.6	7.8	
64	VV	258141.7	597221.5	-0.6	62.0	38.0	3.9	80					0.0		
65	B	259247.4	597221.2	-1.2	38.4	61.6	5.9	39	1246	375	2.32	6.07	1.1	7.5	26.6
66	B	260159.4	597256.9	-1.9	92.3	7.7	1.0	130	2007	1607	0.25	0.65	0.1		
67	B	261221.0	597184.7	-14.9	91.1	8.9	0.9	226	1682	1081	0.56	1.45	0.3	7.7	22.5
68	B	262165.5	597166.3	-6.3	93.7	6.3	0.9	136	1556	877	0.77	2.02	0.1	8.1	29.1
69	B	256177.0	597260.3	-5.5	63.0	37.0	4.9	103	1187	278	3.27	8.53	0.1	8.1	25.2
70	B	256070.6	598056.0	-0.6	90.5	9.5	1.1	123	1243	370	2.36	6.17	0.7	8.1	27.1
71	VT	257147.6	598111.6	-0.2	49.5	50.5	4.7	62	1470	737	0.99	2.60	1.9	8.2	27.5
72	VT	258154.1	598165.8	-0.6	74.0	26.0	2.5	96	1615	972	0.66	1.73	22.1	7.9	
73	B	259194.8	598095.8	-1.5	66.3	33.7	3.3	86	1251	382	2.27	5.94	0.4	7.9	23.6
74	B	260125.6	598157.3	-2.2	45.7	54.3	5.6	50	1447	701	1.07	2.78	1.0	7.5	25.1
75	B	261033.6	598321.7	-14.9	63.2	36.8	4.0	146	1518	815	0.86	2.25	0.6	8.0	26.4
76	B	262062.7	598091.1	-6.4	43.9	56.1	6.0	40	1246	375	2.33	6.07	2.6	7.7	21.9
77	B	255671.3	598600.1	-6.0	92.3	7.7	1.1	137	1195	291	3.10	8.09	1.0	8.1	28.3
78	B	256091.0	599149.6	-0.8	69.3	30.7	2.9	93	1340	527	1.54	4.03	0.3	7.8	28.0
79	VT	257164.2	599176.2	-0.3	62.9	37.1	3.5	83	1438	685	1.10	2.87	1.2	8.0	26.4
80	VT	258240.2	599180.6	-0.5	67.7	32.3	3.5	98	1934	1490	0.30	0.78	0.9		
80	VV	258240.2	599180.6	-0.5	56.4	43.6	4.2	73					0.0		
81	VT	259258.9	599147.0	-1.1	94.1	5.9	0.8	133	2019	1627	0.24	0.63	0.4		
82	B	260198.2	599043.1	-3.7	99.9	0.1	0.0	155	2034	1652	0.23	0.60	0.0		
83	B	261192.8	599077.0	-15.4	89.0	11.0	1.0	423	2157	1851	0.17	0.43	0.0		
84	B	262146.4	599119.4	-2.6	23.7	76.3	4.1	17	1299	460	1.82	4.76	2.2	8.1	27.0
84	VV	262146.4	599119.4	-2.6	20.0	80.0	4.8	16					0.0		
85	B	255647.0	599673.6	-5.6	94.7	5.3	0.4	148	1172	254	3.61	9.43	0.4	7.9	25.3
86	H	255180.5	600151.4	-0.9	48.7	51.3	4.0	61	1826	1314	0.39	1.02	1.2		
86	VV	255180.5	600151.4	-0.9	76.4	23.6	2.2	100					0.0		
87	B	256083.4	600188.2	-0.2	61.8	38.2	3.5	82	1385	600	1.31	3.41	0.8	7.6	26.0
88	B	257148.8	600177.7	-0.9	51.4	48.6	4.5	65	1451	706	1.05	2.75	1.7	7.5	25.1
89	H	258228.2	600178.8	-0.4	82.3	17.7	1.8	112	1745	1183	0.48	1.24	0.4	7.9	24.9
90	B	259171.2	600110.4	-0.4	90.6	9.4	1.2	122	1315	487	1.70	4.45	0.0	8.2	30.0
91	B	260094.3	600174.3	-12.1	95.2	4.8	0.2	206	1990	1580	0.26	0.68	0.1	8.2	
92	B	261208.3	600140.7	-8.7	31.4	68.6	5.6	29	1357	554	1.45	3.78	5.9	8.0	26.4
93	VT	262117.5	600241.3	-0.3	75.7	24.3	2.4	140	1465	730	1.01	2.63	1.3	8.0	25.7
94	H	255064.0	601365.2	0.1	39.4	60.6	5.7	47	1641	1014	0.62	1.61	3.7		
95	B	256101.2	601180.2	-0.6	33.5	66.5	3.3	34	1081	108	9.06	23.64	15.6	7.6	28.8
95	VV	256101.2	601180.2	-0.6	19.4	80.6	11.4	13					0.0		
96	B	257123.3	601228.7	-0.5	30.5	69.5	6.3	22	1145	211	4.42	11.54	2.3	7.6	27.0
97	VT	258243.2	601194.1	-0.4	90.7	9.3	1.1	120	1326	504	1.63	4.26	0.8	8.0	28.6
98	B	259130.1	601094.0	-0.8	93.0	7.0	1.0	121	1175	259	3.54	9.24	0.3	7.9	28.8
99	B	260077.2	601146.9	-9.8	20.0	80.0	3.3	24	1415	648	1.18	3.09	2.3	8.3	23.2
100	B	261097.8	601185.6	-7.4	1.3	98.7	13.0	11	1234	356	2.47	6.45	0.7	7.7	23.5
101	VT	262061.5	601142.9	-0.2	83.4	16.6	1.7	116	1482	756	0.96	2.50	1.1	8.0	25.5
102	VT	256049.2	602177.1	-0.2	87.2	12.8	1.5	132	1986	1574	0.26	0.68	0.3		
103	VT	257184.7	602172.8	-0.1	90.1	9.9	1.1	127	1561	885	0.76	1.99	0.0	8.0	28.2
104	VT	258132.1	602176.5	0.0	99.9	0.1	0.0	143	2088	1739	0.20	0.52	0.0		
105	B	259094.8	602217.8	-14.9	89.6	10.4	1.2	141	1326	504	1.63	4.26	0.0	8.2	24.2
106	B	260155.7	602237.2	-12.4	9.7	90.3	10.5	15	1403	628	1.23	3.22	1.3	7.5	24.4
107	B	261241.6	602143.5	-2.9	43.1	56.9	7.2	35	1450	705	1.06	2.76	0.3	7.7	23.4
108	VT	262093.1	602148.5	0.0	89.2	10.8	1.5	150	1528	832	0.84	2.19	0.9	8.0	25.9
109	B	256115.7	603250.4	-0.3	89.5	10.5	1.2	134	1318	490	1.69	4.40	0.7	7.8	28.8
110	B	257138.7	603209.3	-0.3	95.1	4.9	0.4	159	1989	1578	0.26	0.68	0.3		
111	B	258122.2	603187.5	-8.3	91.0	9.0	1.1	390	2158	1852	0.17	0.43	0.1		
112	B	259165.2	603138.8	-14.7	97.8	2.2	0.4	797	2357	2175	0.08	0.22	0.0		
113	B	260168.3	603130.6	-8.3	16.6	83.4	6.6	26	1400	624	1.24	3.25	3.3	7.7	23.6
114	B	261116.4	603150.7	-2.0	35.7	64.3	6.5	21	1303	466	1.79	4.68	0.5	7.9	26.4
114	VV	261116.4	603150.7	-2.0	13.1	86.9	12.7	9					0.0		
115	VT	262141.4	603188.4	-0.1	87.5	12.5	1.6	140	1343	531	1.53	3.99	0.1	8.0	25.7
116	B	265742.1	594622.9	-6.3	12.1	87.9	6.7	12	1201	301	2.99	7.81	5.4	7.9	22.0
117	B	266761.3	594643.6	-8.1	7.9	92.1	10.6	9	1217	327	2.72	7.10	5.3	7.6	20.5
118	B	268756.0	594761.9	-8.5	54.9	45.1	5.5	81	1223	336	2.63	6.88	1.8	7.8	20.7
119	B	279278.4	595095.7	-3.5	47.7	52.3	3.7	21	1331	512	1.60	4.17	1.1	7.9	
120	VT	274293.9	584875.3	1.1	13.4	86.6	6.6	13	1350	542	1.49	3.89	4.0	7.7	18.9
121	B	274553.9	585524.4	0.9	10.4	89.6	11.6	9	1195	292	3.10	8.09	7.9	7.7	20.0
122	VT	275571.0	585291.5	0.8	12.6	87.4	7.7	12	1206	310	2.89	7.55	5.3	7.6	20.7
123	VT	276408.1	585090.5	0.9	11.8	88.2	7.5	12	1135	195	4.82	12.58	6.5	7.9	19.7
124	VT	270544.4	586621.4	0.9	17.7	82.3	8.0	17	1422	660	1.15	3.01	1.7	8.0	23.4
125	VT	271543.5	586624.3	0.6	31.7	68.3	6.5	35	1393	612	1.28	3.33	1.9	8.0	23.8
126	VT	272538.6	586625.6	0.5	10.9	89.1	7.0	13	1191	285	3.18	8.30	2.8	8.1	24.6
127	VT	273542.7	586626.5	0.6	31.0	69.0	6.0	28	1404	630	1.23	3.21	1.2	7.8	22.0

no	Instr	X (RD) [m]	Y (RD) [m]	Z [m]	sand [%]	mud [%]	clay [%]	d_{50} [µm]	ρ_{bulk} [kg/m^3]	ρ_{dry} [kg/m^3]	W [-]	e_i [-]	OC [%]	pH [-]	sal [psu]
128	B	274395.8	586622.6	-2.8	5.1	94.9	9.0	10	1187	278	3.26	8.52	5.6	8.4	18.4
128	VV	274395.8	586622.6	-2.8	11.1	88.9	9.2	15					0.0		
129	VT	275544.0	586625.3	0.5	26.7	73.3	7.7	28	1239	364	2.41	6.29	3.5	8.1	22.0
130	VT	276544.1	586625.5	0.7	21.4	78.6	8.9	18	1314	485	1.71	4.46	3.8	7.8	18.6
131	VT	268545.1	587625.7	1.1	13.1	86.9	7.6	15	1185	275	3.30	8.62	0.4	8.0	23.3
132	VT	269536.2	587626.7	0.7	38.7	61.3	5.3	46	1401	626	1.24	3.23	0.3	8.2	24.0
133	VT	270537.3	587627.8	0.3	29.3	70.7	6.0	31	1208	313	2.86	7.47	3.6	8.1	24.3
134	VT	271544.5	587625.8	-0.1	36.3	63.7	5.9	42	1137	197	4.76	12.43	0.4	8.0	24.0
135	VT	272549.6	587606.5	0.3	11.9	88.1	5.7	13	1164	241	3.83	10.01	5.8	8.0	23.7
136	B	273602.7	587619.7	-1.1	14.6	85.4	7.3	14	1187	278	3.26	8.52	1.5	7.8	20.4
137	VT	274799.9	587617.5	0.2	41.3	58.7	7.2	42	1540	851	0.81	2.12	0.8	8.0	20.2
138	VT	275553.0	587629.6	0.1	39.8	60.2	5.2	48	1615	973	0.66	1.72	0.5	7.8	20.1
139	VT	276537.1	587639.5	0.2	18.3	81.7	7.9	20	1279	428	1.99	5.19	3.8	8.2	21.3
139	VV	276537.1	587639.5	0.2	15.6	84.4	9.2	19					0.0		
140	VT	277542.2	587622.6	0.4	14.4	85.6	6.4	12	1140	202	4.63	12.09	4.8	7.8	18.6
141	VT	268643.1	588726.7	0.1	33.6	66.4	6.5	39	1203	305	2.95	7.69	1.0	8.0	24.1
142	VT	269413.2	588609.5	0.1	43.1	56.9	5.5	54	1618	978	0.66	1.71	0.6	8.7	
143	B	270302.3	588624.9	-1.3	58.3	41.7	4.3	75	1334	516	1.58	4.13	0.7	8.1	24.4
144	B	271055.4	588621.8	-0.7	19.7	80.3	7.3	13	1424	663	1.15	3.00	2.6	7.7	23.9
144	VV	271055.4	588621.8	-0.7	8.4	91.6	10.2	9					0.0		
145	VT	271535.4	588625.7	-0.1	64.4	35.6	4.2	84	1838	1334	0.38	0.99	0.2		
146	VT	272535.6	588616.6	-0.7	33.1	66.9	6.3	35	1277	425	2.01	5.24	0.1	8.4	24.7
147	B	273558.7	588637.9	-2.8	6.0	94.0	9.2	10	1169	250	3.67	9.59	2.6	7.8	20.3
148	B	273547.7	589111.6	-3.1	12.1	87.9	6.2	11	1309	477	1.75	4.56	3.4	7.6	17.5
148	VV	273547.7	589111.6	-3.1	8.2	91.8	7.4	12					0.0		
149	B	273939.7	589128.9	-2.2	13.6	86.4	10.1	12	1244	371	2.35	6.14	3.7	7.7	18.5
150	B	274538.8	588844.8	-1.4	14.3	85.7	10.2	11	1295	454	1.85	4.83	3.3	7.5	17.7
151	B	275527.0	588625.7	-1.5	50.3	49.7	5.0	64	1282	433	1.96	5.12	1.1	7.5	20.1
152	VT	276550.1	588636.7	-0.1	22.1	77.9	5.3	15	1152	222	4.19	10.93	3.8	7.7	19.0
153	VT	277534.2	588627.7	0.2	17.2	82.8	8.7	12	1142	206	4.54	11.85	1.4	7.9	21.4
154	B	268652.1	589835.8	-0.5	53.5	46.5	5.7	70	1498	783	0.91	2.38	1.0	8.0	24.7
155	B	269137.1	589412.9	0.1	51.8	48.2	5.1	66	1293	450	1.87	4.88	0.4	8.1	23.9
156	B	270594.3	589633.8	-1.8	57.8	42.2	5.2	91	1405	632	1.22	3.19	0.1	8.1	24.5
157	VT	271539.5	589624.8	0.7	78.7	21.3	2.2	108	1219	330	2.69	7.02	0.1	8.0	24.1
158	VT	272544.6	589625.0	0.5	68.8	31.2	3.1	92	1603	953	0.68	1.78	18.4	7.9	24.4
159	B	273541.7	589619.0	-4.3	20.7	79.3	8.0	13	1281	431	1.97	5.15	2.6	7.7	22.6
160	VT	274543.8	589626.0	0.4	76.4	23.6	2.5	119	1164	241	3.82	9.98	1.4	7.8	19.6
161	B	275794.0	589873.0	-2.4	26.2	73.8	6.4	17	1253	386	2.24	5.86	1.5	7.7	21.2
161	VV	275794.0	589873.0	-2.4	42.1	57.9	7.2	31					0.0		
162	B	277037.1	589131.9	0.1	38.0	62.0	5.1	44	1233	354	2.49	6.49	1.4	7.7	20.1
163	B	277277.2	589568.7	-0.9	47.5	52.5	5.9	59	1304	469	1.78	4.65	2.1	7.7	20.3
164	B	268535.1	590611.1	-2.0	7.4	92.6	8.1	9	1132	189	4.98	13.00	7.5	8.1	25.4
165	B	269045.1	590621.9	0.2	61.5	38.5	3.2	78	1362	563	1.42	3.71	0.6	7.8	24.6
166	B	269834.2	590622.9	-2.2	91.2	8.8	0.8	143	1191	286	3.17	8.28	0.0	8.1	24.4
167	B	270050.3	590119.7	-3.7	62.5	37.5	0.7	124	1053	62	16.05	41.90	51.0	8.0	24.4
168	VT	270842.4	590628.0	0.9	72.2	27.8	3.2	103	1446	698	1.07	2.80	0.1	8.0	24.5
169	H	271541.4	590624.1	0.9	80.0	20.0	1.9	109	1747	1186	0.47	1.23	0.9		
170	H	272543.6	590626.1	0.5	80.0	20.0	2.5	112	1911	1452	0.32	0.83	0.4		
171	B	273542.7	590636.2	-4.8	63.4	36.6	0.8	111	1090	121	8.01	20.91	53.9	7.9	19.0
172	B	274588.8	590773.0	-0.9	24.0	76.0	6.2	15	1242	368	2.38	6.21	0.3	8.0	21.5
173	B	275288.9	590376.0	-1.2	9.9	90.1	6.4	9	1171	253	3.63	9.49	2.7	8.1	24.6
174	B	276047.0	591124.3	-1.6	20.6	79.4	8.6	16	1206	310	2.89	7.55	4.4	8.1	20.4
175	B	276567.1	590634.1	-1.4	42.9	57.1	4.6	51	1157	230	4.04	10.54	3.7	7.7	21.1
176	B	277035.1	590101.1	-1.0	39.6	60.4	6.5	41	1220	333	2.66	6.96	1.8	7.9	20.5
177	B	277539.2	590630.0	0.4	27.1	72.9	9.5	19	1397	619	1.26	3.28	3.6	8.7	20.9
178	B	268288.0	591117.0	0.4	46.0	54.0	5.0	53	1245	373	2.34	6.10	1.6	8.1	24.9
179	B	268543.1	591620.0	-2.9	12.0	88.0	6.6	12	1329	508	1.61	4.21	1.0	8.1	24.9
180	B	269625.2	591634.2	-1.5	93.0	7.0	0.7	308	1239	364	2.41	6.29	0.0	8.1	23.9
181	VT	270539.3	591632.0	0.1	81.9	18.1	2.0	122	1459	719	1.03	2.68	0.0	8.0	24.0
182	B	271540.4	591626.0	-0.4	76.7	23.3	2.3	122	1301	464	1.80	4.71	1.1	7.6	24.6
183	B	272557.6	591621.9	0.0	54.1	45.9	5.1	72	1278	427	1.99	5.21	0.7	7.7	21.8
184	B	273566.7	591600.0	-5.5	20.0	80.0	3.5	24	1117	165	5.76	15.04	32.5	7.9	20.3
185	B	274573.8	591631.0	-3.6	26.3	73.7	6.3	17	1244	370	2.36	6.15	1.8	7.8	20.4
186	B	275312.9	591388.3	-0.4	4.1	95.9	5.9	10	1312	482	1.72	4.50	0.7	7.6	19.7
187	B	276534.1	591615.2	0.1	53.8	46.2	5.6	73	1408	637	1.21	3.16	1.4	7.7	20.7
188	B	277545.2	591614.2	0.2	35.6	64.4	7.9	31	1262	400	2.16	5.63	2.8	7.8	20.5
189	B	264542.5	592214.1	-0.2	47.3	52.7	5.1	59	1561	885	0.76	1.99	1.9	7.8	22.9
190	B	265553.7	592219.9	-0.6	43.8	56.2	5.7	53	1492	774	0.93	2.43	2.0	8.4	20.9
191	B	266560.8	592230.1	-0.9	60.9	39.1	3.6	77	1421	658	1.16	3.03	1.2	8.2	21.6
192	B	267548.9	592238.3	-0.8	47.4	52.6	5.7	59	1561	884	0.76	2.00	1.4	7.8	22.1
193	B	268554.0	592650.1	-1.7	92.9	7.1	0.9	143	1263	403	2.14	5.58	0.1	7.9	22.6

no	Instr	X (RD) [m]	Y (RD) [m]	Z [m]	sand [%]	mud [%]	clay [%]	d_{50} [µm]	ρ_{bulk} [kg/m^3]	ρ_{dry} [kg/m^3]	W [-]	e_i [-]	OC [%]	pH [-]	sal [psu]
194		270551.3	592630.3	-1.5	70.2	29.8	3.5	105	1318	492	1.68	4.39	16.9	7.9	22.8
195		271546.4	592638.2	-1.4	70.6	29.4	3.7	97	1125	178	5.31	13.87	0.7	8.0	22.3
196	B	272633.6	592728.1	-5.9	99.5	0.5	0.0	129	1356	553	1.45	3.79	0.2	7.8	21.1
196	VV	272633.6	592728.1	-5.9	90.1	9.9	1.3	129					0.0		
197	B	273206.6	592270.3	-6.7	13.8	86.2	5.7	20					0.0	7.8	19.0
198	B	273694.7	592759.3	-4.0	7.4	92.6	11.2	8	1165	244	3.78	9.87	2.7	7.8	22.0
199	B	274581.8	592850.1	0.0	28.4	71.6	11.3	22	1252	384	2.26	5.91	1.8	7.9	22.3
200	B	275566.0	592526.1	-0.4	54.5	45.5	6.6	76	1179	265	3.44	8.99	0.4	7.9	22.2
201	B	276553.1	592476.2	0.1	26.6	73.4	6.8	23	1319	494	1.67	4.37	2.4	8.4	21.1
201	VV	276553.1	592476.2	0.1	4.3	95.7	13.8	7					0.0		
202	VT	277544.2	592626.3	0.5	49.9	50.1	5.2	63	1406	634	1.22	3.18	2.3	7.8	20.6
203	B	264042.5	592923.0	-2.1	56.0	44.0	3.2	75	1514	809	0.87	2.28	0.9	7.8	21.1
203	VV	264042.5	592923.0	-2.1	78.7	21.3	2.1	103					0.0		
204	B	265047.6	592924.3	-4.5	47.8	52.2	6.5	49	1504	793	0.90	2.34	2.1	7.7	17.7
206	B	267053.8	592921.1	-2.5	13.4	86.6	9.3	10	1347	539	1.50	3.92	2.9	7.7	20.2
207	B	268048.0	593121.1	-1.9	100.0	0.0	0.0	146	1762	1211	0.46	1.19	0.0	8.2	21.2
208	B	269047.1	593121.4	-8.5	91.5	8.5	0.9	172	1627	992	0.64	1.67	0.1	7.9	20.4
209	B	263551.4	593638.1	-10.4	24.9	75.1	8.1	23	1358	555	1.44	3.77	6.5	7.8	23.3
210	B	264541.5	593633.4	-10.4	84.9	15.1	2.0	151	1239	364	2.41	6.29	0.1	7.8	24.4
211	B	265545.6	593634.4	-8.9	31.6	68.4	8.2	17	1316	487	1.70	4.44	2.1	7.8	18.4
212	B	266551.8	593631.4	-7.6	36.8	63.2	4.7	31	1332	514	1.59	4.15	8.3	7.7	21.6
213	B	267543.9	593622.3	-6.8	33.5	66.5	5.5	28	1209	315	2.84	7.42	16.4	7.7	25.3
214	B	268547.0	593628.5	-15.0	76.0	24.0	3.6	253	1730	1159	0.49	1.29	0.2	7.9	22.8
215	B	269557.2	593629.2	-9.8	33.8	66.2	5.8	25	1238	361	2.43	6.34	19.4	8.1	19.9
216	B	270538.3	593624.2	-7.3	98.4	1.6	0.1	258	1720	1143	0.51	1.32	0.0	7.9	
217	B	271549.4	593633.4	-6.5	14.7	85.3	7.9	15	1167	247	3.73	9.73	28.0	7.9	18.8
218	B	272200.5	593281.5	-6.4	13.3	86.7	8.5	15	1279	429	1.99	5.18	9.5	7.8	19.6
219	VT	272547.6	593630.2	-4.3	29.0	71.0	4.1	24	1073	94	10.43	27.23	31.9	8.0	22.5
220	VT	273193.6	593288.4	-2.0	39.3	60.7	6.2	24	1323	500	1.65	4.30	1.5	8.0	24.6
221	VT	273533.7	593617.5	-1.0	74.7	25.3	3.1	110	1914	1457	0.31	0.82	0.8		
222	VT	274543.8	593626.4	-0.6	68.8	31.2	3.7	96	1905	1443	0.32	0.84	0.6		
223	VT	275543.9	593626.4	0.0	62.1	37.9	4.3	84	1565	892	0.75	1.97	1.0	7.8	21.5
224	VT	276544.0	593626.6	0.6	45.9	54.1	5.0	55	1430	672	1.13	2.94	2.4	8.1	18.0
225	VT	277544.2	593626.5	1.0	42.9	57.1	4.8	51	1539	849	0.81	2.12	1.5	7.8	17.6
226	VT	278544.3	593626.3	0.8	21.6	78.4	6.2	15	1289	444	1.90	4.97	3.8	7.8	13.8
227	VT	269532.2	594625.3	-1.2	88.9	11.1	0.3	139	1709	1125	0.52	1.36	8.2	8.1	
228	VT	270518.3	594619.3	-1.4	88.5	11.5	0.4	154	1449	703	1.06	2.77	0.3	8.1	
229	VT	271520.4	594626.5	-1.1	78.7	21.3	2.1	123	1546	860	0.80	2.08	0.4	8.2	22.1
230	VT	272529.6	594625.3	-0.5	72.1	27.9	1.6	90	1240	365	2.40	6.26	7.7	8.2	21.4
230	VV	272529.6	594625.3	-0.5	67.5	32.5	2.5	98					0.0		
231	VT	273234.6	594212.4	-0.9	69.3	30.7	3.9	104	1712	1130	0.51	1.34	0.9	7.9	
232	VT	273543.7	594626.4	0.1	82.5	17.5	2.2	109	1201	302	2.98	7.77	1.0	7.7	22.3
233	VT	274543.8	594626.6	0.7	65.2	34.8	3.5	95	1521	821	0.85	2.23	0.5	7.8	20.7
234	VT	275543.9	594626.6	0.7	38.8	61.2	6.2	40	1313	483	1.72	4.49	1.9	7.9	19.4
235	VT	255049.2	602177.1	-5.9	33.4	66.6	5.6	34	1427	668	1.14	2.96	3.4	7.5	29.6
236	VT	255115.7	603250.4	-6.3	10.4	89.6	11.6	13	1301	463	1.81	4.73	0.3	7.8	29.2
236	VV	255115.7	603250.4	-6.3	19.1	80.9	10.7	14					0.0		
237	VT	254082.2	604298.9	0.0	23.5	76.5	6.6	19	1232	351	2.51	6.54	1.9	8.0	28.2
238	B	254946.1	604171.6	-5.8	4.4	95.6	12.2	10	1153	223	4.16	10.87	1.1	8.0	26.6
239	VT	256094.1	604264.1	0.1	92.7	7.3	0.8	155	1988	1578	0.26	0.68	0.0		
240	B	257146.5	604248.7	-6.3	88.8	11.2	1.1	434	1500	786	0.91	2.37	0.4	8.0	28.6
241	B	258134.1	604175.6	-10.9	93.6	6.4	0.6	233	1291	448	1.88	4.92	0.6	8.0	28.9
242	B	259119.5	604207.6	-13.6	18.5	81.5	7.0	22	1204	306	2.93	7.66	1.9	8.1	28.6
243	B	260162.6	604184.1	-3.8	13.4	86.6	10.3	9	1198	297	3.03	7.92	6.8	7.9	27.8
244	B	261091.0	604211.8	-1.0	65.8	34.2	3.3	93	1474	744	0.98	2.56	0.0	8.0	26.6
245	VT	262051.7	604203.9	-0.7	54.3	45.7	4.4	70	1243	370	2.36	6.16	2.3	8.2	26.7
246	B	269350.0	592582.0	-7.9	91.0	9.0	0.7	380	2077	1722	0.21	0.54	0.0		
247	B	269132.0	591630.0	-4.2	5.0	95.0	4.9	10	1245	372	2.34	6.12	2.3	8.0	24.8
247	VV	269132.0	591630.0	-4.2	16.9	83.1	7.7	17					0.0		
248	B	269424.0	596625.0		86.3	13.7	1.6	440	1654	1036	0.60	1.56	0.1	8.5	25.6
249	B	275575.0	585117.1	-3.0	6.8	93.2	11.6	9	1285	437	1.94	5.07	0.0	8.3	
249	VV	275575.0	585117.1	-3.0	9.0	91.0	9.1	10					0.0		
5711	B	280198.5	594607.7	-6.2	21.8	78.2	3.4	9	1099	158	5.96	15.77	4.3	8.1	18.6
5712	B	281179.6	594624.7	-6.3	31.8	68.2	3.9	11	1196	313	2.82	7.47	4.6	8.1	14.4
5713	B	282026.6	594570.8	-6.2	20.5	79.5	3.9	8	1102	163	5.77	15.26	11.4	8.1	9.7
5714	B	283118.6	594488.2	-6.9	36.4	63.6	3.4	14	1152	243	3.74	9.90	0.6	8.3	15.4
5715	B	284092.3	594592.7	-9.6	30.6	69.4	4.4	11	1156	250	3.63	9.62	2.0	8.2	
5716	B	284918.4	594246.9	-5.7	23.0	77.0	6.7	18	1273	437	1.91	5.06	0.9		
5717	B	285314.6	593323.1	-3.2	12.6	87.4	9.9	11	1208	333	2.63	6.96	4.3	8.5	
5718	B	285738.9	592369.1	-4.5	20.7	79.3	5.5	8	1147	235	3.89	10.29	7.5	8.4	
5719	B	286628.2	591868.8	-7.8	5.5	94.5	11.4	11	1169	270	3.33	8.81	3.7	7.7	5.5

no	Instr	X (RD) [m]	Y (RD) [m]	Z [m]	sand [%]	mud [%]	clay [%]	d_{50} [µm]	ρ_{bulk} [kg/m^3]	ρ_{dry} [kg/m^3]	W [-]	e_i [-]	OC [%]	pH [-]	sal [psu]
5720	B	287586.3	591963.9	-6.1	11.5	88.5	9.6	11	1188	301	2.95	7.81	2.6	7.8	5.5
5721	B	288646.6	591659.1	-7.7	25.0	75.0	4.8	19	1140	224	4.10	10.85	5.9	8.2	3.7
5722	B	289011.8	590722.5	-4.9	5.6	94.4	8.4	9	1169	270	3.32	8.80	4.1		
5723	B	289002.0	589788.8	-5.6	7.5	92.5	9.0	9	1139	222	4.13	10.93	3.2	8.0	3.9
5724	B	289065.0	588792.6	-6.7	3.9	96.1	9.8	9	1105	168	5.60	14.82	7.2	8.2	
5725	B	288956.8	587825.1	-6.0	8.8	91.2	6.2	13	1133	213	4.33	11.45	5.4	8.4	3.6
5726	B	289015.0	586800.9	-5.9	2.7	97.3	7.8	9	1135	216	4.26	11.27	6.6	8.0	
5727	B	289002.8	585859.7	-5.6	6.7	93.3	8.1	10	1129	205	4.50	11.91	5.5	8.0	3.8
5728	B	289514.4	584944.2	-7.5	12.7	87.3	6.3	12	1161	257	3.52	9.32	3.4	8.3	2.9
5729	B	290460.3	584717.0	-6.6	8.6	91.4	7.6	12	1247	396	2.15	5.69	2.7	8.0	
5730	B	291239.6	584146.5	-5.4	9.7	90.3	8.5	15	1173	276	3.25	8.60	2.6	8.0	2.5
5731	B	291175.6	583293.5	-6.6	4.1	95.9	6.8	10	1211	338	2.58	6.84	3.8		
5731	VV	291175.6	583293.5	-6.6	9.2	90.8	7.0	12					0.0		
5732	B	290782.6	582239.2	-6.1	18.3	81.7	5.6	23	1354	568	1.39	3.67	3.1	7.8	
5733	B	290221.2	581482.0	-4.7	11.3	88.7	6.4	16	1203	325	2.70	7.15	2.5	7.9	3.3
5734	B	290002.3	580513.0	-6.4	27.2	72.8	2.8	39	1287	460	1.80	4.76	3.2	7.8	
5735	B	289815.2	579740.7	-5.4	13.0	87.0	5.9	16	1271	433	1.93	5.12	4.3	8.1	3.0
5736	B	289007.7	579302.8	-5.8	8.3	91.7	6.7	12	1195	311	2.84	7.52	4.8	8.0	
5737	B	288355.0	578512.5	-4.8	12.5	87.5	6.8	13	1264	423	1.99	5.26	4.1		
5738	B	287618.0	577881.7	-4.2	6.0	94.0	9.9	10	1191	305	2.90	7.68	3.3		
5739	B	287780.5	576724.7	-4.4	26.7	73.3	6.0	23	1344	551	1.44	3.81	2.6	8.5	
5740	B	287942.2	575815.3	-4.9	6.5	93.5	4.6	13	1202	323	2.72	7.20	3.5	8.2	
5741	B	287858.8	574862.0	-4.8	17.3	82.7	7.5	18	1259	414	2.04	5.40	2.3	8.9	1.3
5742	B	287475.8	574022.6	-5.5	17.3	82.7	6.9	18	1267	427	1.97	5.21	3.2		
5743	B	287923.4	572849.4	-4.2	6.8	93.2	5.3	13	1206	329	2.66	7.05	5.0	7.8	
5744	B	288069.2	572321.9	-4.8	8.7	91.3	7.6	13	1205	328	2.67	7.07	5.2	7.6	
5745	B	287831.2	571336.6	-4.2	10.9	89.1	7.0	13	1164	261	3.45	9.14	3.7	8.4	0.9
5745	VV	287831.2	571336.6	-4.2	17.8	82.2	6.0	21					0.0		
6000	B	291309.0	582527.0	2.8	14.0	86.0	7.8	16	1177	283	3.17	8.38	3.4	8.2	2.2

Explanation:

no	number of sample
Instr	type of sampling instrument: B = Box corer, VV = Van Veen grab, VT = Vacuum tube, H = Hand
X	x-coordinate of the sampling location in Rijksdriehoek-coordinates [m]
Y	y-coordinate of the sampling location in Rijksdriehoek-coordinates [m]
Z	estimated z-coordinate of the sampling location [m], defined positive up, derived from vaklodingen data of 2012 and 2005 (in Ems River), based on (x,y)-position
sand	percentage of sand (d > 63 µm), derived from Malvern data
mud	percentage of mud (d < 63 µm), derived from Malvern data
clay	percentage of clay (d < 2 µm), derived from Malvern data
d_{50}	median grain size in [µm], derived from Malvern data
ρ_{bulk}	bulk density [kg/m^3]
ρ_{dry}	dry density [kg/m^3]
W	water content [-]
e_i	void ratio [-]
OC	organic content [%]
pH	pH [-]
sal	salinity [psu], computed with the UNESCO formula, based on the conductivity [mS/cm] measured at a temperature of 17^{o}C.

B Overview of experiments

	Experiments						
Sample no	Zeta Potential	CST	Atterberg Limits	Vane	Sedigraph	Settling column	
7	x			x			Box corer / Vacuum tube
19	x		x	x	x		
27	x	x	x	x	x		
35	x						
38	x		x		x		
40	x						
42	x		x		x		
46	x						
47				x			
49						x	
55	x			x			
87	x			x			
90	x			x			
93	x			x			
119						x	
126	x		x		x		
135						x	
139	x			x			
142	x	x	x	x	x		
145	x			x			
149	x		x		x		
160	x			x			
166	x			x			
170	x			x			
173	x	x	x	x	x		
183	x		x		x		
192	x		x	x	x		
193							
199	x		x	x	x		
200	x		x		x		
202	x		x	x	x		
213	x		x		x		
214	x			x			
222	x			x			
229	x			x			
246	x			x			
5714	x		x		x		
5721	x		x		x		
5726	x	x	x		x		
5731	x		x		x		
5734						x	
5736	x		x		x		
5739	x		x		x		
5745	x		x		x		
55			x		x		Van Veen grab
139			x		x		
5731			x		x		
5745			x		x		

C Settling column test results

In this appendix the results of the settling column test for phase I and II are visualized. At the top of each figure the characteristics of the samples are shown (sample number, concentration, initial water level in the column, initial water content and the amount of sand in each sample. In the legend the values obtained for K_k, D and K_p are listed, together with a reference to the equation which is used to obtain the results.

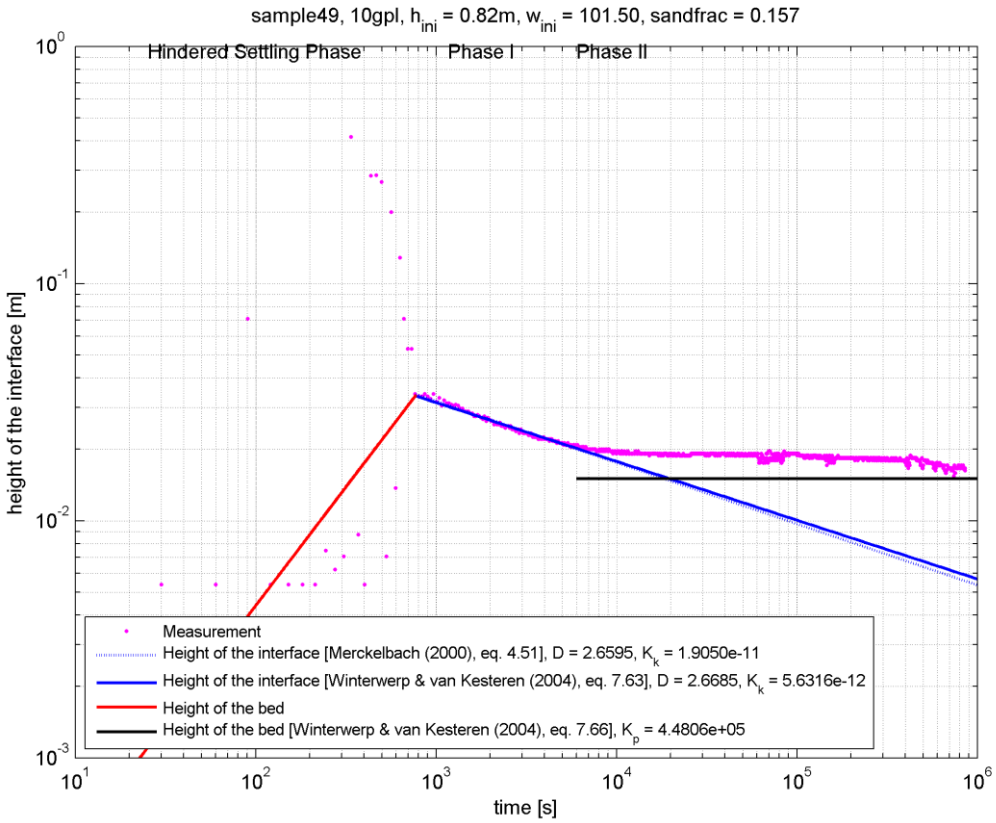

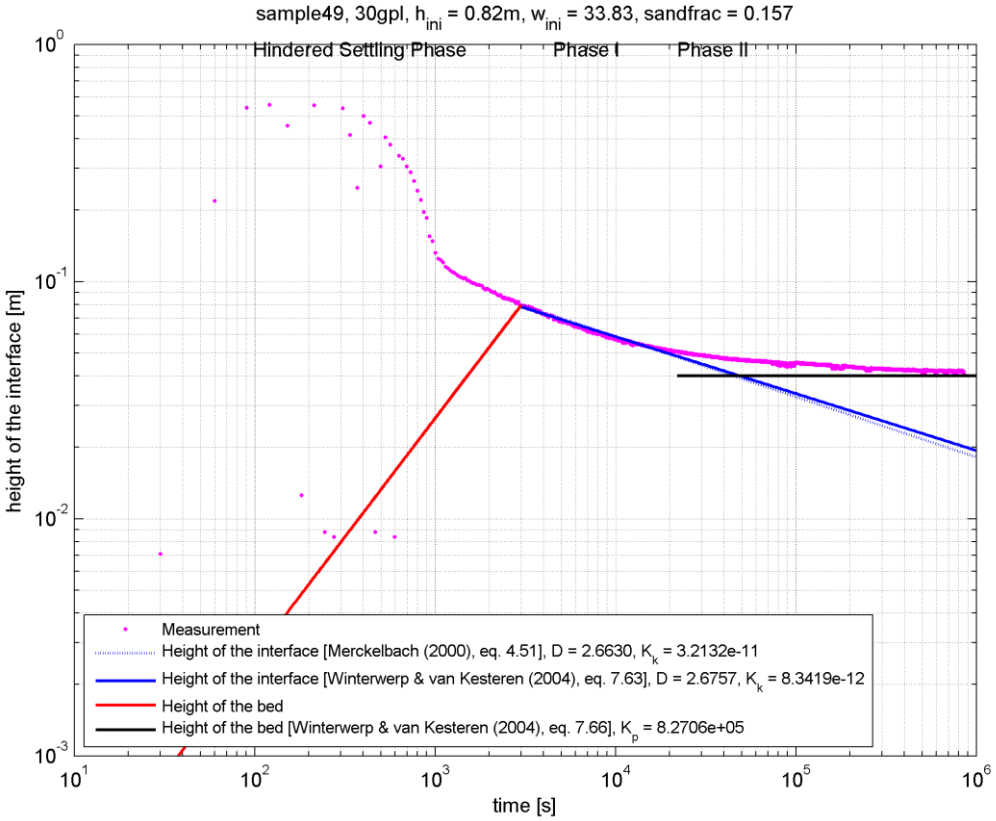
sample49, 30gpl, h_ini = 0.82m, w_ini = 33.83, sandfrac = 0.157
Hindered Settling Phase
Phase I
Phase II
height of the interface [m]
time [s]
Measurement
Height of the interface [Merckelbach (2000), eq. 4.51], D = 2.6630, K_k = 3.2132e-11
Height of the interface [Winterwerp & van Kesteren (2004), eq. 7.63], D = 2.6757, K_k = 8.3419e-12
Height of the bed
Height of the bed [Winterwerp & van Kesteren (2004), eq. 7.66], K_p = 8.2706e+05

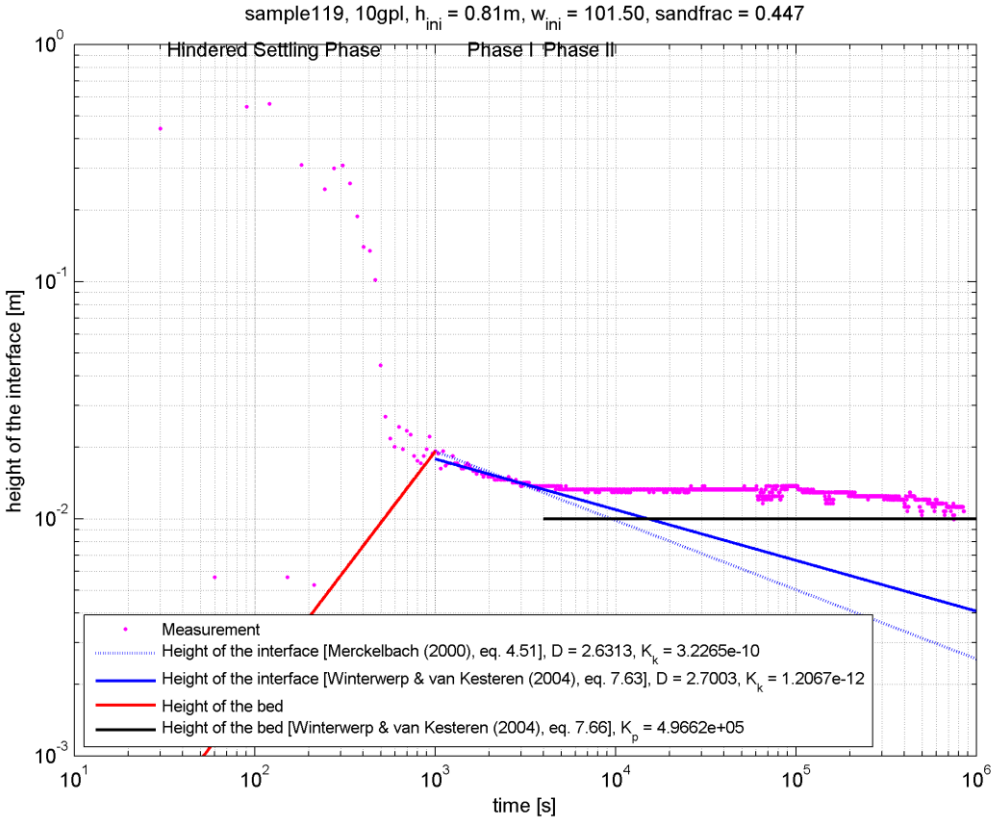
sample119, 10gpl, h_ini = 0.81m, w_ini = 101.50, sandfrac = 0.447
Hindered Settling Phase
Phase I
Phase II
height of the interface [m]
time [s]
Measurement
Height of the interface [Merckelbach (2000), eq. 4.51], D = 2.6313, K_k = 3.2265e-10
Height of the interface [Winterwerp & van Kesteren (2004), eq. 7.63], D = 2.7003, K_k = 1.2067e-12
Height of the bed
Height of the bed [Winterwerp & van Kesteren (2004), eq. 7.66], K_p = 4.9662e+05

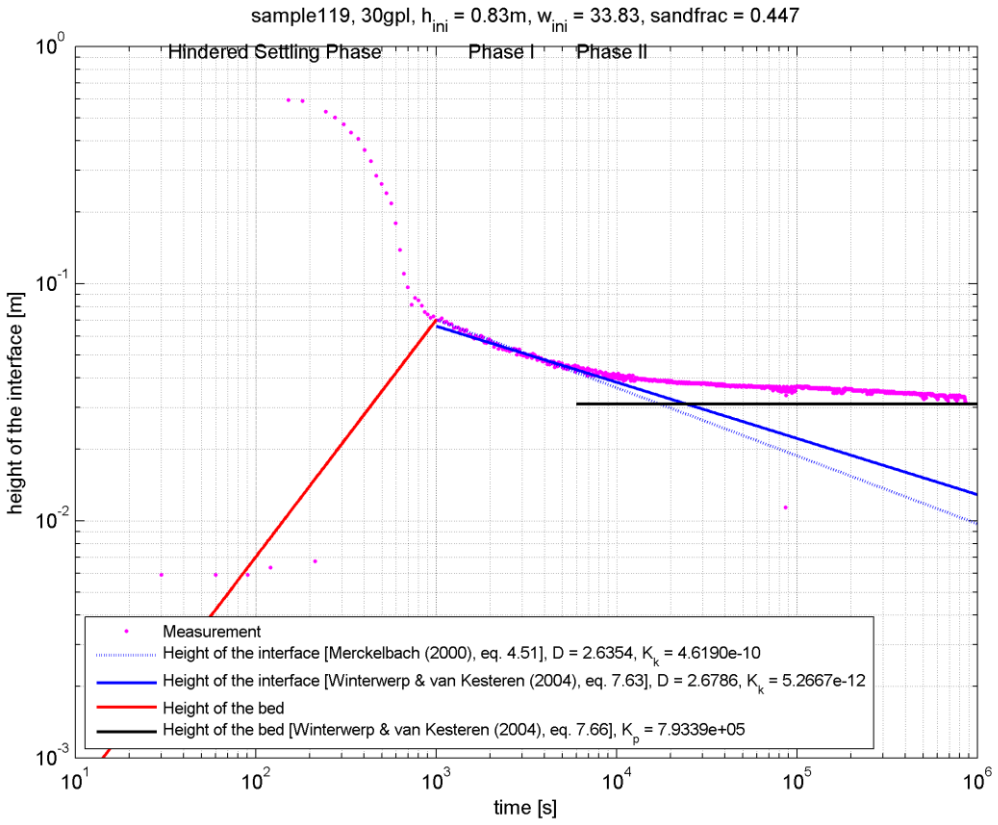
sample119, 30gpl, h_ini = 0.83m, w_ini = 33.83, sandfrac = 0.447
Hindered Settling Phase
Phase I
Phase II
height of the interface [m]
time [s]
Measurement
Height of the interface [Merckelbach (2000), eq. 4.51], D = 2.6354, K_k = 4.6190e-10
Height of the interface [Winterwerp & van Kesteren (2004), eq. 7.63], D = 2.6786, K_k = 5.2667e-12
Height of the bed
Height of the bed [Winterwerp & van Kesteren (2004), eq. 7.66], K_p = 7.9339e+05

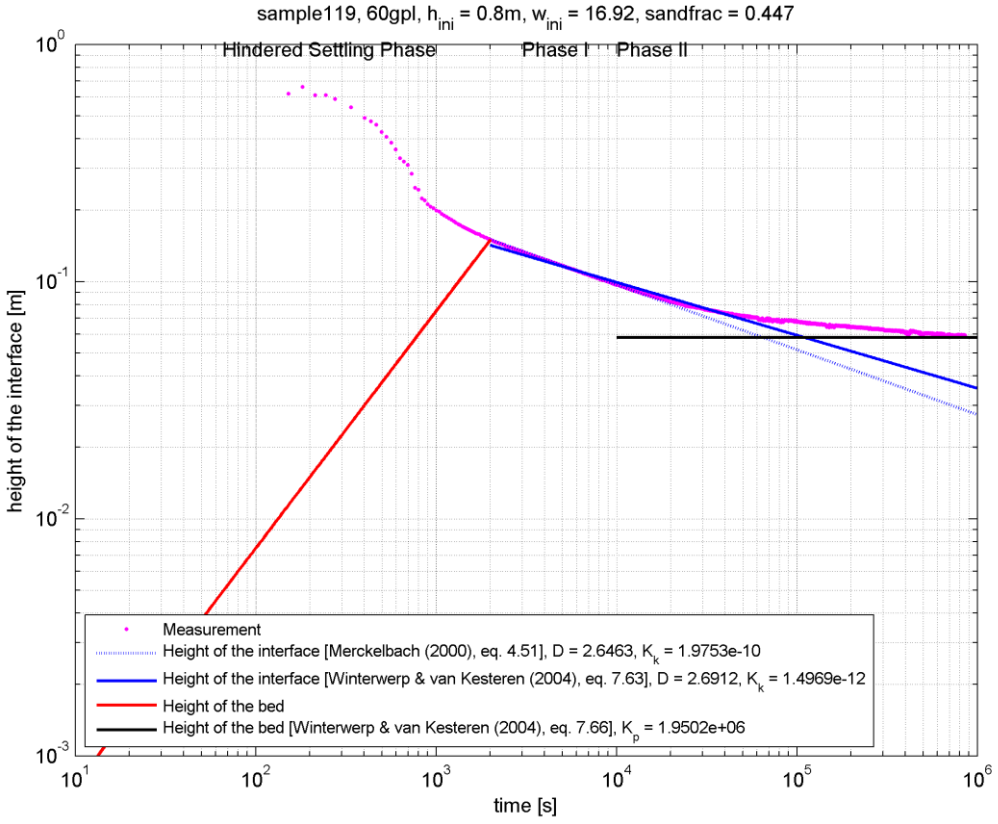
sample119, 60gpl, h_ini = 0.8m, w_ini = 16.92, sandfrac = 0.447
Hindered Settling Phase
Phase I
Phase II
height of the interface [m]
time [s]
Measurement
Height of the interface [Merckelbach (2000), eq. 4.51], D = 2.6463, K_k = 1.9753e-10
Height of the interface [Winterwerp & van Kesteren (2004), eq. 7.63], D = 2.6912, K_k = 1.4969e-12
Height of the bed
Height of the bed [Winterwerp & van Kesteren (2004), eq. 7.66], K_p = 1.9502e+06

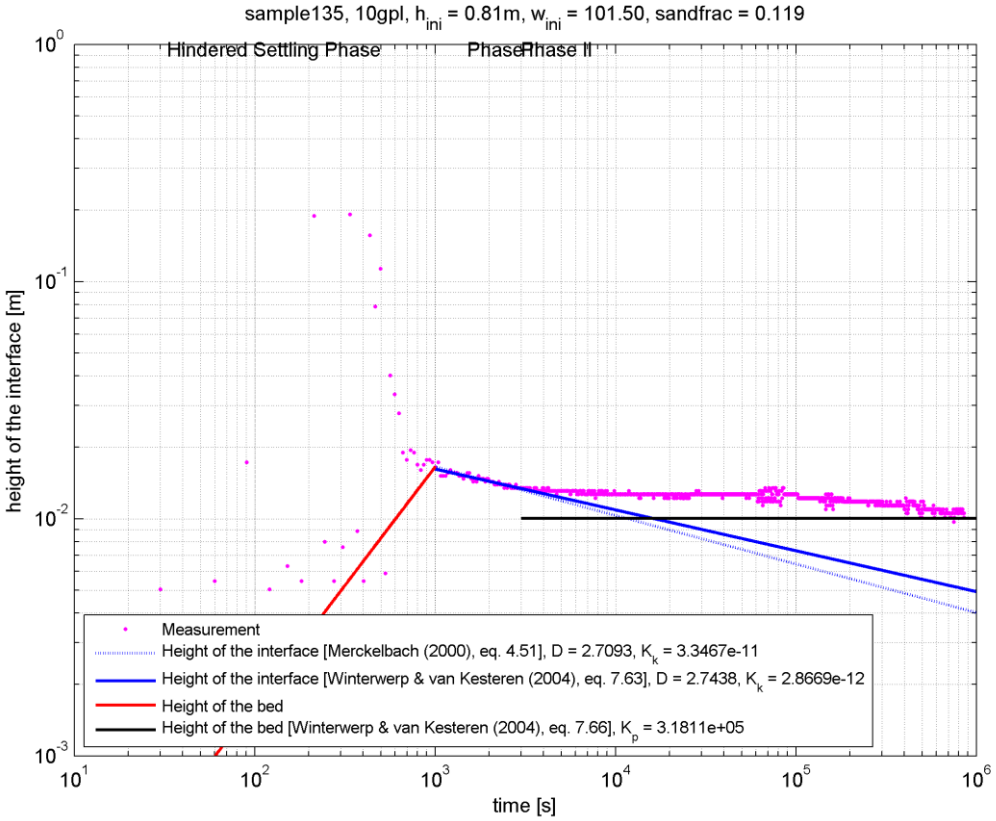
sample135, 10gpl, h_ini = 0.81m, w_ini = 101.50, sandfrac = 0.119
Hindered Settling Phase
Phase
Phase II
height of the interface [m]
time [s]
Measurement
Height of the interface [Merckelbach (2000), eq. 4.51], D = 2.7093, K_k = 3.3467e-11
Height of the interface [Winterwerp & van Kesteren (2004), eq. 7.63], D = 2.7438, K_k = 2.8669e-12
Height of the bed
Height of the bed [Winterwerp & van Kesteren (2004), eq. 7.66], K_p = 3.1811e+05

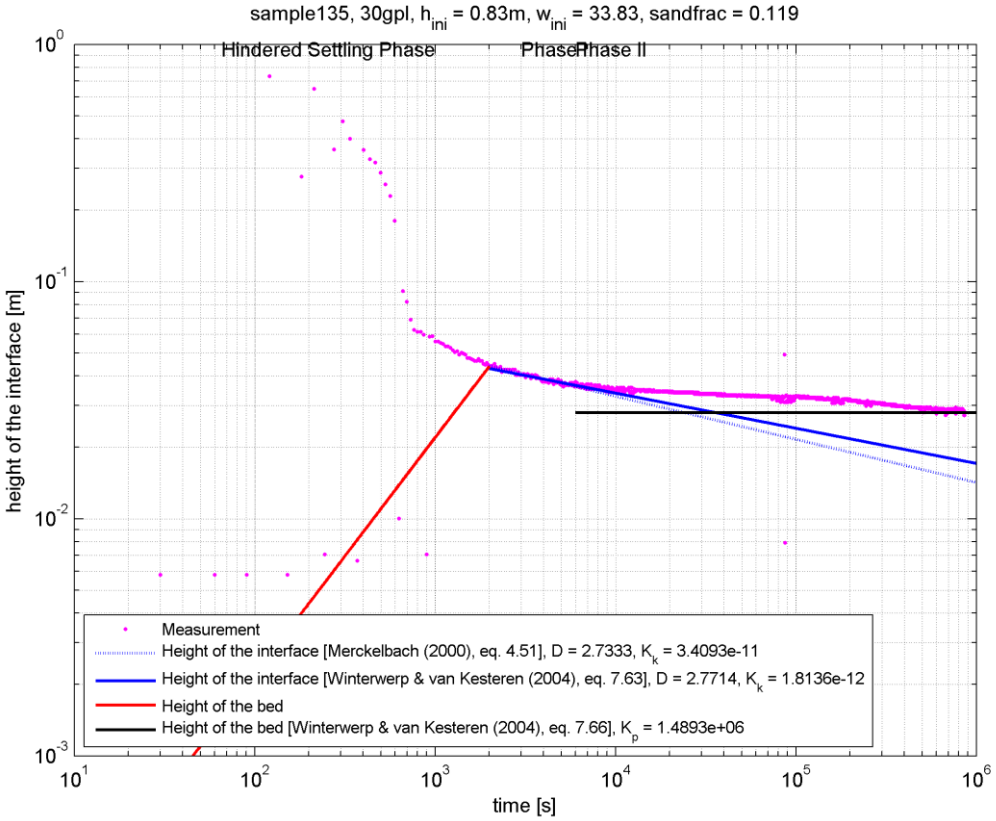
sample135, 30gpl, h_ini = 0.83m, w_ini = 33.83, sandfrac = 0.119
Hindered Settling Phase
Phase
Phase II
height of the interface [m]
time [s]
Measurement
Height of the interface [Merckelbach (2000), eq. 4.51], D = 2.7333, K_k = 3.4093e-11
Height of the interface [Winterwerp & van Kesteren (2004), eq. 7.63], D = 2.7714, K_k = 1.8136e-12
Height of the bed
Height of the bed [Winterwerp & van Kesteren (2004), eq. 7.66], K_p = 1.4893e+06

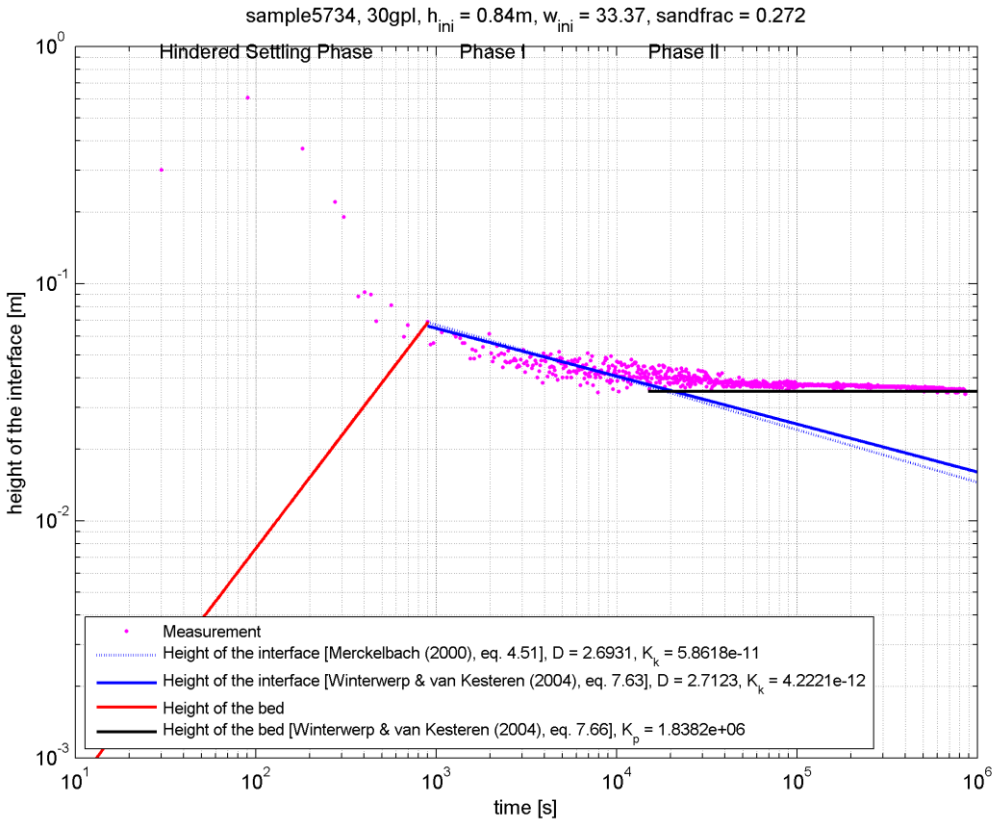
sample5734, 30gpl, h_ini = 0.84m, w_ini = 33.37, sandfrac = 0.272
Hindered Settling Phase
Phase I
Phase II
height of the interface [m]
time [s]
Measurement
Height of the interface [Merckelbach (2000), eq. 4.51], D = 2.6931, K_k = 5.8618e-11
Height of the interface [Winterwerp & van Kesteren (2004), eq. 7.63], D = 2.7123, K_k = 4.2221e-12
Height of the bed
Height of the bed [Winterwerp & van Kesteren (2004), eq. 7.66], K_p = 1.8382e+06

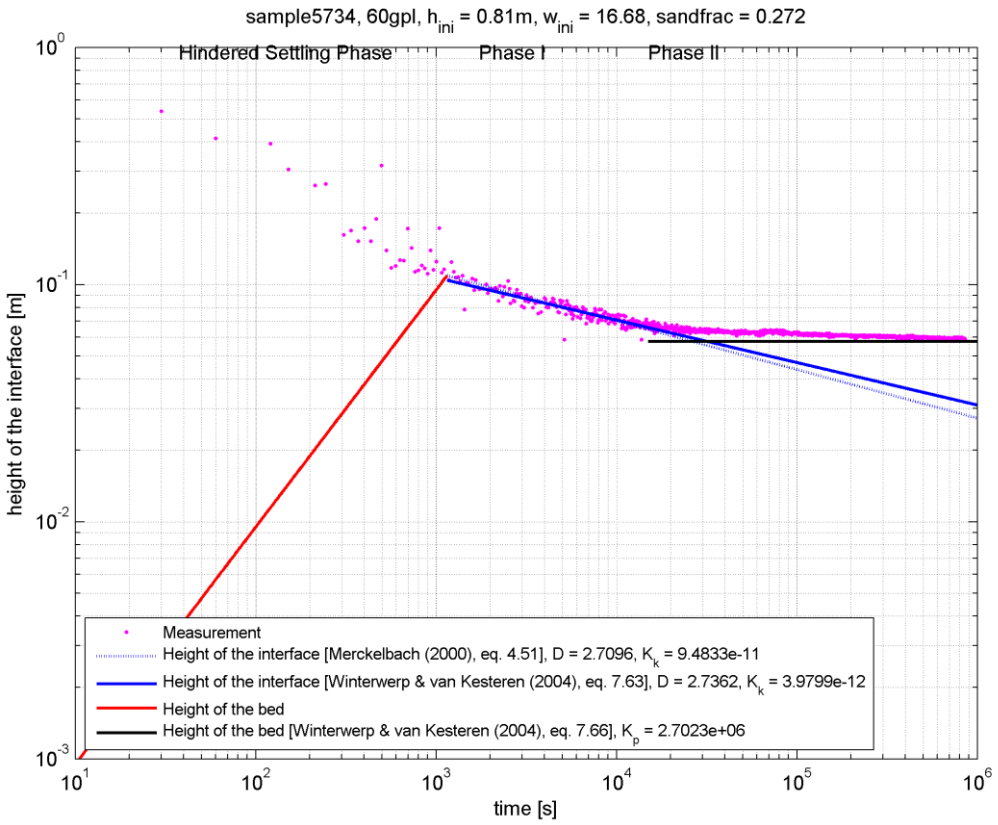
sample5734, 60gpl, h_ini = 0.81m, w_ini = 16.68, sandfrac = 0.272
Hindered Settling Phase
Phase I
Phase II
height of the interface [m]
time [s]
Measurement
Height of the interface [Merckelbach (2000), eq. 4.51], D = 2.7096, K_k = 9.4833e-11
Height of the interface [Winterwerp & van Kesteren (2004), eq. 7.63], D = 2.7362, K_k = 3.9799e-12
Height of the bed
Height of the bed [Winterwerp & van Kesteren (2004), eq. 7.66], K_p = 2.7023e+06